ABSTRACT

GREELEY, LAURA ANN. The GRIK-SnRK1 Kinase Cascade: Characterizing Phosphorylation of TCP Transcription Factors and Motifs in Arabidopsis Proteins. (Under the direction of Drs. Michael B. Goshe and Linda Hanley-Bowdoin.)

Abiotic and biotic stresses often reduce the yields of native plants and economically important crop plants significantly. Due to their sessile nature, plants have evolved complicated response pathways to react to environmental stresses and signals. SNF1-related kinase 1 (SnRK1) is the plant homolog of mammalian AMPK (AMP-activated protein kinase) and yeast SNF1 (Sucrose Non-fermenting-1). SnRK1 is part of a protein kinase cascade that includes the GRIKs (Geminivirrus Rep Interacting Kinases), which activate SnRK1 by phosphorylating its activation loop. SnRK1 is critical for the regulation of many plant signaling pathways including global regulation of metabolism and energy conservation, and responses to abiotic and biotic stresses. SnRK1 also plays a role in regulation of plant development, most likely by modulating transcription factors to alter transcriptional gene expression programs.

Teosinte branched 1/Cycloidea/PROLIFERATING CELL FACTORS (TCPs) are a family of transcription factors that are unique to green algae and plants. TCPs fall into two classes that play opposing roles in plant development. Class I TCPs promote cell proliferation early in plant development, while Class II TCPs inhibit proliferation and promote differentiation. Although the knowledge about the functions of TCPs and the regulation of their mRNAs have been accumulating, very little is known about regulation of the proteins themselves.

The work described in this thesis characterized TCP phosphorylation by the GRIK-SnRK1 cascade. These studies established that the majority of TCPs are phosphorylated by

GRIK and/or by GRIK-activated SnRK1 *in vitro*. Analysis of truncated proteins revealed that TCP3 is phosphorylated in its C-terminus after the TCP domain. A combination of mass spectroscopy and site-directed mutagenesis showed that SnRK1 phosphorylates TCP18 on Ser-36 or Ser-38 and Thr-233, TCP20 on Ser-237, and TCP22 on Ser-140. All of these sites are also located outside of the TCP domain. Comparison of wild-type TCP20 and TCP22 with their corresponding phosphomutants and phosphomimics at Ser-237 and Ser-140, respectively, revealed that SnRK1 phosphorylation does not impact protein-DNA binding *in vitro*. In contrast, TCP20 and TCP22 phosphomimics were impaired for binding to BRM, a subunit of the SWI/SNF chromatin remodeling complex. These results suggested that SnRK1 phosphorylation of TCP20 and TCP22 regulates their transcription activity by altering their protein interactions.

This thesis also describes a proteomic approach to reveal a more specific consensus phosphorylation motif for SnRK1. This strategy used LC/MS/MS analysis to identify phosphopeptides derived from Arabidopsis culture cell lysates incubated with GRIK-activated SnRK1 *in vitro*. The sequence -xxxRSxsFxxxxx- was identified as a motif for GRIK-SnRK1 cascade phosphorylation. This motif is a more specific variation of one of the motifs in the literature.

The GRIK-SnRK1 Kinase Cascade: Characterizing Phosphorylation of TCP Transcription Factors and Motifs in Arabidopsis Proteins

by
Laura Ann Greeley

A dissertation submitted to the Graduate Faculty of
North Carolina State University
in partial fulfillment of the
requirements for the Degree of
Doctor of Philosophy

Biochemistry

Raleigh, North Carolina

2016

APPROVED BY:

_____	_____
Linda Hanley-Bowdoin Committee Chair	Michael B. Goshe
_____	_____
Robert Rose	Steven Clouse

DEDICATION

To my friends and family for loving me through all the ups and downs.

BIOGRAPHY

Laura Ann Greeley was raised in suburban New Jersey by her parents, David and Laura Greeley and her brother, Jonathan. Laura was the first to complete the biochemistry curriculum for BS at Misericordia University, before interning at NIAAA of NIH for two years. Laura later pursued a doctorate in Biochemistry at North Carolina State University under the direction of Dr. Linda Hanley-Bowdoin and Dr. Michael B. Goshe.

ACKNOWLEDGMENTS

First, I would like to thank Dr Linda Hanley-Bowdoin and Dr. Michael Goshe for being their polar mentoring styles and how they balanced. Linda's enthusiasm, encouragement, dedication and support centered me and inspired me throughout these years. Mike's relaxed composure enabled me to make mistakes without out falling too far.

I also want to thank my committee members, Dr. Bob Rose and Dr. Steve Clouse for their advice and support.

I would like to thank my family, especially my parents. My father for his faith and unending pride and my mother for her laughter and regular counsel. Additionally, I want to thank my friends for years of smile even under the greatest stress.

I want to thank my lab mates Mary Beth, Tara, Trino, Mariana, Ashley, Leandro, Lorenzo, Emilie, Cyprian, Catherine, Kevin, Mialy, Koyi, Fan, Laura H., and all of the others who have come and gone for their great advice, memories and support, with special thanks to Wei for his assay training and continual support as a sounding board.

I would also like to acknowledge the financial support from NIH MBTP fellowship and NSF grants (MCB-1052218 and DBI-1126244).

TABLE OF CONTENTS

LIST OF TABLES

LIST OF FIGURES

CHAPTER 4:

CHAPTER I

Introduction to GRIK-SnRK1 Cascade and TCP Transcription Factors

INTRODUCTION

SNF1-related kinase 1

Proteins are dynamic molecules whose functions affect an organism's physiology in both subtle and striking ways (*1*). Post-translational modifications (PTM) are enzymatic processes that the primary structure of a protein after it is synthesized from translation of an mRNA (*1*). These changes are key factors in how and where a protein functions (*1*).

One such PTM is the addition of a phosphoryl group to a specific amino acid of a protein by covalent bond, known as phosphorylation (*1*). In eukaryotes, phosphorylation of tyrosine, serine, or threonine by protein kinases (*1*) plays a central role in the regulation of cellular processes (*2, 3*). It is hypothesized that approximately 30% of the proteins in an organism are phosphorylated, most frequently on serine or threonine (*4*). These covalent bonds can be broken via protein phosphatases, thus, protein phosphorylation is reversible (*1*).

Phosphorylation introduces a bulk negative charge to a region that was previously moderately polar (*1, 5*). This chemical change can repel other negative groups as well as form hydrogen bonds, both of which have the potential to have significant effects on protein structure (*1*). Additionally, if the phosphorylation is in a catalytic domain or in regions that bind to other proteins or nucleic acid, the negative charge can directly modulate ligand, protein or nucleic acid binding (*5*). This reversible chemical change not only affects activity and protein binding but many cells also utilize this modification to affect localization of a protein within a cell (*5*).

Plant growth and development can easily be impacted by adverse environmental conditions due to the sessile nature of plants. Abiotic and biotic stresses are often detrimental to yield of native plants and economically important crop plants. Since plants are stationary, they must be able to respond to their natural environment by undergoing changes in their physiology and development through one of many adaptive mechanisms (*6*). Up to 4% of the annotated proteins in Arabidopsis are annotated as kinases (*7*). When compared to 1.7% of the proteins in humans (*8*), a significant expansion in protein kinases is apparent and can be attributed to plant-specific kinase families such as the calcium-dependent protein kinase and SNF1-related kinase superfamilies (*2, 3*).

The CDPK-SnRK superfamily is comprised of seven types of serine-threonine protein kinases: calmodulin-dependent protein kinases (CaMKs), phosphoenolpyruvate carboxylase kinases (PPCKs), PEP carboxylase kinase-related kinases (PEPRKs), calcium-dependent protein kinase (CDPKs), CDPK-related kinases (CRKs), calcium and calmodulin-dependent protein kinases (CCaMKs), and SnRKs (*3*). Members of the CDPK-SnRK superfamily are Ser/Thr protein kinases (*2*). Most members have a C-terminus that regulates kinase activity and mediates interactions with other proteins (*3*). The C-terminal domains of SnRKs are highly variable but in many cases are thought to function in protein-protein interactions (*3*). The SnRK subfamily is related to the classical SNF1 (Sucrose Non-fermenting-1)-type kinases from yeast and are known as SNF1-related kinase (SnRK) (*3*). The family contains three recognized subgroups: SnRK1, SnRK2, and SnRK3. SnRK1 is a true homologue of

SNF1 (3). SnRK2 and SnRK3 kinases are distinct from SNF1 and have different primary structures (*3*).

Arabidopsis contains 38 protein kinases classified as SnRK proteins (*3*). SnRK2 and SnRK3 kinases are unique to plants (*9*). The SnRK2 subfamily contains 10 kinases (*3*). SnRK2 proteins are about 40 kD in size, making them 140 to 160 amino acids shorter than SnRK1, and have a characteristic sequences of acidic amino acids in their C-termini (*9*). SnRK2 kinases are key components of abscisic acid (ABA) signaling pathways (Fig.1) (*10*). SnRK2 kinases phosphorylate ABA-Responsive Element Binding factors (AREBs) that regulate ABA-responsive genes. The targets include genes encoding the ion channels Slow Anion Channel-Associated 1 and K^+ channel in *Arabidopsis thaliana* 1, which regulate ABA-dependent stomatal movement, and Respiratory Burst Oxidase Homolog F, which responds to ABA generation induction by reactive oxygen species (ROS) (*10*). The SnRK3 subfamily has 25 members (3). SnRK3 kinases are involved in ABA responses during root elongation, seed germination, and gene expression (*11*).

SnRK1 is the plant homologue of SNF1 from yeast and AMPK (AMP-activated protein kinase) from mammals (*12*). The primary functions of the SNF1/AMPK/SnRK1 are regulating metabolic and energy homeostasis pathways (*12*) and protecting against falling energy levels by inhibiting energy-consuming pathways and activating energy-producing pathways (*13*). SNF1 is key to survival during glucose deprivation and growth utilizing other metabolic sources (*14*). AMPK is also pivotal to metabolic homeostasis (*15*). SnRK1 is known to phosphorylate and modulate several biosynthetic and assimilatory enzymes (*16*).

This is vital for survival of plants during dark periods and the during abiotic stresses like sugar deprivation, salt and osmotic stress, and hypoxia (*17*). SnRK1 is also responsive to herbivore wounding, and viral infection (*17*).

SNF1/AMPK/SnRK1 exist as heterotrimeric complexes containing a catalytic asubunit, α, and two regulatory subunits, β and γ (Fig. 2) (*18*). Each subunit has multiple forms in Arabidopsis and different combinations of heterotrimeric complexes are hypothesized to affect regulation (*19*). The N-terminal half of the α subunit, which displays the highest degree of conservation across species, contains the kinase domain with a conserved threonine residue in the activation loop (*20*). SNF1/AMPK/SnRK1 activity depends on phosphorylation of a specific threonine residue in the kinase domain T–loop (*21*) by upstream kinases. The C-terminal half has an autoinhibitory regulatory sequence (*3, 20*).

The β subunits are characterized by N–terminal myristoylation sites, mid-molecule family 48 carbohydrate-binding modules (CBM), and C–terminal association to the complex domains that anchor α and γ subunits (*13*). The myristoylation site regulates localization within the cell and kinase activity (*14*). The protein-binding domain is essential for heterotrimer formation (*22*). The γ subunits possess four-tandem cystathionine β–synthase (CBS) motifs. CBS motifs bind to adenine nucleotides (*23*). Binding of AMP (adensine monophosphate) and ADP (adensine diphosphate), which compete with ATP (adensine triphosphate), stimulate AMPK kinase activity (*24*), and ADP stimulates SNF1 (*23*), but there is no evidence that either impacts SnRK1 activity (*13*).

Arabidopsis thaliana encodes three α subunits – SnRK1.1/AKIN10 (At3g01090), SnRK1.2/AKIN11 (At3g29160) (*25, 26*), and SnRK1.1T, an alternative intron-exon splicing of SnRK1.1 (*27*). SnRK1.1 and SnRK1.2 catalytic subunits are regulated by phosphorylation of the T- loop (*28*) at T175 and T176, respectively (*26*). Although, these homologs have similar kinase domains, they differ in the domain architecture of their C–termini (Fig. 2). Arabidopsis encodes two typical β subunits (β1 and β2) and one γ subunit (γ). Additionally, Arabidopsis encodes β3 and βγ subunits with atypical domain architecture (Fig. 2) that are unique to green algae and plants (*13*). The β3 subunit, which can rescue β deficient yeast lines, has only a C–terminal domain (*29*). The βγ subunit contains an N–terminal family 48 CBM, similar to the β subunits of SNF1 and AMPK. Contrary to its β like N-terminal domain, the βγ complements γ-deficient yeast (*30*). β1 and β2 are N–myristoylated, affecting subcellular localization (*31*). Despite having genes for two γ subunits, it has been demonstrated that only the βγ isoform participates in SnRK1 heterotrimeric complexes (*13*). Another difference between SnRK1 and AMPK/SNF1 is that SnRK1 βγ conserves only one of six amino acids for nucleotide binding, disrupting AMP binding and its regulation of SnRK1. SnRK1 is inhibited by a large heat-labile soluble proteinaceous factor, and SnRK1 CBMs associate with different carbohydrate than AMPK/SNF1 (*13*).

Bacterial artificial chromosomes fluorescence studies in plants showed that SnRK1 accumulates to high levels in the meristematic, elongating and differentiating zones of primary and lateral roots and leaf primordial (*19*). SnRK1 was found in the cytoplasm in ring-shaped structures around nuclei of cells in these tissues (*19*). However, in differentiated

epidermal cells of hypocotyls, leaves and sepals, SnRK1.1 was localized in the cytoplasm and at plasma membranes, while stomatal cells accumulated SnRK1 in nuclei (*19*). Detection of SnRK1.1 at the plasma membrane of different cell types is consistent with potential assembly of trimeric kinase complexes with membrane-bound myristoylated SnRK1 β1 and β2 (*19*). GFP-tagged SnRK1.1 accumulates in the cytoplasm of stigmas and pistils of young flowers, particularly in tip papillae cells of pistils and various cell types of stamens (*19*). GFP-tagged SnRK1.1 was also detected upon fertilization in developing embryos, but not in petals of flowers (*19*). SnRK1.1 is expressed throughout the seedling, but more abundantly in leaf primordia, vascular tissue, and root tips (*27*). In contrast, SnRK1.2 is only in the hydathodes, leaf primordia, and cotyledon vascular tissue of seedlings (*27*). SnRK1.1 and SnRK1.2 are found in the cytoplasm and nucleus, but SnRK1.1T is found in puncta after manual wounding (*27*).

SnRK1 is a metabolic sensor protein (*32*) and regulates several pathways. It plays a key role in environmental stress responses, global regulation of metabolism, energy conservation, antiviral defense and development (*20*). SnRK1 is regulated allosterically by metabolites (*33*), such as activation by 2-deoxyglucose (*34*) and sucrose (*35*) or deactivation by glucose-6-phosphate (*36*), or by phosphorylation of the T-loop (*28*). SnRK1.1 transcription is repressed by sucrose, glucose, fructose or mannitol, and SnRK1.2 expression increase in the presences of trehalose (*27*). Mathematical models indicated that SnRK1 protein concentrations do not need to vary for regulation by changing sugar concentration (*37*). SnRK1 plays a key role in abscisic acid (ABA) sensory pathways. Over-expressing

SnRK1.1 mutant plants are hypersensitive to ABA (*38*). ABI1 and PP2Cs (type 2 protein phosphotases) repress ABA pathways by interacting with and dephosphorylating SnRK1.1 (*39*). Additionally, 600 genes are either activated or repressed by SnRK1.1 (*26*). Many of these genes are also regulated by are microRNA pathways, such as miR319 (*40*). Seedlings over expressing SnRK1.1 display enhanced primary root growth and development in low light and inverse in high sucrose conditions relative to SnRK1.1 silenced lines (*26*) SnRK1.1 over-expressing lines are delayed in both flowering and the onset of senescence, down-regulated in expression of the sugar-induced gene FLZ (*41*), and reduced in size when grown in soil under long-day conditions (*26*). SnRK1.2 over-expressing mutants display early flowering and larger rosettes (*27*). Together, these observations indicate that SnRK1 plays a role in development.

SnRK1's roles in environmental responses are often linked to sugar responses. SnRK1 phosphorylates adenosine kinases, ADK1 and ADK2, to modulate the conversion of adenosine to AMP (*42*). SNRK1.1 also undermines the MYC2-dependent salt response (*43*) and phosphorylates cyclin-dependent kinase inhibitor $p27^{KIP1}$ homologues AtKRP6 and AtKRP7 (*44*).

SnRK1 is also thought to phosphorylate transcription factors to reprogram gene expression (*26, 45*). SnRK1.1 interacts with Petal Loss (PTL) (*46*), bZIP11 (*47*), bZIP63 (*48*), FUSCA3 (*49*), IDD8 (Indeterminate domain 8) (*50*), FUS5, JAZ3, and TOE2 (*27*). Both SnRK1.1 and SnRK1.2 interact with DUF581 transcription factor (*51*). FUSCA3 and IDD8 are both inactivated via phosphorylation by SnRK1 to delay flowering (*38, 50*).

The amino acid modified within a target protein is the site of phosphorylation and is part of a primary structure known as the consensus sequence or motif (*1*). Consensus sequences are a key part of kinase recognition and confer kinase specificity (*2*). However, regulation of phosphorylation is a complicated process, depending on the structure of the target protein, other phosphorylation events, and competition with other kinases modulating phosphorylation (*1*). There are two consensus motifs for SnRK1 predicted in the literature. A study performing semi-degenerate peptide array screening to determine putative substrates indicated that the SnRK1 consensus motif is LxRxxSxxxL (*2*). Meta-analysis of known SnRK1 phosphorylation sites indicated the consensus motif is xxxxxxSxx(D/E)xx, where x is any amino acid (*52*). However when comparing these consensus motifs to experimentally determined sites, such as -IGDFSVSQVFKD- (GRIK1 S261) (*28*), there are incongruities.

GRIK

Many signaling pathways contain kinases that are themselves phosphorylated. These series of kinases are known as phosphorylation cascades (*5*). In these cascades, one kinase is activated via phosphorylation and can in turn phosphorylated another target (*5*). Both AMPK and SNF1 are members of cascades (*12, 21*). AMPK is phosphorylated by LKB1 (Liver kinase B1) and CaMKKα (calcium/calmodulin-dependentprotein kinase kinase α) *(12)* and SNF1 is activated by PAK1/Tos3/ELM1 (*21*).

Pak1, Tos3, and Elm1 protein kinases contribute to activation of SNF1 *in vivo (53)*. Studies suggest that each of these kinases play distinct roles with respect to regulation of

SNF1 function. Pak1 specifically contributes to the nuclear enrichment of SNF1-Gal83 (*54*). SNF1-Gal83 is the only complex of the kinase that is enriched in the nucleus during glucose deficiency (*55*). Tos3 is the primary activator of SNF1 during growth on nonfermentable carbon sources, an important response for yeast in a natural environment (*56*). Elm1 regulates cell cycle progression, cell morphology, and filamentous invasive growth (*57*), which are not known functions of SNF1.

AMPK is activated by LKB1 or CAMKKα when ATP declines and AMP rises intercellularly (*12*), such as during nutrient deprivation or hypoxia (*58*). Biochemical and genetic studies in worms, flies and mice indicate that LKB1 is the major kinase that phosphorylates AMPKα (*59*). LKB1 also phosphorylates and activates other AMPK-related proteins, such as the microtubule-associated protein (MAP) and microtubule affinity-regulating kinase (MARK) family (*60*). These are homologs of the C. elegans PAR-1 kinase, which is a key part of early embryonic partitioning and polarity (*60*). CaMKKα, but not CaMKKβ, is also an upstream regulator of AMPK in nonmuscle cells (*12*) and skeletal muscle cells in mammals (*61*).

Although less is known about SnRK1 cascades, GRIK (geminivirus Rep *i*nteracting kinase) is a homolog of CaMKKα and PAK1/Tos3/ELM1 with 41-53% similarity (*62*). GRIK is a Ser/Thr kinase (*63*) with ATP- binding and catalytic domains (*62*). In Arabidopsis, there are two genes that code for GRIK1 (At3g45240) and GRIK2 (At5g60550). These GRIKs are 88% identical and 93% similarin amino acids (*62*). GRIK is activated by autophosphorylation (*64*). GRIK phosphorylates SnRK1 *in vitro* (*64, 65*) and GRIK can

rescue yeast *tos3pak1elm1* knockout mutants (*62*). In healthy plants, GRIK is found in young leaves, shoot apical meristem, leaf primordia, emerging petioles, flowers, buds, and siliques (*62*). CaMKKα, which phosphorylates AMPK, interacts and recruits substrates to AMPK, including transcription factors, for phosphorylation (*12*). Because GRIK is a homolog of CaMKKα, it may also interact with transcription factors that are substrates of SnRK1.

TCP Transcription Factors

In eukaryotes, transcription factors are proteins required to initiate or regulate transcription (*5*). Because of the direct effect of transcription factors have on gene expression, they are major components for phenotypic evolution (*66*). Transcription factors can play important roles in chromatin remodeling, cell division and differentiation, and cells tightly control transcription regulation (*67*). Eukaryotic transcription factors are divided into two categories based on their binding to the core promoter or to proximal/distal promoter elements (*68*). Factors that bind to proximal/distal promoter elements include DNA-binding proteins that specifically interact through a secondary structure (*68*). Members of the basic helix-loop-helix (bHLH) family of transcription factors are defined by a basic region that interacts directly with the DNA followed by two alpha helices connected by a disordered region that can dimerize (Fig. 4) (*69*).

SnRK1 deactivates FUSCA3 and IDD8 via phosphorylation (*38, 50*), setting a precedent for SnRK1 targeting and altering the activities of transcription factors. GRIK is a homolog of ELM1, an upstream regulator of SNF1 which interacts with transcription factors

(*70*). A yeast-two-hybrid screen of an Arabidopsis cDNA library using GRIK1 as bait (unpublished data) identified five transcription factors, three of which are members of the TCP family and candidates for SnRK1 phosphorylation.

TCP transcription factors constitute a family with a basic helix-loop-helix DNA binding domain (Fig. 4) (*71, 72*) that is specific to plant and fresh water algae (*73*). The name TCP is derived from teosinte branched 1 (TB1) from maize (*71*), cycloidea from Antirrhinum (*74*), and PROLIFERATING CELL FACTORS 1 (PCF1) and PCF2 from rice (*72*). TB1 controls apical dominance, sex determination and inflorescence(*75, 76*). Cycloidea (CyC) play a vital role in the formation of floral structure (*74*). PCF1 and PCF2 interact with the promoter region for PCNA (*72*), which is involved in DNA replication and repair, chromatin structure maintenance, chromosome segregation and cell-cycle progression (*77*). TCP family members are defined by the DNA binding domain, which is a 60-residue conserved region (*71*). The primary structure of the Arabidopsis TCP domain has an over representation of serine and alanine (*73*). The TCP DNA binding domain contains a sequence of 18 amino acids that is 80% similar between the 45 family members found in Arabidopsis and rice (*78*). Secondary structure predictions (see Fig. 4) indicate that helix I (dark and light green) extends to Pro-58 in the basic region and that most residues in the basic segment (dark green) are exposed with most of the buried residues on helix II (light green) (*79*). Outside of DNA binding domain, TCPs have no significant similarity to each other or any known motifs (*73*). TCPs interact with DNA as homo or heterodimers (*80*), although heterodimers appear to bind more efficiently (*81*). These dimers interact with a DNA sequence of 5´-GGNCC-3´ with

additional specificity to family members provided by surrounding nucleic acids (*81*). TCPs predominantly target nuclear genomes but also interact with organelle genomes (*82*).

TCPs are divided into two classes: Class I or the PCF class and Class II or the CyC/TB1 class (*77*). Class II TCPs can be divided into two subclades – the CIN clade and the CYC/TB1 clade or ECE clade (*82*). In Arabidopsis, there are 24 family members, 13 class I and 11 class II (*83*). The structural difference between these classes is a four-amino acid deletion in the basic domain of class I proteins (*77*). An analysis of 206 TCP domains in multiple species determined in 93% of cases the domain sequence starts with a Lys (*79*). Class I TCP domains ended with Ala for 85% of domains tested, with approximately 98% of the domain contain unique residue frequency, (URF) scores greater than 50%. Class II TCP domains had a 91% probability of ending with a Leu, with approximately 80% of the domains containing URF scores of greater than 50% (*79*). This suggests that TCP domains have a higher degree of similarity to each other than other transcription factors (*79*). Class I TCP have a conserved Cys at position 20, which is at the beginning of helix I in the HLH domain, and is thought to be responsible for redox sensitivity (*84*).

Class I TCPs predominantly control cell proliferation and growth (*77*). Light induction of Arabidopsis seedlings is associated with expression of class II in cotyledons and class I in shoot apical meristems (*85*). Phenotypic studies of repression mutants and over-expressing plants indicate that class II members regulate growth in different organs, mainly through the inhibition of cell proliferation or growth (*86*). Additionally, mRNA levels of

class I and class II are reported to be inversely expressed (*78*). TCPs also play important roles in hormone response and signaling (*87-90*).

Examples of class I members are TCP20 and TCP22 from Arabidopsis. TCP20 binds the promoter region of ribosomal proteins RPL24 and RPS27 (*91*), PCNA2, PS4, and CycB1;1 (*92*). TCP20 protein accumulates in areas of cell proliferation like embryos, root buds and tips, cotyledons and meristems (*92*). Expression of TCP20:EAR repressors causes delayed germination, drastic shoot arrest, hypocotyl calluses, and yellowing of cotyledons (*92*). TCP20 targets LIPOXYGENASE2 (LOX2) and TCP9 (*93*). TCP20 represses subgroup Ib bHLH expression (*94*). TCP20 binds the promoter region of two key components of the systemic signaling pathway for nitrate foraging, NIA1.1 and NRT2.1, mediating root response to nitrate concentrations (*95*). TCP20 interacts with the isochorismate synthaase 1 (ICS1) gene, which encodes the key enzyme in salicylic acid biosynthesis, and may regulate it along with TCP8 (*96*). In cross-sections of young leaves, it was indicated that GUS-tagged TCP22 was located at the surface of lateral organs (*97*). The *tcp7 tcp8 tcp22 tcp23* knockout mutants display weak phenotypes (*97*). These mutants showed changes in leaf development with reduced number of rosette leaves (*97*). The *tcp8 tcp14 tcp15 tcp22* knockout mutants exhibit dwarfism and reduced response to gibberellin (*98*).

Class II TCPs regulate organ growth, mainly through the inhibition of cell proliferation or growth (*86*). Examples of class II members are TCP3 and TCP18 from Arabidopsis. TCP3 is a AS2-interacting Class II member *(77).* AS2 represses class I KNOX genes and impacts the development of shoot apical meristems (*99*). TCP3SRDX, a repressor

of TCP3, plants have wavy, serrated leaves, small ectopic shoots on cotyledons and various defects in organ development. Expression of TCP3SRDX induced ectopic expression of the CUP-SHAPED COTYLEDON (CUC) genes, a boundary-specific gene (*100*). TCP3 interacts with R2R3-MYB effecting activation of flavanoid biosynthesis and control of early flavaniod biosynthesis (*101*). TCP18 or BRC1 is the Arabidopsis homolog of teosinte branched 1 and is expressed in axillary buds retarding their growth (*102*). Similar functions are observed for the homologues of TCP18 in maize (*75, 76*), tomato (*103*), and rice (*104*).

Regulation of TCPs is not well understood. The only report of post-transcriptional modification of a Class I TCP genes is phosphorylation of TCP8 (*105*). Reports of regulation of Class II members indicate that a subset of CIN-type genes are targets of the microRNA, miR319 (*106*). Class I TCPs and NAC transcription factors may also be regulated by miR319 (*107*). This microRNA, as well as others, is down regulated by SnRK1 during energy deficient periods (*40*). TCP4 regulates miR167, which is part of the miR159-miR167-miR319 circuit, indicating indirect TCP modulation of other TCP functions (*108*). Regulation of TCPs by protein interactions was recently shown. TCPs can be negatively regulated by PNM1, a transcription factor found in both the nucleus and mitochondria, and acts as a messenger from the mitochondria (*109*). TCP Interactor containing EAR motif protein (TIE1) modulates TCP activity, and when over-expressed causes curly leaves similar to miR319 over-expressing mutants (*110*). TCP5, TCP13, and TCP17 are also negatively regulated by RABBIT EARS (RBE) (*111*). Introns might also have regulatory roles in these genes (*77*).

SWI/SNF Chromatin Remodeling Complex

SWI/SNF (switch/sucrose non-fermentable) ATPases are conserved in yeast, animals, and plants (*112*). In plants, there are three types of SWI/SNF chromatin remodeling ATPases: BRAHMA (BRM), SPLAYED (SYD), and MINUSCULEs (MINU1 and MINU2) (*112-114*). Arabidopsis SWI/SNF complexes also contain an ortholog of SNF5/INI1, BUSHY (BSH) (*115*), two of the four orthologs of SWI3/BAF170/BAF155 (SWI3A, SWI3B, SWI3C, and SWI3D) (*116*), and one of the two possible orthologs of SWP73/BAF60 (SWP73A and SWP73B) (*114, 117*). The large protein complex is required for full activity *in vivo*. SWI/SNF complexes hydrolyze ATP to alter histone–DNA interactions (*117, 118*). The increase or decrease of accessibility of genomic DNA activates or represses transcription (*116, 119, 120*). SYD and BRM are recruited to DNA through physical interactions with transcription factors (*121*).

The SWI/SNF complexes play important roles in leaf development as seen for *brm* and *swi3c* mutants, which have rosette leaves that are strongly curled downward (*116, 120*). BRM and SYD up-regulate expression of CUC genes (*114*). This correlated with TCP3 functions (*100*). BRM plays a role in modulating 75% of flowering pathways in Arabidopsis, including the photoperiod, gibberellin, and autonomous pathways (*119, 120*). TCP22 plays a role in the gibberellin response (*98*). SnRK1 also regulates floral timing (*27*). These overlapping functions may indicate possible interactions with a GRIK-SnRK1 pathway through the TCPs. TCP4 arrests leaf growth and promotes maturation and interacts with

BRM and SWI3C (*122*). TCP4 interaction with BRM activates ARR16 gene expression, inhibiting cytokinin signaling. BRM and SWI3C have also been implicated in interactions with a few other TCP via a large library yeast two-hybrid study (*122*).

In this report, I asked if members of the TCP family are phosphorylation substrates of the GIRK-SnRK1 kinase cascade and mapped SnRK1 phosphorylation sites in TCP18, TCP20 and TCP22. I then asked if SnRK1 phosphorylation impacts the activities of TCP20 and TCP22 and performed a proteomic screen of SnRK1 phosphorylation sites in Arabidopsis proteins.

FIGURES

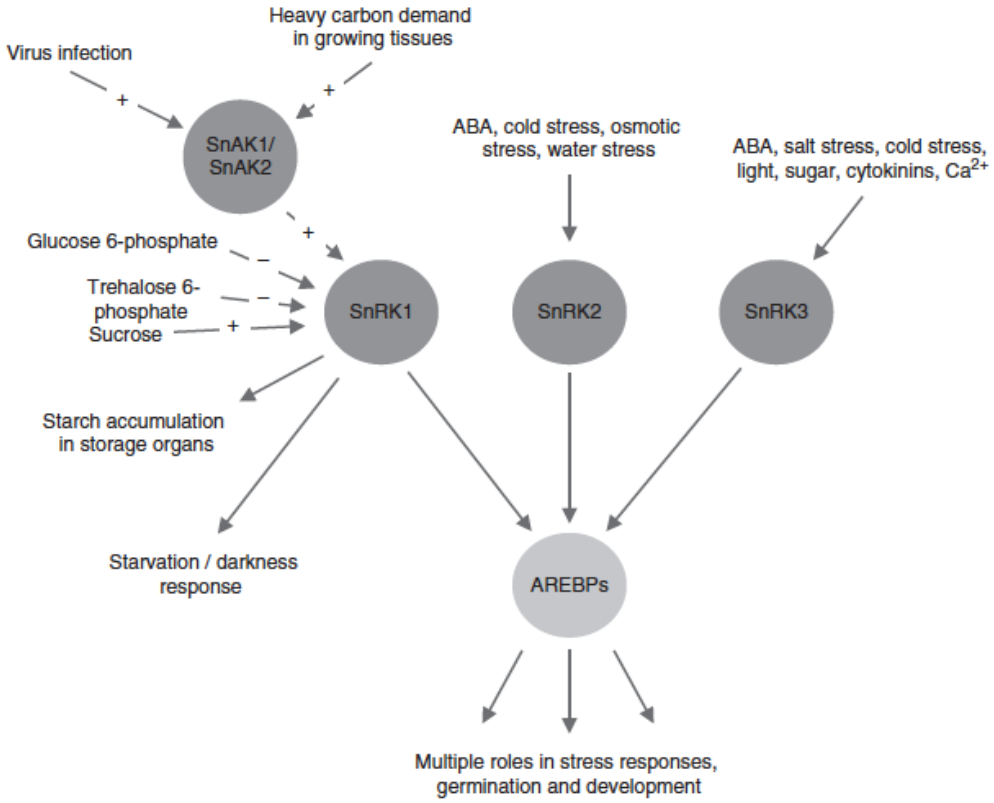

Figure 1. ABA response element binding proteins (AREBPs) as hubs at the interface between metabolic and stress signalling networks, potentially targeted for phosphorylation by all three SNF1-related protein kinases (SnRK1 to 3) and with multiple roles in stress responses, germination and development *(123)*. (Figure and legend from Hey et al 2010.)

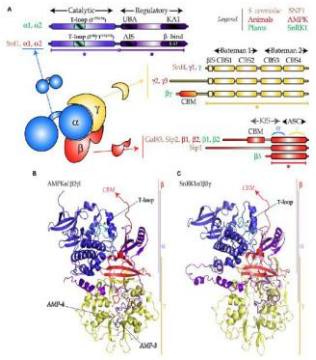

Figure 2. Heterotrimeric structure of the SNF1/AMPK/SnRK1 complexes,.(A) The α-subunit (in blue) is composed of a catalytic domain (in blue with the T-loop in cyan) and a autoinhibitory regulatory domain (in purple-blue), which encompasses an auto-inhibitory sequence (AIS) or an ubiquitin-associated (UBA) domain, and a kinase-associated (KA1) domain for binding the β- and γ-subunits. The γ-subunit (in yellow) is composed four CBS (cystathionine-β-synthase) domains and a β-interacting sequence (βIS). The AMPKγ2 and γ3 bear an N-terminal extension and the plant-specific SnRK1βγ possesses a carbohydrate binding module (CBM). The β-subunit (in red) harbors an ASC (association to the complex) domain, containing the sites of interaction with γ and α, a CBM and an N-terminal extension. The plant-specific SnRK1β3 is atypical as it does not possess the CBM or the N-terminal extension. (B) Cartoon representation of the 3D-structure (PDB:2Y94) of the AMPKα1β2γ1 complex. Asterisks designate parts in (A) that were crystallized. Arrows indicate missing parts (CBM), the T-loop, and the two AMP molecules. (C) 3D-structure model of SnRK1α1β1γ, generated with Swiss-Model using as template the AMPK structure presented in (B). Color code in (B,C) as described in (A). (*18*) (Figure and modified legend from Crozet et al. 2014.)

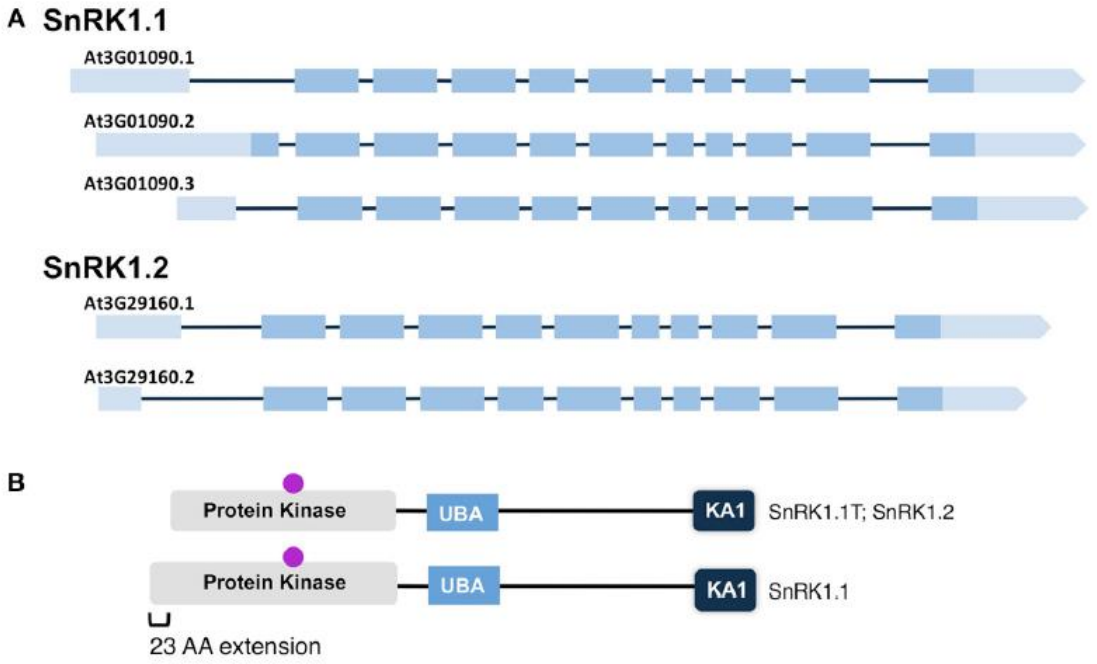

Figure 3. Maps of SnRK1 Isoforms and Domain Structures. A) The reported intron-exon maps of SnRK1 genes. Dark boxes denote exons while light boxes denote 5′ and 3′ UTRs. (B) SnRK1 kinases contain 3 domains: Protein Kinase, Ubiquitin Associated (UBA), and Kinase Associated1 (KA1). The location of the active site residues are indicated by a purple circle. *(27)* (Figure and legend from Williams et al. 2014)

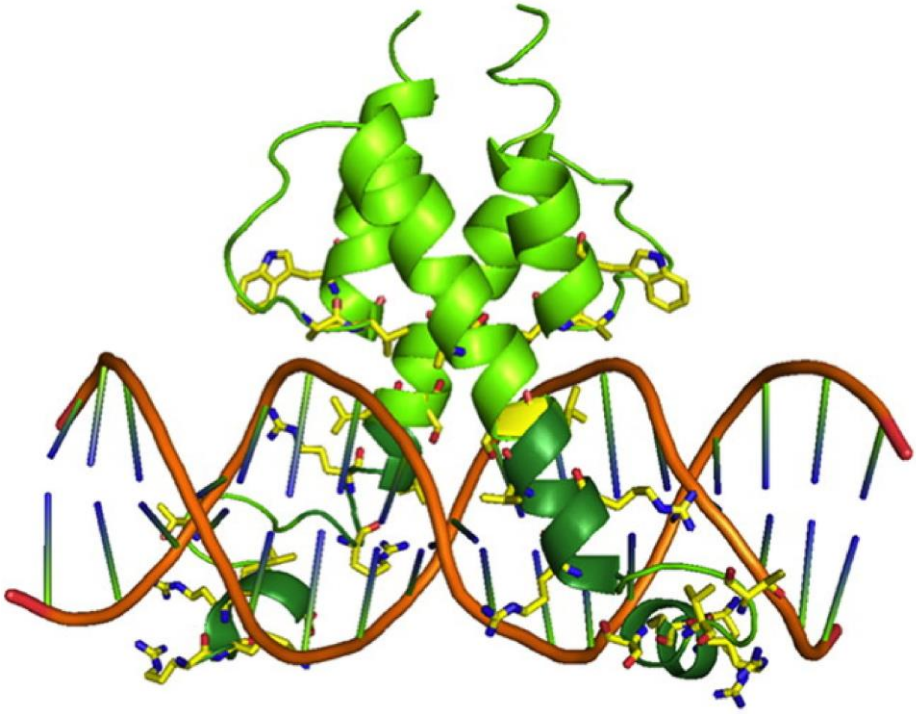

Figure 4. Modeling the Three-Dimensional Structure of the TCP4-DNA Complex. Model of TCP4 domain in dimer form bound to the B-form target DNA sequence GTGGTCCC (in orange). The basic domain is shown in dark green, and residues that interact with the DNA backbone are shown in yellow.*(79)* (Figure and legend from Aggarwal et al. 2010.)

REFERENCES

1. Nelson, D. L. (2005) *Lehninger Principles of Biochemistry*, 4th ed., W. H. Freeman and Company, New York, New York.

2. Vlad, F., Turk, B. E., Peynot, P., Leung, J., and Merlot, S. (2008) A versatile strategy to define the phosphorylation preferences of plant protein kinases and screen for putative substrates, *Plant J 55*, 104-117.

3. Hrabak, E. M., Chan, C. W., Gribskov, M., Harper, J. F., Choi, J. H., Halford, N., Kudla, J., Luan, S., Nimmo, H. G., Sussman, M. R., Thomas, M., Walker-Simmons, K., Zhu, J. K., and Harmon, A. C. (2003) The Arabidopsis CDPK-SnRK superfamily of protein kinases, *Plant Physiol 132*, 666-680.

4. Cohen, P. (2000) The regulation of protein function by multisite phosphorylation--a 25 year update, *Trends Biochem Sci 25*, 596-601.

5. Alberts, B. (2002) *Molecular biology of the cell*, 4th ed., Garland Science, New York.
6. Osakabe, Y., Yamaguchi-Shinozaki, K., Shinozaki, K., and Tran, L. S. (2013) Sensing the environment: key roles of membrane-localized kinases in plant perception and response to abiotic stress, *J Exp Bot 64*, 445-458.

7. Wang, D., Harper, J. F., and Gribskov, M. (2003) Systematic trans-genomic comparison of protein kinases between Arabidopsis and *Saccharomyces cerevisiae*, *Plant Physiol 132*, 2152-2165.

8. Manning, G., Whyte, D. B., Martinez, R., Hunter, T., and Sudarsanam, S. (2002) The protein kinase complement of the human genome, *Science 298*, 1912-1934.

9. Halford, N. G., Bouly, J. P., and Thomas, M. (2000) SNF1-related protein kinases (SnRKs): regulators at the heart of the control of carbon metabolism and partitioning, *Adv Bot Res*, 405-434.

10. Wang, P., Xue, L., Batelli, G., Lee, S., Hou, Y. J., Van Oosten, M. J., Zhang, H., Tao, W. A., and Zhu, J. K. (2014) Quantitative phosphoproteomics identifies SnRK2 protein kinase substrates and reveals the effectors of abscisic acid action, *Proc Natl Acad Sci U S A 110*, 11205-11210.

11. Zhou, X., Hao, H., Zhang, Y., Bai, Y., Zhu, W., Qin, Y., Yuan, F., Zhao, F., Wang, M., Hu, J., Xu, H., Guo, A., Zhao, H., Zhao, Y., Cao, C., Yang, Y., Schumaker, K. S., Guo, Y., and Xie, C. G. (2015) PKS5/CIPK11 Modulates ABA Signaling via ABI5, *Plant Physiology*.

12. Hawley, S. A., Pan, D. A., Mustard, K. J., Ross, L., Bain, J., Edelman, A. M., Frenguelli, B. G., and Hardie, D. G. (2005) Calmodulin-dependent protein kinase kinase-beta is an alternative upstream kinase for AMP-activated protein kinase, *Cell Metab 2*, 9-19.

13. Emanuelle, S., Hossain, M. I., Moller, I. E., Pedersen, H. L., van de Meene, A. M., Doblin, M. S., Koay, A., Oakhill, J. S., Scott, J. W., Willats, W. G., Kemp, B. E., Bacic, A., Gooley, P. R., and Stapleton, D. I. (2015) SnRK1 from *Arabidopsis thaliana* is an atypical AMPK, *Plant J 82*, 183-192.

14. Hedbacker, K., and Carlson, M. (2008) SNF1/AMPK pathways in yeast, *Front Biosci 13*, 2408-2420.

15. Hardie, D. G. (2007) AMP-activated/SNF1 protein kinases: conserved guardians of cellular energy, *Nat Rev Mol Cell Biol 8*, 774-785.

16. Kulma, A., Villadsen, D., Campbell, D. G., Meek, S. E., Harthill, J. E., Nielsen, T. H., and MacKintosh, C. (2004) Phosphorylation and 14-3-3 binding of Arabidopsis 6-phosphofructo-2-kinase/fructose-2,6-bisphosphatase, *Plant J 37*, 654-667.

17. Baena-Gonzalez, E., and Sheen, J. (2008) Convergent energy and stress signaling, *Trends Plant Sci 13*, 474-482.

18. Crozet, P., Margalha, L., Confraria, A., Rodrigues, A., Martinho, C., Adamo, M., Elias, C. A., and Baena-Gonzalez, E. (2014) Mechanisms of regulation of SNF1/AMPK/SnRK1 protein kinases, *Front Plant Sci 5*, 190.

19. Bitrian, M., Roodbarkelari, F., Horvath, M., and Koncz, C. (2011) BAC-recombineering for studying plant gene regulation: developmental control and cellular localization of SnRK1 kinase subunits, *Plant J 65*, 829-842.

20. Ghillebert, R., Swinnen, E., Wen, J., Vandesteene, L., Ramon, M., Norga, K., Rolland, F., and Winderickx, J. (2011) The AMPK/SNF1/SnRK1 fuel gauge and energy regulator: structure, function and regulation, *FEBS J 278*, 3978-3990.

21. Hong, S. P., Momcilovic, M., and Carlson, M. (2005) Function of mammalian LKB1 and Ca2+/calmodulin-dependent protein kinase kinase alpha as Snf1-activating kinases in yeast, *J Biol Chem 280*, 21804-21809.

22. Iseli, T. J., Walter, M., van Denderen, B. J., Katsis, F., Witters, L. A., Kemp, B. E., Michell, B. J., and Stapleton, D. (2005) AMP-activated protein kinase beta subunit

tethers alpha and gamma subunits via its C-terminal sequence (186-270), *J Biol Chem 280*, 13395-13400.

23. Mayer, F. V., Heath, R., Underwood, E., Sanders, M. J., Carmena, D., McCartney, R. R., Leiper, F. C., Xiao, B., Jing, C., Walker, P. A., Haire, L. F., Ogrodowicz, R., Martin, S. R., Schmidt, M. C., Gamblin, S. J., and Carling, D. (2011) ADP regulates SNF1, the *Saccharomyces cerevisiae* homolog of AMP-activated protein kinase, *Cell Metab 14*, 707-714.

24. Gowans, G. J., Hawley, S. A., Ross, F. A., and Hardie, D. G. (2013) AMP is a true physiological regulator of AMP-activated protein kinase by both allosteric activation and enhancing net phosphorylation, *Cell Metab 18*, 556-566.

25. Polge, C., and Thomas, M. (2007) SNF1/AMPK/SnRK1 kinases, global regulators at the heart of energy control?, *Trends Plant Sci 12*, 20-28.

26. Baena-Gonzalez, E., Rolland, F., Thevelein, J. M., and Sheen, J. (2007) A central integrator of transcription networks in plant stress and energy signalling, *Nature 448*, 938-942.

27. Williams, S. P., Rangarajan, P., Donahue, J. L., Hess, J. E., and Gillaspy, G. E. (2014) Regulation of Sucrose non-Fermenting Related Kinase 1 genes in *Arabidopsis thaliana, Front Plant Sci 5*, 324.

28. Shen, W., Reyes, M. I., and Hanley-Bowdoin, L. (2009) Arabidopsis protein kinases GRIK1 and GRIK2 specifically activate SnRK1 by phosphorylating its activation loop, *Plant Physiol 150*, 996-1005.

29. Polge, C., Jossier, M., Crozet, P., Gissot, L., and Thomas, M. (2008) Beta-subunits of the SnRK1 complexes share a common ancestral function together with expression and function specificities; physical interaction with nitrate reductase specifically occurs via AKINbeta1-subunit, *Plant Physiol 148*, 1570-1582.

30. Lumbreras, V., Alba, M. M., Kleinow, T., Koncz, C., and Pages, M. (2001) Domain fusion between SNF1-related kinase subunits during plant evolution, *EMBO Rep 2*, 55-60.

31. Pierre, M., Traverso, J. A., Boisson, B., Domenichini, S., Bouchez, D., Giglione, C., and Meinnel, T. (2007) N-myristoylation regulates the SnRK1 pathway in Arabidopsis, *Plant Cell 19*, 2804-2821.

32. Tome, F., Nagele, T., Adamo, M., Garg, A., Marco-Llorca, C., Nukarinen, E., Pedrotti, L., Peviani, A., Simeunovic, A., Tatkiewicz, A., Tomar, M., and Gamm, M. (2014) The low energy signaling network, *Front Plant Sci 5*, 353.

33. Nunes, C., Primavesi, L. F., Patel, M. K., Martinez-Barajas, E., Powers, S. J., Sagar, R., Fevereiro, P. S., Davis, B. G., and Paul, M. J. (2013) Inhibition of SnRK1 by metabolites: tissue-dependent effects and cooperative inhibition by glucose 1-phosphate in combination with trehalose 6-phosphate, *Plant Physiol Biochem 63*, 89-98.

34. Harthill, J. E., Meek, S. E., Morrice, N., Peggie, M. W., Borch, J., Wong, B. H., and Mackintosh, C. (2006) Phosphorylation and 14-3-3 binding of Arabidopsis trehalose-phosphate synthase 5 in response to 2-deoxyglucose, *Plant J 47*, 211-223.

35. Bhalerao, R. P., Salchert, K., Bako, L., Okresz, L., Szabados, L., Muranaka, T., Machida, Y., Schell, J., and Koncz, C. (1999) Regulatory interaction of PRL1 WD protein with Arabidopsis SNF1-like protein kinases, *Proc Natl Acad Sci U S A 96*, 5322-5327.

36. Toroser, D., Plaut, Z., and Huber, S. C. (2000) Regulation of a plant SNF1-related protein kinase by glucose-6-phosphate, *Plant Physiol 123*, 403-412.

37. Nagele, T., and Weckwerth, W. (2014) Mathematical modeling reveals that metabolic feedback regulation of SnRK1 and hexokinase is sufficient to control sugar homeostasis from energy depletion to full recovery, *Front Plant Sci 5*, 365.

38. Tsai, A. Y., and Gazzarrini, S. (2012) Overlapping and distinct roles of AKIN10 and FUSCA3 in ABA and sugar signaling during seed germination, *Plant Signal Behav 7*, 1238-1242.

39. Rodrigues, A., Adamo, M., Crozet, P., Margalha, L., Confraria, A., Martinho, C., Elias, A., Rabissi, A., Lumbreras, V., Gonzalez-Guzman, M., Antoni, R., Rodriguez, P. L., and Baena-Gonzalez, E. (2013) ABI1 and PP2CA phosphatases are negative regulators of Snf1-related protein kinase1 signaling in Arabidopsis, *Plant Cell 25*, 3871-3884.

40. Confraria, A., Martinho, C., Elias, A., Rubio-Somoza, I., and Baena-Gonzalez, E. (2013) miRNAs mediate SnRK1-dependent energy signaling in Arabidopsis, *Front Plant Sci 4*, 197.

41. Jamsheer, K. M., and Laxmi, A. (2015) Expression of Arabidopsis FCS-Like Zinc finger genes is differentially regulated by sugars, cellular energy level, and abiotic stress, *Front Plant Sci 6*, 746.

42. Mohannath, G., Jackel, J. N., Lee, Y. H., Buchmann, R. C., Wang, H., Patil, V., Adams, A. K., and Bisaro, D. M. (2014) A complex containing SNF1-related kinase (SnRK1) and adenosine kinase in Arabidopsis, *PLoS One 9*, e87592.

43. Im, J. H., Cho, Y. H., Kim, G. D., Kang, G. H., Hong, J. W., and Yoo, S. D. (2014) Inverse modulation of the energy sensor Snf1-related protein kinase 1 on hypoxia adaptation and salt stress tolerance in *Arabidopsis thaliana*, *Plant Cell Environ 37*, 2303-2312.

44. Guerinier, T., Millan, L., Crozet, P., Oury, C., Rey, F., Valot, B., Mathieu, C., Vidal, J., Hodges, M., Thomas, M., and Glab, N. (2013) Phosphorylation of p27(KIP1) homologs KRP6 and 7 by SNF1-related protein kinase-1 links plant energy homeostasis and cell proliferation, *Plant J 75*, 515-525.

45. Shen, Q., Liu, Z., Song, F., Xie, Q., Hanley-Bowdoin, L., and Zhou, X. (2011) Tomato SlSnRK1 protein interacts with and phosphorylates betaC1, a pathogenesis protein encoded by a geminivirus beta-satellite, *Plant Physiol 157*, 1394-1406.

46. O'Brien, M., Kaplan-Levy, R. N., Quon, T., Sappl, P. G., and Smyth, D. R. (2015) PETAL LOSS, a trihelix transcription factor that represses growth in *Arabidopsis thaliana*, binds the energy-sensing SnRK1 kinase AKIN10, *J Exp Bot 66*, 2475-2485.

47. Ma, J., Hanssen, M., Lundgren, K., Hernandez, L., Delatte, T., Ehlert, A., Liu, C. M., Schluepmann, H., Droge-Laser, W., Moritz, T., Smeekens, S., and Hanson, J. (2011) The sucrose-regulated Arabidopsis transcription factor bZIP11 reprograms metabolism and regulates trehalose metabolism, *New Phytol 191*, 733-745.

48. Mair, A., Pedrotti, L., Wurzinger, B., Anrather, D., Simeunovic, A., Weiste, C., Valerio, C., Dietrich, K., Kirchler, T., Nagele, T., Vicente Carbajosa, J., Hanson, J., Baena-Gonzalez, E., Chaban, C., Weckwerth, W., Droge-Laser, W., and Teige, M. (2015) SnRK1-triggered switch of bZIP63 dimerization mediates the low-energy response in plants, *Elife 4*.

49. Tsai, A. Y., and Gazzarrini, S. (2012) AKIN10 and FUSCA3 interact to control lateral organ development and phase transitions in Arabidopsis, *Plant J 69*, 809-821.

50. Jeong, E. Y., Seo, P. J., Woo, J. C., and Park, C. M. (2015) AKIN10 delays flowering by inactivating IDD8 transcription factor through protein phosphorylation in Arabidopsis, *BMC Plant Biol 15*, 110.

51. Nietzsche, M., Schiessl, I., and Bornke, F. (2014) The complex becomes more complex: protein-protein interactions of SnRK1 with DUF581 family proteins provide a framework for cell- and stimulus type-specific SnRK1 signaling in plants, *Front Plant Sci 5*, 54.

52. van Wijk, K. J., Friso, G., Walther, D., and Schulze, W. X. (2014) Meta-Analysis of *Arabidopsis thaliana* Phospho-Proteomics Data Reveals Compartmentalization of Phosphorylation Motifs, *Plant Cell 26*, 2367-2389.

53. Sutherland, C. M., Hawley, S. A., McCartney, R. R., Leech, A., Stark, M. J., Schmidt, M. C., and Hardie, D. G. (2003) Elm1p is one of three upstream kinases for the *Saccharomyces cerevisiae* SNF1 complex, *Curr Biol 13*, 1299-1305.

54. Hedbacker, K., Hong, S. P., and Carlson, M. (2004) Pak1 protein kinase regulates activation and nuclear localization of Snf1-Gal83 protein kinase, *Mol Cell Biol 24*, 8255-8263.

55. Vincent, O., Townley, R., Kuchin, S., and Carlson, M. (2001) Subcellular localization of the Snf1 kinase is regulated by specific beta subunits and a novel glucose signaling mechanism, *Genes Dev 15*, 1104-1114.

56. Kim, M. D., Hong, S. P., and Carlson, M. (2005) Role of Tos3, a Snf1 protein kinase kinase, during growth of *Saccharomyces cerevisiae* on nonfermentable carbon sources, *Eukaryot Cell 4*, 861-866.

57. Sreenivasan, A., Bishop, A. C., Shokat, K. M., and Kellogg, D. R. (2003) Specific inhibition of Elm1 kinase activity reveals functions required for early G1 events, *Mol Cell Biol 23*, 6327-6337.

58. Shackelford, D. B., and Shaw, R. J. (2009) The LKB1-AMPK pathway: metabolism and growth control in tumour suppression, *Nat Rev Cancer 9*, 563-575.

59. Carling, D., Sanders, M. J., and Woods, A. (2008) The regulation of AMP-activated protein kinase by upstream kinases, *Int J Obes (Lond) 32 Suppl 4*, S55-59.

60. Watts, J. L., Morton, D. G., Bestman, J., and Kemphues, K. J. (2000) The *C. elegans* par-4 gene encodes a putative serine-threonine kinase required for establishing embryonic asymmetry, *Development 127*, 1467-1475.

61. Witczak, C. A., Fujii, N., Hirshman, M. F., and Goodyear, L. J. (2007) Ca2+/calmodulin-dependent protein kinase kinase-alpha regulates skeletal muscle glucose uptake independent of AMP-activated protein kinase and Akt activation, *Diabetes 56*, 1403-1409.

62. Shen, W., and Hanley-Bowdoin, L. (2006) Geminivirus infection up-regulates the expression of two Arabidopsis protein kinases related to yeast SNF1- and mammalian AMPK-activating kinases, *Plant Physiol 142*, 1642-1655.

63. Hanks, S. K., and Hunter, T. (1995) Protein kinases 6. The eukaryotic protein kinase superfamily: kinase (catalytic) domain structure and classification, *FASEB J 9*, 576-596.

64. Crozet, P., Margalha, L., Confraria, A., Rodrigues, A., Martinho, C., Adamo, M., Elias, C. A., and Baena-Gonzalez, E. (2010) Mechanisms of regulation of SNF1/AMPK/SnRK1 protein kinases, *Front Plant Sci 5*, 190.

65. Halford, N. G., and Hey, S. J. (2009) Snf1-related protein kinases (SnRKs) act within an intricate network that links metabolic and stress signalling in plants, *Biochem J 419*, 247-259.

66. Wray, G. A. (2003) Transcriptional regulation and the evolution of development, *Int J Dev Biol 47*, 675-684.

67. Masuda, H. P., Cabral, L. M., De Veylder, L., Tanurdzic, M., de Almeida Engler, J., Geelen, D., Inze, D., Martienssen, R. A., Ferreira, P. C., and Hemerly, A. S. (2008) ABAP1 is a novel plant Armadillo BTB protein involved in DNA replication and transcription, *EMBO J 27*, 2746-2756.

68. Tan, S., and Richmond, T. J. (1998) Eukaryotic transcription factors, *Curr Opin Struct Biol 8*, 41-48.

69. Atchley, W. R., and Fitch, W. M. (1997) A natural classification of the basic helix-loop-helix class of transcription factors, *Proc Natl Acad Sci U S A 94*, 5172-5176.

70. Manderson, E. N., Malleshaiah, M., and Michnick, S. W. (2008) A novel genetic screen implicates Elm1 in the inactivation of the yeast transcription factor SBF, *PLoS One 3*, e1500.

71. Cubas, P., Lauter, N., Doebley, J., and Coen, E. (1999) The TCP domain: a motif found in proteins regulating plant growth and development, *Plant J 18*, 215-222.

72. Kosugi, S., and Ohashi, Y. (1997) PCF1 and PCF2 specifically bind to cis elements in the rice proliferating cell nuclear antigen gene, *Plant Cell 9*, 1607-1619.

73. Navaud, O., Dabos, P., Carnus, E., Tremousaygue, D., and Herve, C. (2007) TCP transcription factors predate the emergence of land plants, *J Mol Evol 65*, 23-33.

74. Luo, D., Carpenter, R., Vincent, C., Copsey, L., and Coen, E. (1996) Origin of floral asymmetry in Antirrhinum, *Nature 383*, 794-799.

75. Doebley, J., Stec, A., and Gustus, C. (1995) teosinte branched1 and the origin of maize: evidence for epistasis and the evolution of dominance, *Genetics 141*, 333-346.

76. Doebley, J., Stec, A., and Hubbard, L. (1997) The evolution of apical dominance in maize, *Nature 386*, 485-488.

77. Martin-Trillo, M., and Cubas, P. (2010) TCP genes: a family snapshot ten years later, *Trends Plant Sci 15*, 31-39.

78. Yao, X., Mal, H., Wang, J., and Zhang, D. (2007) Genome- Wide Comparative Analysis and Expression Pattern of TCP Gene Families in *Arabidopsis thaliana* and *Oryza sativa*, *Journal of Integrative Plant Biology 49*, 885−897.

79. Aggarwal, P., Das Gupta, M., Joseph, A. P., Chatterjee, N., Srinivasan, N., and Nath, U. (2010) Identification of specific DNA binding residues in the TCP family of transcription factors in Arabidopsis, *Plant Cell 22*, 1174-1189.

80. Jonsson, Z. O., and Hubscher, U. (1997) Proliferating cell nuclear antigen: more than a clamp for DNA polymerases, *Bioessays 19*, 967-975.

81. Kosugi, S., and Ohashi, Y. (2002) DNA binding and dimerization specificity and potential targets for the TCP protein family, *Plant J 30*, 337-348.

82. Damerval, C., Le Guilloux, M., Jager, M., and Charon, C. (2007) Diversity and evolution of CYCLOIDEA-like TCP genes in relation to flower development in Papaveraceae, *Plant Physiol 143*, 759-772.

83. Cubas, P., Coen, E., and Zapater, J. M. (2001) Ancient asymmetries in the evolution of flowers, *Curr Biol 11*, 1050-1052.

84. Viola, I. L., Guttlein, L. N., and Gonzalez, D. H. (2013) Redox modulation of plant developmental regulators from the class I TCP transcription factor family, *Plant Physiol 162*, 1434-1447.

85. Lopez-Juez, E., Dillon, E., Magyar, Z., Khan, S., Hazeldine, S., de Jager, S. M., Murray, J. A., Beemster, G. T., Bogre, L., and Shanahan, H. (2008) Distinct light-initiated gene expression and cell cycle programs in the shoot apex and cotyledons of Arabidopsis, *Plant Cell 20*, 947-968.

86. Viola, I. L., Uberti Manassero, N. G., Ripoll, R., and Gonzalez, D. H. (2011) The Arabidopsis class I TCP transcription factor AtTCP11 is a developmental regulator with distinct DNA-binding properties due to the presence of a threonine residue at position 15 of the TCP domain, *Biochem J 435*, 143-155.

87. Gonzalez, N., De Bodt, S., Sulpice, R., Jikumaru, Y., Chae, E., Dhondt, S., Van Daele, T., De Milde, L., Weigel, D., Kamiya, Y., Stitt, M., Beemster, G. T., and Inze, D. (2010) Increased leaf size: different means to an end, *Plant Physiol 153*, 1261-1279.

88. Guo, Z., Fujioka, S., Blancaflor, E. B., Miao, S., Gou, X., and Li, J. (2010) TCP1 modulates brassinosteroid biosynthesis by regulating the expression of the key biosynthetic gene DWARF4 in *Arabidopsis thaliana*, *Plant Cell 22*, 1161-1173.

89. Rueda-Romero, P., Barrero-Sicilia, C., Gomez-Cadenas, A., Carbonero, P., and Onate-Sanchez, L. (2012) *Arabidopsis thaliana* DOF6 negatively affects germination in non-after-ripened seeds and interacts with TCP14, *J Exp Bot 63*, 1937-1949.

90. Yanai, O., Shani, E., Russ, D., and Ori, N. (2011) Gibberellin partly mediates LANCEOLATE activity in tomato, *Plant J 68*, 571-582.

91. Li, C., Potuschak, T., Colon-Carmona, A., Gutierrez, R. A., and Doerner, P. (2005) Arabidopsis TCP20 links regulation of growth and cell division control pathways, *Proc Natl Acad Sci U S A 102*, 12978-12983.

92. Herve, C., Dabos, P., Bardet, C., Jauneau, A., Auriac, M. C., Ramboer, A., Lacout, F., and Tremousaygue, D. (2009) *In vivo* interference with AtTCP20 function induces severe plant growth alterations and deregulates the expression of many genes important for development, *Plant Physiol 149*, 1462-1477.

93. Danisman, S., van der Wal, F., Dhondt, S., Waites, R., de Folter, S., Bimbo, A., van Dijk, A. D., Muino, J. M., Cutri, L., Dornelas, M. C., Angenent, G. C., and Immink, R. G. (2012) Arabidopsis class I and class II TCP transcription factors regulate

jasmonic acid metabolism and leaf development antagonistically, *Plant Physiol 159*, 1511-1523.

94. Andriankaja, M. E., Danisman, S., Mignolet-Spruyt, L. F., Claeys, H., Kochanke, I., Vermeersch, M., De Milde, L., De Bodt, S., Storme, V., Skirycz, A., Maurer, F., Bauer, P., Muhlenbock, P., Van Breusegem, F., Angenent, G. C., Immink, R. G., and Inze, D. (2014) Transcriptional coordination between leaf cell differentiation and chloroplast development established by TCP20 and the subgroup Ib bHLH transcription factors, *Plant Mol Biol 85*, 233-245.

95. Guan, P., Wang, R., Nacry, P., Breton, G., Kay, S. A., Pruneda-Paz, J. L., Davani, A., and Crawford, N. M. (2014) Nitrate foraging by Arabidopsis roots is mediated by the transcription factor TCP20 through the systemic signaling pathway, *Proc Natl Acad Sci U S A 111*, 15267-15272.

96. Wang, X., Gao, J., Zhu, Z., Dong, X., Wang, X., Ren, G., Zhou, X., and Kuai, B. (2015) TCP transcription factors are critical for the coordinated regulation of isochorismate synthase 1 expression in *Arabidopsis thaliana*, *Plant J 82*, 151-162.

97. Aguilar-Martinez, J. A., and Sinha, N. (2013) Analysis of the role of Arabidopsis class I TCP genes AtTCP7, AtTCP8, AtTCP22, and AtTCP23 in leaf development, *Front Plant Sci 4*, 406.

98. Daviere, J. M., Wild, M., Regnault, T., Baumberger, N., Eisler, H., Genschik, P., and Achard, P. (2014) Class I TCP-DELLA interactions in inflorescence shoot apex determine plant height, *Curr Biol 24*, 1923-1928.

99. Li, Z., Li, B., Shen, W. H., Huang, H., and Dong, A. (2012) TCP transcription factors interact with AS2 in the repression of class-I KNOX genes in *Arabidopsis thaliana*, *Plant J 71*, 99-107.

100. Koyama, T., Furutani, M., Tasaka, M., and Ohme-Takagi, M. (2007) TCP transcription factors control the morphology of shoot lateral organs via negative regulation of the expression of boundary-specific genes in Arabidopsis, *Plant Cell 19*, 473-484.

101. Li, S., and Zachgo, S. (2013) TCP3 interacts with R2R3-MYB proteins, promotes flavonoid biosynthesis and negatively regulates the auxin response in *Arabidopsis thaliana*, *Plant J 76*, 901-913.

102. Aguilar-Martinez, J. A., Poza-Carrion, C., and Cubas, P. (2007) Arabidopsis BRANCHED1 acts as an integrator of branching signals within axillary buds, *Plant Cell 19*, 458-472.

103. Parapunova, V., Busscher, M., Busscher-Lange, J., Lammers, M., Karlova, R., Bovy, A. G., Angenent, G. C., and de Maagd, R. A. (2014) Identification, cloning and characterization of the tomato TCP transcription factor family, *BMC Plant Biol 14*, 157.

104. De Paolo, S., Gaudio, L., and Aceto, S. (2015) Analysis of the TCP genes expressed in the inflorescence of the orchid Orchis italica, *Sci Rep 5*, 16265.

105. Valsecchi, I., Guittard-Crilat, E., Maldiney, R., Habricot, Y., Lignon, S., Lebrun, R., Miginiac, E., Ruelland, E., Jeannette, E., and Lebreton, S. (2013) The intrinsically disordered C-terminal region of *Arabidopsis thaliana* TCP8 transcription factor acts both as a transactivation and self-assembly domain, *Mol Biosyst 9*, 2282-2295.

106. Nag, A., King, S., and Jack, T. (2009) miR319a targeting of TCP4 is critical for petal growth and development in Arabidopsis, *Proc Natl Acad Sci U S A 106*, 22534-22539.

107. Zhou, M., Li, D., Li, Z., Hu, Q., Yang, C., Zhu, L., and Luo, H. (2013) Constitutive expression of a miR319 gene alters plant development and enhances salt and drought tolerance in transgenic creeping bentgrass (*Agrostis stolonifera L.*), *Plant Physiol*.

108. Rubio-Somoza, I., and Weigel, D. (2013) Coordination of flower maturation by a regulatory circuit of three microRNAs, *PLoS genetics 9*, e1003374.

109. Hammani, K., Gobert, A., Small, I., and Giege, P. (2011) A PPR protein involved in regulating nuclear genes encoding mitochondrial proteins?, *Plant Signal Behav 6*, 748-750.

110. Tao, Q., Guo, D., Wei, B., Zhang, F., Pang, C., Jiang, H., Zhang, J., Wei, T., Gu, H., Qu, L. J., and Qin, G. (2013) The TIE1 transcriptional repressor links TCP transcription factors with TOPLESS/TOPLESS-RELATED corepressors and modulates leaf development in Arabidopsis, *Plant Cell 25*, 421-437.

111. Huang, T., and Irish, V. F. (2015) Temporal Control of Plant Organ Growth by TCP Transcription Factors, *Curr Biol 25*, 1765-1770.

112. Flaus, A., Martin, D. M., Barton, G. J., and Owen-Hughes, T. (2006) Identification of multiple distinct Snf2 subfamilies with conserved structural motifs, *Nucleic Acids Res 34*, 2887-2905.

113. Sang, Y., Silva-Ortega, C. O., Wu, S., Yamaguchi, N., Wu, M. F., Pfluger, J., Gillmor, C. S., Gallagher, K. L., and Wagner, D. (2012) Mutations in two non-canonical Arabidopsis SWI2/SNF2 chromatin remodeling ATPases cause embryogenesis and stem cell maintenance defects, *Plant J 72*, 1000-1014.

114. Kwon, C. S., and Wagner, D. (2007) Unwinding chromatin for development and growth: a few genes at a time, *Trends Genet 23*, 403-412.

115. Brzeski, J., Podstolski, W., Olczak, K., and Jerzmanowski, A. (1999) Identification and analysis of the *Arabidopsis thaliana* BSH gene, a member of the SNF5 gene family, *Nucleic Acids Res 27*, 2393-2399.

116. Sarnowski, T. J., Rios, G., Jasik, J., Swiezewski, S., Kaczanowski, S., Li, Y., Kwiatkowska, A., Pawlikowska, K., Kozbial, M., Kozbial, P., Koncz, C., and Jerzmanowski, A. (2005) SWI3 subunits of putative SWI/SNF chromatin-remodeling complexes play distinct roles during Arabidopsis development, *Plant Cell 17*, 2454-2472.

117. Hargreaves, D. C., and Crabtree, G. R. (2011) ATP-dependent chromatin remodeling: genetics, genomics and mechanisms, *Cell Res 21*, 396-420.

118. Clapier, C. R., and Cairns, B. R. (2009) The biology of chromatin remodeling complexes, *Annu Rev Biochem 78*, 273-304.

119. Farrona, S., Hurtado, L., March-Diaz, R., Schmitz, R. J., Florencio, F. J., Turck, F., Amasino, R. M., and Reyes, J. C. (2011) Brahma is required for proper expression of the floral repressor FLC in Arabidopsis, *PLoS One 6*, e17997.

120. Archacki, R., Buszewicz, D., Sarnowski, T. J., Sarnowska, E., Rolicka, A. T., Tohge, T., Fernie, A. R., Jikumaru, Y., Kotlinski, M., Iwanicka-Nowicka, R., Kalisiak, K., Patryn, J., Halibart-Puzio, J., Kamiya, Y., Davis, S. J., Koblowska, M. K., and Jerzmanowski, A. (2009) BRAHMA ATPase of the SWI/SNF chromatin remodeling complex acts as a positive regulator of gibberellin-mediated responses in arabidopsis, *PLoS One 8*, e58588.

121. Wu, M. F., Sang, Y., Bezhani, S., Yamaguchi, N., Han, S. K., Li, Z., Su, Y., Slewinski, T. L., and Wagner, D. (2012) SWI2/SNF2 chromatin remodeling ATPases overcome polycomb repression and control floral organ identity with the LEAFY and SEPALLATA3 transcription factors, *Proc Natl Acad Sci U S A 109*, 3576-3581.

122. Efroni, I., Han, S. K., Kim, H. J., Wu, M. F., Steiner, E., Birnbaum, K. D., Hong, J. C., Eshed, Y., and Wagner, D. (2013) Regulation of leaf maturation by chromatin-mediated modulation of cytokinin responses, *Developmental cell 24*, 438-445.

123. Hey, S. J., Byrne, E., and Halford, N. G. (2010) The interface between metabolic and stress signalling, *Ann Bot 105*, 197-203.

124. Danisman, S., van Dijk, A. D., Bimbo, A., van der Wal, F., Hennig, L., de Folter, S., Angenent, G. C., and Immink, R. G. (2013) Analysis of functional redundancies within the Arabidopsis TCP transcription factor family, *J Exp Bot 64*, 5673-5685.

CHAPTER II

Embryonic Phenotypes of *grik1-grik2* Knockout Mutants

INTRODUCTION

Phosphorylation, a posttranslational modification that is often a key regulator of signal transduction and regulatory pathways in all eukaryotes (*1*, *2*), is the attachment of a phosphate group to tyrosine, serine, or threonine by protein kinases (*3*). It is hypothesized that approximately 30% of the proteins in a living organism are phosphorylated at any given time, most frequently on serine and threonine (*4*). These covalent bonds are formed by kinases and broken by phosphatases (*3*).

Geminivirus Rep Interacting Kinase (GRIK), as discussed in chapter I, is a plant homolgue to LKB1 and CaMKKα from animals (*5*) and PAK1/Tos3/ELM1 kinases in yeast (*6*), which are the upstream activators of AMPK and SNF1, respectively (*7*). GRIK is a Ser/Thr kinase (*8*) with ATP binding and catalytic domains (*7*). In Arabidopsis there are two genes that code for GRIK; GRIK1 (At3g45240) and GRIK2 (At5g60550). The GRIKs are 88% identical and 93% similar in amino acids (*7*). GRIK is activated via autophosphorlytion (*9*) and is phosphorylated by SnRK1 *in vitro* (*9, 10*). GRIK also rescues *tos3pak1elm1* knockout mutants (*7*).

In healthy plants, GRIK mRNA is expressed ubiquitously but GRIK protein is only found in young leaves, shoot apical meristem, leaf primordia, emerging petioles, flowers, buds, and maybe siliques (*7*). GRIK protein levels are regulated by protein degradation via the 26S proteasome pathway. Further studies are required to determine the exact function of GRIK in plants. Here I endeavor to determine if there is a phenotype of a *grik1grik2* double knockout mutant during embryo development.

MATERIALS AND METHODS

Development of *grik1 grik2* Double Knockout Mutants

Generation and verification of *grik1grik2* double knockout mutants were performed by Wei Shen. Two *grik1 grik2* double mutants CR1 and CR2, were made by crossing Arabidopsis Col-0 lines of T-DNA insertional mutation of either *grik1* or *grik2* (Fig. 1) and screening for homozygotes in the F2 plants from self-fertilization of F1 plants. CR1 is from a crossing between SALK_142938-3 (*grik1-1*) and SALK_015230-1 (*grik2-1*); CR2 is from a crossing between SALK_142938-3 (*grik1-1*) and SALK_000044-1 (*grik2-2*). The double mutations were screened for by PCR to locate T-DNA insertion at the *grik1* or *grik2* locus on leaf genomic DNA with 2 pairs of primers. One pair was two gene specific primers (GSP) flanking the site of insertion for confirming the disruption; the other pair contained one GSP and one corresponding to the T-DNA boarder sequences (TDP) for confirming the presence of T-DNA (Table 1). Verification of successful double knockout mutations were determined by immunoblotting utilizing GRIK1 protein antibodies and GRIK2 C-terminus peptide antibodies, specific for GRIK1 and GRIK2 respectively (*11*).

Fixation of Arabidopsis Siliques

Siliques from wild-type and mutant Col-0 plants were fixed in ethanol:acetic acid (v/v 9:1) for 2 h. They were then washed twice in 90% ethanol for 30 min each. Siliques of varying maturities were selected by counting 5, 9, or 13 slilques down from the last petaled

flower without a visible silique. These siliques were dissected under a dissecting microscope before being mounted on a slide with in 70% chloral hydrate, 4% glycerol, and 5% gum arabic.

Imaging Arabidopsis Emryos

Slides were imaged using a Leica DMI4000 inverted microscope (HXC PL fluotar 10× objective) with differential interference contrast (DIC; Nomarski) optics, a Leica DFC360FX camera, and LAS AF (Leica Microsystems) software according to Azhakanandam et al 2008 (*12*).

RESULTS

The knockout mutations were confirmed by the loss of GRIK1 and GRIK2 protein expression in leaves by GRIK1 protein antibodies and GRIK2 peptide antibodies, specific for GRIK1 and GRIK2 respectively (Fig. 2).

The reproductive structures of ten plants representing five different genotypes were fixed. The plants included wild-type, two independent lines of CR2 (homozygous *grik1-1/grik2-2*), two lines of *grik1-1/*WT, *grik2-1/grik2-1*, two lines of *grik1-1/grik1-1*, *grik 2-1/*WT and two lines of CR1 (homozygous *grik1-1/grik2-1*) with a background of Col-0. Microscopic examination revealed that wild-type plants (Col-0-1 and Col-0-2) and plants carrying one wild-type GRIK1 allele (CR1-2-17, CR2-2-21, CR1-2-9, and CR1-2-2) had similar embryonic defects and abortion frequencies. In contrast, early stage embryos showed

a range of defects in the four homozygous *grik1 grik2* knockout plants. Examples of these defects are shown in Figure 1. The percentage of total embryos that had phenotypic defects in each case was high during early development (silique number 5), but dropped dramatically by the torpedo stage (silique number 13). The decrease in the frequency of abnormal embryos during development was accompanied by an increase in the number of aborted seeds (Figure 2). However, approximately 40% of *the grik1-1/grik1-2* embryos appeared normal, and the homozygous mutants produced viable seed that germinated normally and resulted in normal progeny.

DISCUSSION

GRIK1 and GRIK2 proteins have only been detected in young tissue of healthy plants, while activated SnRK1 is detected in mature as well as young tissues (*11*). Hence, it is unlikely that the GRIKs are the only upstream activating kinases of SnRK1. We hypothesize that the GRIKs are the primary SnRK1 activating kinases during early embryo development but other unknown SnRK1 activator(s) can partially overcome the defect, especially at later stages of embryogenesis. AMPK, the mammalian homolog of SnRK1, has multiple activators (*5*), and provides precedence for this hypothesis. Alternatively, a previous study analyzed at least 100 seeds from cross breading of grik1 and grik2 knockout mutants, which yielded no homozygotes for both mutations. They concluded that that double knockout is either gametophytic or embryo lethal (*13*). This suggests that our mutations were slightly leaky and that recovery was due to low level GRIK expression.

FIGURES AND TABLES

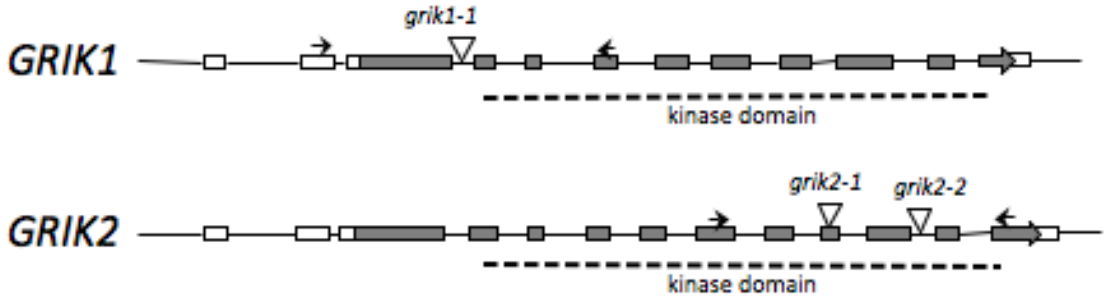

Figure 1. Diagram of T-DNA insertion positions in *grik1* and *grik2* mutants. Boxes indicate transcribed genomic sequences, of which the coding regions are filled with gray color. The direction of transcription is shown by boxed arrows. The kinase catalytic domains are shown by dashed lines underneath the genomic DNA. Positions of T-DNa insertions are indicated by upside-down triangles. *grik1-1*, SALK_142938-3. *grik2-1*, SALK_015230-1. *grik2-2*, SALK_000044-1.

Table 1. GSP and TDP Primers

PCR type	Primer name	Primer sequence
*grik*1-1 GSP+GSP	GRIK1T1F	CGAAGCTTACCGGGCTTTGAAG
	GRIK1T1R	ACTTTCCCATAACTACCAGATC
*grik*1-1 GSP+TDP	GRIK1T1R	ACTTTCCCATAACTACCAGATC
	LBB1	GCGTGGACCGCTTGCTGCAACT
*grik*2-1 GSP+GSP	GHRTF2	CGGGATATTGTTACTGGACT
	GRIK2T1R	GATACTCGTTGATTCTCCATTC
*grik*2-1 GSP+TDP	GRIK2T1R	GATACTCGTTGATTCTCCATTC
	LBB1	GCGTGGACCGCTTGCTGCAACT
*grik*2-2 GSP+GSP	GRIK2T2F	ATAGTGGCAGAGCTGCGGATAC
	GRIK2T2R	TGTACGGTTAAGTAGATGCATC
*grik*2-2 GSP+TDP	GHRTF2	CGGGATATTGTTACTGGACT
	LBB1	GCGTGGACCGCTTGCTGCAACT

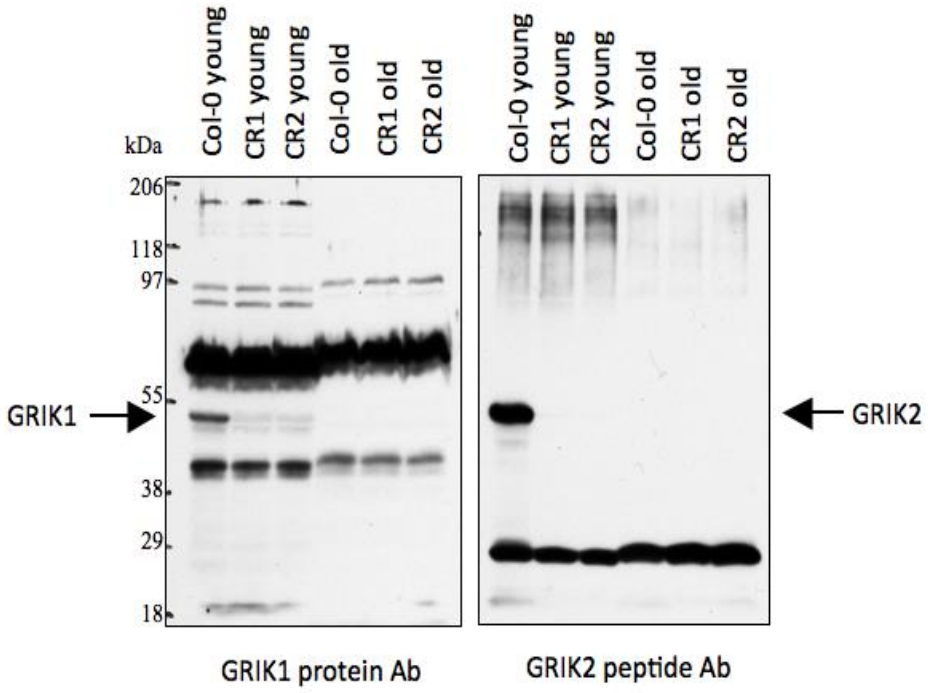

Figure 2. Immunoblotting of proteins from young and old leaves of wild-type Arabidopsis Col-0 plants and the CR1 and CR2 *grik1 grik2* double knockout mutants with GRIK1 and GRIK2 specific antibodies. The positions of GRIK1 and GRIK2 proteins are indicated by the arrows.

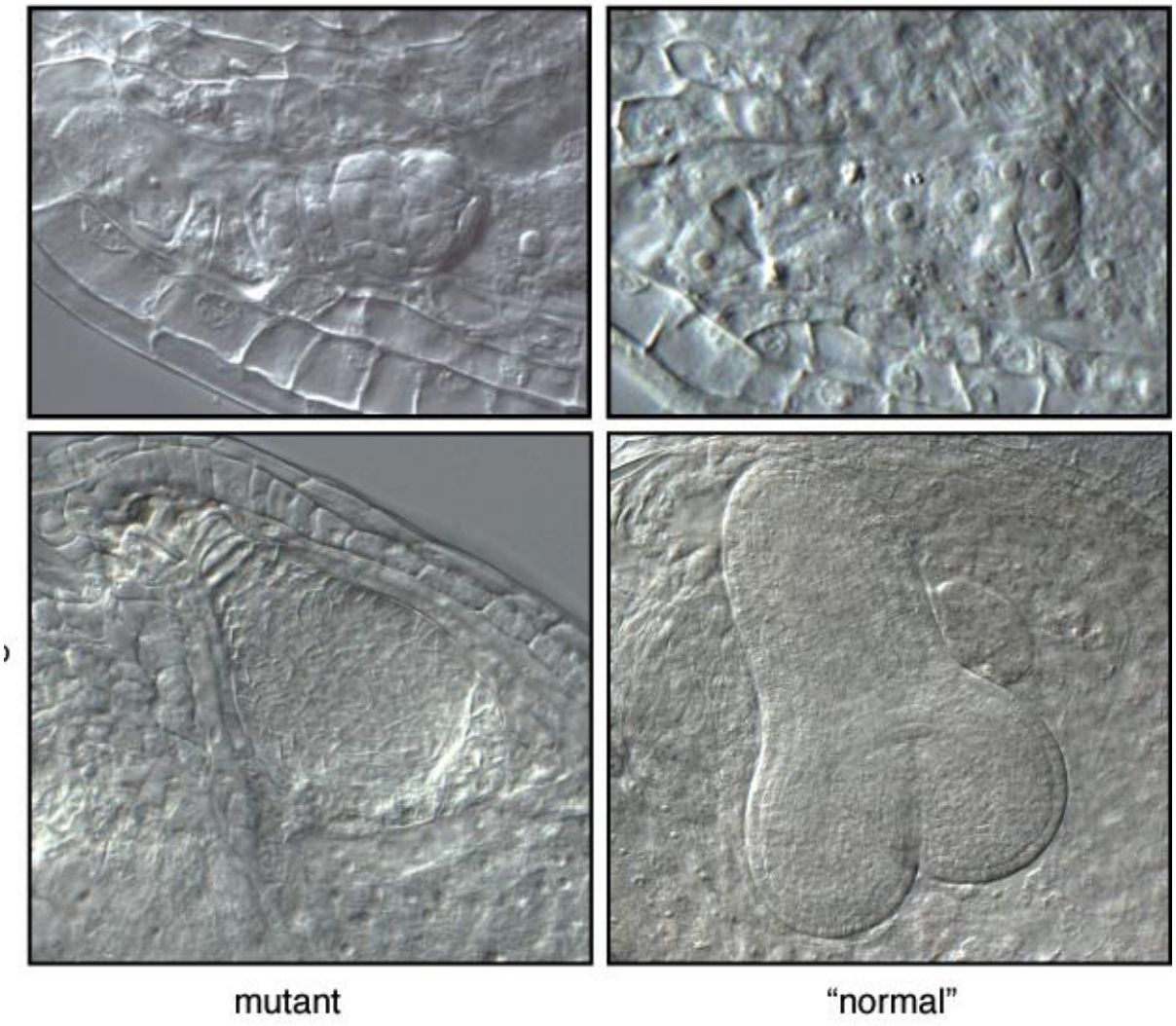

Figure 3. Fixed embryos from the homozygous CR2 *grik1-1/grik 2-2* knockout Top left, a globular stage embryo with visible defect in the apical domain. Top right, a wild-type globular stage embryo. Bottom left, early torpedo stage embryo with a visible defect in cotyledon formation. Bottom right, a wild-type early torpedo stage embryo.

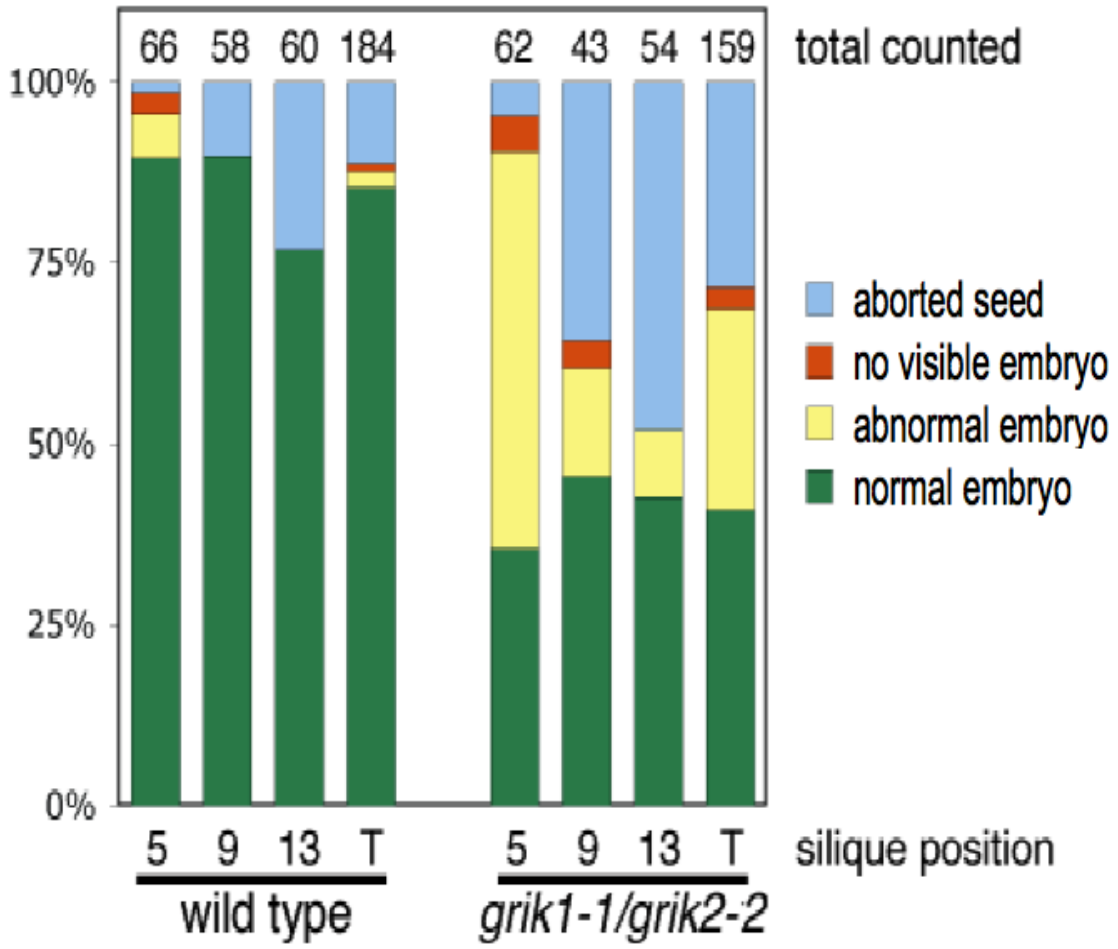

Figure 4. Comparison of the number of abnormal embryos or aborted seeds between wild-type Arabidopsis Col-0 plants and the *grik1-1*/*grik 2-2* knockout mutants. The percent of normal, abnormal, absent embryos and aborted seed at 3 developmental stages (silique positions 5, 9 and 13) and the total (T) are given. The numbers of embryos counted are indicated at the top of each column.

REFERENCES

1. Vlad, F., Turk, B. E., Peynot, P., Leung, J., and Merlot, S. (2008) A versatile strategy to define the phosphorylation preferences of plant protein kinases and screen for putative substrates, *Plant J 55*, 104-117.

2. Hrabak, E. M., Chan, C. W., Gribskov, M., Harper, J. F., Choi, J. H., Halford, N., Kudla, J., Luan, S., Nimmo, H. G., Sussman, M. R., Thomas, M., Walker-Simmons, K., Zhu, J. K., and Harmon, A. C. (2003) The Arabidopsis CDPK-SnRK superfamily of protein kinases, *Plant Physiol 132*, 666-680.

3. Nelson, D. L. (2005) *Lehninger Principles of Biochemistry*, 4th ed., W. H. Freeman and Company, New York, New York.

4. Cohen, P. (2000) The regulation of protein function by multisite phosphorylation--a 25 year update, *Trends Biochem Sci 25*, 596-601.

5. Hawley, S. A., Pan, D. A., Mustard, K. J., Ross, L., Bain, J., Edelman, A. M., Frenguelli, B. G., and Hardie, D. G. (2005) Calmodulin-dependent protein kinase kinase-beta is an alternative upstream kinase for AMP-activated protein kinase, *Cell Metab 2*, 9-19.

6. Hong, S. P., Momcilovic, M., and Carlson, M. (2005) Function of mammalian LKB1 and Ca2+/calmodulin-dependent protein kinase kinase alpha as Snf1-activating kinases in yeast, *J Biol Chem 280*, 21804-21809.

7. Shen, W., and Hanley-Bowdoin, L. (2006) Geminivirus infection up-regulates the expression of two Arabidopsis protein kinases related to yeast SNF1- and mammalian AMPK-activating kinases, *Plant Physiol 142*, 1642-1655.

8. Hanks, S. K., and Hunter, T. (1995) Protein kinases 6. The eukaryotic protein kinase superfamily: kinase (catalytic) domain structure and classification, *FASEB J 9*, 576-596.

9. Crozet, P., Margalha, L., Confraria, A., Rodrigues, A., Martinho, C., Adamo, M., Elias, C. A., and Baena-Gonzalez, E. (2010) Mechanisms of regulation of SNF1/AMPK/SnRK1 protein kinases, *Front Plant Sci 5*, 190.

10. Halford, N. G., and Hey, S. J. (2009) Snf1-related protein kinases (SnRKs) act within an intricate network that links metabolic and stress signalling in plants, *Biochem J 419*, 247-259.

11. Shen, W., Reyes, M. I., and Hanley-Bowdoin, L. (2009) Arabidopsis protein kinases GRIK1 and GRIK2 specifically activate SnRK1 by phosphorylating its activation loop, *Plant Physiol 150*, 996-1005.

12. Azhakanandam, S., Nole-Wilson, S., Bao, F., and Franks, R. G. (2008) SEUSS and AINTEGUMENTA mediate patterning and ovule initiation during gynoecium medial domain development, *Plant Physiol 146*, 1165-1181.

13. Bolle, C., Huep, G., Kleinbolting, N., Haberer, G., Mayer, K., Leister, D., and Weisshaar, B. (2013) GABI-DUPLO: a collection of double mutants to overcome genetic redundancy in Arabidopsis thaliana, *Plant J 75*, 157-171.

CHAPTER III

Characterization of TCP Phosphorylation Sites by the GRIK-SnRK1 Kinase Cascade

INTRODUCTION

In eukaryotes, protein phosphorylation plays a central role in the regulation of cellular processes (*1*, *2*). It is the attachment of a phosphate group to tyrosine, serine, or threonine residues by protein kinases (*3*). This modification is important since up to 4% of the annotated proteins in Arabidopsis are kinases (*4*). One of the subfamilies of Ser/Thr protein kinases appears to be related to the classical SNF1-type kinases from yeast and the mammalian AMPK and are known as SNF1-related kinase (SnRK) (*2*). As desicribed in chapter I, there are three recognized subgroups: SnRK1, SnRK2, and SnRK3, but only SnRK1s are true homolgues of SNF1 and AMPK (*2*).

In plante, SnRK1 is a heterotrimeric complex(*5*) comprised of a catalytic α subunit and two regularly subunits, γ and β (*6*). For more detail about these subunits see chapter I. The *Arabidopsis thaliana* genome codes for two α subunits SnRK1.1 and SnRK1.2 (*6*), and have the highest degree of conservation in the N-terminal half of the protein, particularly in the conserved threonine residue in the activation loop (*5*). SnRK1.1 and SnRK1.2 catalytic subunits are activated by phosphorylation of the T- loop (*7*) at T175 and T176, respectively (*8*).

SnRK1 is functionally responsible the regulation of several pathways. It plays a key role in environmental stress response, global regulation of metabolism, energy conservation, antiviral defense, and fundamental development (*5*). SnRK1 is also allosterically regulated by metabolites (*9*).

A series of kinases that are phosphorylated before phosphorylating a target form a phosphorylation cascade (*10*). In these cascades, a kinase of focus must be activated via phosphorylation before it can phosphorylate another target (*10*). Both AMPK and SNF1 are known members of cascades (*11, 12*). AMPK is phosphorylated by LBK1 and CaMKKα (*11*) and SNF1 is activated by PAK1/Tos3/ELM1 (*12*). Although less is known about the SnRK1 cascades, there are plant homologues to CaMKKα and PAK1/Tos3/ELM1 with 41-53% amino acid sequence similarity and are known as Geminivirus Rep Interacting Kinases (GRIKs) (*13*). In Arabidopsis there are two genes that code for GRIK: GRIK1 and GRIK2 (*7*). GRIK is activated via autophosphorlytion (*14*) and has been shown to phosphorylated by SnRK1 *in vitro* (*14, 15*) and rescue the yeast *tos3pak1elm1* knockout mutants (*13*). Therefore, GRIK likely forms a cascade with SnRK1.

Evidence indicates SnRK1 uses phosphorylation to modulate transcriptional reprogramming; likely through modulating DNA binding proteins known as transcription factors (*8, 16*). CaMKKα phosphorylated AMPK but it also interacts with and recruits substrates of AMPK, in particular transcription factors (TFs), for phosphorylation (*11*). Because GRIK is a homologue of CaMKKα, it is likely that if a transcription factor interacts with GRIK it could be a substrate of SnRK1.

In eukaryotes, transcription is initiated or regulated by TFs (*10*). TFs have important roles in chromatin remodeling, cell division and cell differentiation (*17*). Because of the importance of TFs in cell division and differentiation states, cells must tightly control transcription regulation (*17*).

Wei Shen and Maria Reyes in the laboratory of Linda Hanley-Bowdoin preformed a yeast-two-hybrid screening of an Arabidopsis cDNA library (see Table 1) with GRIK1 and GRIK2 as baits (unpublished data). Three of the five transcription factors that interact with GRIK1 are members of the TCP (teosinte branched 1/ cycloidea/ PROLIFERATING CELL FACTORS) family, and are candidates for members of a putative GRIK-SnRK1 cascade phosphorylation.

TCP transcription factors are a specific plant and fresh water algae (*18*) family of basic helix-loop-helix DNA binding proteins (*19, 20*). TCPs interact with DNA as homo or heterodimers (*21*).These dimers interact with the nucleic acid sequences of 5´-GGNCC-3´ with additional specificity to family members on the surrounding nucleic acids (*22*). TCPs are divided into two classes: class I and class II (*23*). In Arabidopsis, there are 24 family members, 13 class I and 11 class II (*24*).

Regulation of TCP is minimally understood. Thus far the only report of post-transcriptional regulation of class I TCP proteins is phosphorylation of TCP8 (*25*). Reports of regulation of class II members indicate that a subset of CIN-type genes are microRNA miR319 targets (*26*). Introns might also have a regulatory role in these genes (*23*).

Here we identify new post-translational modifications of TCP via phosphorylation by the GRIK-SnRK1 cascade, including possible sites of phosphorylation on 4 TCPs, TCP3, TCP18, TCP20 and TCP22, by SnRK1 (for details of the functions of these TCPs see chapter I), and show possible functional relevance of class I TCP phosphorylation.

MATERIALS AND METHODS

Recombinant Fusion Protein Clones

Bacterial expression cassettes for His-SnRK1.1 fl (full-length; pNSB1490) and His-SnRK1.1 kd (kinase domain; pNSB1494) were described previously (*7*). Bacterial expression cassettes for His-GRIK1 (pNSB1451), GST-GRIK1 (pNSB1554), and GST-GRIK1 K137A (pNSB1555) were also described previously (*13*). Expression cassettes corresponding to all other recombinant proteins were cloned via PCR with primers made by IDT, purified using a Qiagen PCR Purification kit, digested by restriction enzymes, and ligated with QuickLigase (New England BioLabs). For specific construct details see Table 2 and Table 3. Ligation products were transformed into *E. coli* DH5α cells. Single colonies were selected using LB medium agar plates supplemented with 100 μg/ml carbenicillin (Carb100) or 50 μg/ml kanamycin (Kan50) (dependent on antibiotics resistance marker of the plasmid) and inoculated into 6 mL LB medium containing Carb100 or Kan50. Cultures were grown overnight at 37°C and plasmids were isolated via Qiagen Plasmid MiniPrep kit. Plasmids were verified by restriction enzyme mapping and DNA sequencing (Eton Biosciences), transformed into *E. coli* BL21 (DE3) cells, and recombinant protein was expressed and purified as described below.

Mutagenesis

The SnRK1 or TCP coding sequence was subjected to site-directed mutagenesis using Pfu polymerase Ultra (New England Biolabs) or Q5 polymerase (New England Biolabs). For

template see Table 2 and primers see Table 3. DNA products from thermal cycles were transformed into *E. coli* DH5α and plated onto LB agar plates supplemented with Carb100 or Kan50 (dependent on plasmid resistance). The bacteria were grown overnight in LB supplemented with Carb100 or Kan50 (dependent on plasmid resistance), and plasmid DNA was purified using a Qiagen Plasmid Mini Prep kit and sequenced (Eton Biosciences). Plasmids carrying the desired mutations were transformed into *E. coli* BL21 (DE3) cells, and recombinant protein was expressed and purified as described below.

Recombinant Fusion Protein Expression

E. coli BL21 (DE3) lines carrying verified plasmids were grown in one flask of 250 mL (or multiples for lines with low expression) LB medium with Carb100 or Kan50 at 37°C for 1-3 h to an OD at 600 nm of 0.8-1.0 and induced with 0.5-1.0 mM IPTG overnight at 16°C with shaking. Each flask of culture was then pelleted, rinsed with 5-10 mL PBS (10 mM Na_2HPO_4, 1.8 mM KH_2PO_4, 140 mM NaCl, 2.7 mM KCl) and repelleted . These pellets were frozen at -20°C for a minimum of 30 min before being resuspended in 20 mL PBS with 0.1% Trition-X 100 (PBST) with Protease Inhibitor for bacterial cells (Sigma, catalog # P8465) and lysed via 12 sonicating pulses of 10 s at a setting of 30% intensity. After pelleting debris via centrifugation at 32,500 ×g for 30 min, GST-fusion proteins were purified by incubating the total volume of the soluble lysate component to a 0.3 mL bed volume of pre-washed glutathione-Sepharose (GE) beads for 30 min with rotation (40 rpm) at 4°C. After batch loading, the beads were washed three times for 10, 30, and 10 min with

rotation (40 rpm) at 4°C in 10-14 mL PBST, and eluted with 1.2 mL of 50 mM glutathione (Sigma).

The His-fusion proteins were expressed, pelleted, and frozen in the same manner as described for the GST-fusion proteins. The His-fusion protein pellets were then resuspended in 20 mL 20 mM Tris-HCl, pH 8, 500 mM NaCl, 5 mM imidizole with Protease Inhibitor Cocktail for Hisidine-Tagged Proteins (Sigma, catalog # P8849) and lysed via 12 sonicating pulses of 10 s at a setting of 30% intensity. After pelleting debris via centrifugation, His-fusion proteins were purified by binding the total volume of the soluble lysate component to 0.3 mL bed volume of pre-washed Ni-NTA Agarose (Qiagen) beads for 30 min with rotation (40 rpm) at 4°C. After batch loading, the beads were washed three times for 10, 30, and 10 min with rotation (40 rpm) at 4°C in 10-14 mL of His wash buffer (20 mM Tris-HCl, pH 8, 500 mM NaCl, 20 mM imidizole), and eluted with 1.2 mL of His elution buffer (20 mM Tris-HCl, pH 8, 500 mM NaCl, 500 mM imidizole) on ice. With the exception of His-SnRK1.1 kd, which was stored in a 1:1 ratio of His elution buffer and glycerol with 1 mM DTT, all proteins were subjected to diafiltration with TBS (25 mM Tris-HCl, pH 7.5, 140 mM NaCl, 2.7 mM KCl) using an Amicon Ultra 30K 0.5 mL tubes (Millipore). Glycerol was added to concentrated proteins in a 1:1 ratio with 1 mM DTT. Concentrations were measured using the Bradford assay (BioRad) and protein purity was assessed using SDS-PAGE analysis.

Preactivation of SnRK1

Recombinant His-SnRK1.1 kd (0.5 μg) and recombinant GST-GRIK (1 μg) were incubated together in kinase buffer (50 mM Tris-HCl, pH 7.4, 10 mM $MgCl_2$, 1 mM EGTA, 1 mM DTT) and 1 mM ATP in a total volume of 50 μL for 30 min at 30°C. The reaction was then incubated at room temperature with 50 μL of pre-washed glutathione-sepharose (GE) beads for 30 min with rotation (40 rpm). The supernatant was recovered by centrifugation at 16,100 ×g, combined with 50 μL of pre-washed Ni-NTA Agarose (Qiagen) and then incubated at room temperature for 30 min with rotation (40 rpm). Ni-NTA beads were washed three times with 1 mL His wash buffer for 10 min. Preactivated SnRK1 was eluted with 400 μL His elution buffer containing 0.5 mM DTT. Conversely, recombinant GST-SnRK1.1 (fl) (1 μg) and recombinant His-GRIK (0.5 μg) were incubated together in kinase buffer and 1 mM ATP in a total volume of 50 μL of kinase buffer for 30 min at 30°C. The reaction was incubated at room temperature with 50 μL of pre-washed Ni-NTA Agarose beads for 30 min with rotation (40 rpm). The supernatant was recovered by centrifugation at 16,100 ×g, combined with 50 μL pre-washed glutathione-sepharose and then incubated at room temperature for 30 min with rotation (40 rpm). The glutathione-sepharose beads were washed three times with 1 mL kinase buffer for 10 min. Preactivated SnRK1 was eluted with 400 μL of 50 mM glutathione in TBS containing 0.5 mM DTT. SnRK1 kinase activity was assessed by reacting 38 μL of preactivated SnRK1 and/or 1.0 μg GST-GRIK with 0.2 mM of the synthetic peptide acetyl-KGRMRRISSVEMMK (Genscript) in kinase buffer in a reaction volume of 50 μL in the presence of 1 mM ATP and 0.5 μCi/μl [γ-^{32}P]-ATP (Perkin Elmer)

for 20 min at 30°C. The reactions, which were performed in triplicate, were stopped by spotting onto p81 filter discs (Whatman) and rinsed for four times with 250 mL of 75 mM H_3PO_4; the discs were air dried and then submerged in Scintiverse II Sintillation Fluid (Fisher Scientific). Samples were analyzed with a scintillation counter (Packard Tri-Carb Model 2900 TR).

GRIK and SnRK1 Kinase Assays

Kinases (0.25-0.5μg) His-SnRK1.1 kd and His-GRIK1 or GST-GRIK, dependent on the molecular mass of the substrate protein, were incubated in kinase buffer (50 mM Tris-HCl, pH 7.4, 10 mM $MgCl_2$, 1 mM EGTA, 1 mM DTT) with 10 nmol ATP for 1 h at 30°C, before adding substrate. Substrates (5-30 pmol, consistent in each assay) were added with 2 μL of 2.5 μCi/μl [γ-^{32}P]-ATP (Perkin Elmer) and incubated with the kinases for 30 min at 30°C. Reactions were quenched with one volume of 2x SDS-PAGE running buffer (0.125 mM Tris-HCl, pH 6.8, 20% (v/v) glycerol, 4% (w/v) SDS, 10% (v/v) β-mercaptoethanol, 0.02 mg/mL bromophenol blue). Half of the quenched reaction volume was separated on a 10% acrylamide SDS-PAGE gel or a 4-12% NuPAGE gel (Novex). Gels were either transferred to nitrocellulose membrane (Whatman) and immunoblotted with anti-His antibody (1:40,000 dilution of mouse anti-HIS6x (Clontech)) followed by incubation with 1:10,000 dilution of donkey anti-mouse Alexa800 (LiCor) or goat anti-GST antibody (GE Healthcare) (1:10,000 dilution) and then with 1:10,000 dilution of donkey anti-goat

Alexa680 (LiCor) or stained with Coomassie blue, destained in 40% methanol, 10% acetic acid, and 3% glycerol, then dried. Radioactivity was visualized by autoradiography.

Sample Preparation for LC/MS/MS Analysis

Recombinant proteins were purified as described above except instead of PBST, PSB with 1 mM dodecyl maltoside was used. For the kinase assays, His-SnRK1.1 kd and His-GRIK1 (1 μg each) were incubated with 1 μg substrate protein in kinase buffer with 10 nmol ATP for 1 h at 30°C in a reaction volume of 100 μL. The reactions, which were performed in triplicate, were quenched with 1 μg/μL RapiGest (Waters) and 10 mM DTT. The proteins were dried and resuspended in 50 μL 50 mM ammonium bicarbonate pH 8 (for trypsin digestion) or 50 mM Tris, pH 8 (for chymotrypsin or Asp-N digestion). Each solution was reduced with 10 mM DTT for 30 min at 57°C, alkylated with 50 mM iodoacetamide for 30 min at room temperature in the dark, and then digested with trypsin (1:100, w/w)(Promega), chymotrypsin (1:100, w/w) (Roche), or Asp-N (1:100, w/w) (Promega) overnight at 37°C. The digested samples were acidified with the addition of 1 μL formic acid (FA). Samples were then split 1:2 aliquots (v/v) to generate an unenriched sample for LC/MS/MS analysis and IMAC phosphopeptide enrichment, respectively.

For phosphopeptide enrichment, IMAC resin was prepared by washing 400 μL of suspended NTA agarose slurry (Qiagen) with 1 mL water twice before chelation with 1 mL 40 mM EDTA (pH ~7.4). The resin was then washed twice with 1 mL water before acidifying with 1 mL 1% acetic acid. Acidified resin was incubated 4-16 h with 1 mL 100

mM $FeCl_3$ in 1% acetic acid in the dark at room temperature and stored at 4°C until sample enrichment was performed. The resin (40 µL of the IMAC-Fe resin slurry) was washed with 100 µL 1% acetic acid, then the sample aliquot for enrichment was loaded and sequentially washed with 100 µL 1% acetic acid, twice. Flowthrough of both the load and washes were collected. To reduce nonspecific hydrophobic peptide content, an additional wash with 100 µL 100mM NaCl/acetonitrile/acetic acid solution (v/v/v 74/25/1), was preformed twice. Peptides were eluted twice with 100 µL water and twice with 100 µL 5% NH_4OH. The eluate was acidified using 5 µL 100% formic acid. The unenriched aliquot, IMAC and flow-through samples were vacuum-dried. The dried samples were resuspended in 20 µL 0.1% formic acid and filtered prior to LC/MS/MS analysis.

LC/MS/MS Analysis

An Easy nLC 1000 coupled to an ETD-enabled Orbitrap Elite (Thermo Scientific) was used for nano-LC/MS/MS analyses. A Self-Pack PicoFrit® column with 10 Å frit (OD/ID 360/75, Tip ID 10, New Objective) packed with Magic C18 -5 µm particles (Bruker) was used as an analytical column, which was preceded with an inline Acclaim Pepmap C18, 5um particles, 100um id x 2cm length trapping column (Thermo Scientific). Each sample was run twice: once with higher-energy collisional dissociation (HCD)/electron transfer dissociation (ETD) and once with collision-induced dissociation (CID)/ETD. Samples were injected with a 5 µL volume and sprayed at 300 nL min^{-1} and 4.0 kV. The mobile phases consisted of 2% acetonitrile and 0.1% formic acid (A) and 0.5% formic acid in acetonitrile

(B). A three-step linear gradient (0% to 7% B in 1 min, 7% to 40% B in 39 min, 40% to 95% B in 1 min, and 95% B for 15 min) was used. The MS scan range was m/z 200 to 4,000. The top 10 precursor ions were selected in the MS scan by Orbitrap FTMS analyzer with full scantype, resolution = 60,000, and positive polarity. Scan events had a minimum signal intensity of 1,000, a default charge state of +2 or greater, isolation width of *m/z* 3.0, and a normalized collision energy setting of 27. MS/MS acquisitions utilized Decision Tree software with the FTMS analyzer using mass charge cut-offs of +3 at *m/z* 650, +4 at *m/z* 900, and +5 at *m/z* 950.

Post LC/MS/MS Data Processing and Analysis

Raw data was processed with Proteome Discover 1.3 and spectra were searched against a modified *E. coli* database with added standards, such as BSA, and recombinant fusion proteins using Mascot (Matrix Science). Proteome Discoverer created mgf files for the CID, HCD, and ETD acquisition with monoisotopic precursor mass tolerances of 10 ppm for all acquisitions and fragment ion tolerances of 0.6 Da, 0.01 Da, and 0.6 Da, respectively, with strict trypsin, chymotrypsin, or Asp_N specificity, allowing for up to two missed cleavages. Database searches included carbamidomethylation of Cys set as a fixed modification, while oxidation of Met and phosphorylation of Ser, Thr, and Tyr were allowed as variable modifications. Peptides were considered identified if the Mascot score was over 20 with a p-value < 0.05.

GB-Tag Removal

GB-Ent-TCP20-His plasmids were created by PCR cloning of TCP20 with a primer containing the sequence to code for an enterokinase cleavage site (see Table 2 and Table 3 for details) and ligated into the pET30A plasmid containing the sequence for IgG-binding-B domain. GB-Ent-TCP20-His recombinant protein was expressed and purified via His tag affinity purification. Ni-NTA beads (50 μL) were washed in Ent Reaction buffer (20 mM Tris-HCl, pH 8, 500 mM NaCl, 2 mM $CaCl_2$). GB-Ent-TCP20-His protein sample (50 μg) was incubated with the beads in 1.0 mL Ent Reaction buffer for 30 min with shaking at 40 rpm at room temperature. The supernatant was then removed and Enterokinase (1 μL of 10:1 diltion of NEB stock) in 50 μL Ent Reaction buffer was added. The cleavage was preformed overnight at 25°C. After the cleavage reaction, the beads were collected by centrifugation at 16,100 ×g and washed three times in 1 mL Ent Reaction buffer before TCP20-His was eluted using 150 μL His elution buffer. All samples including the beads were diluted with running buffer and then analyzed by SDS-PAGE using a 10% acrylamide gel.

Native PAGE Analysis

TCP20-His, GB-TCP20-His, and GST-TCP 20 (0.25 mM) were incubated for 1 h in the dark at room temperature with or without 5 μM preannealed GTGGG$^{A}/_{C}$CCGG double stranded oligonucleotides in a reaction volume of 20 μL in binding buffer (20 mM HEPES, pH 7.5, 50 mM KCl, 2 mM $MgCl_2$, 0.5 mM EDTA, 1 mM DTT, 0.5% Triton-X 100, 22

ng/μL BSA, 0.5 μg/μL polydIdC, and 10% glycerol). The reactions were resolved by 10% acrylamide native PAGE and proteins were stained with Coomassie dye.

Fluorescent EMSA

Double stranded DNA (except the RPL24 promoter region) was generated by annealing an IRD-labeled forward primer with its unlabeled reverse complementary primer. DNA oligonucleotides containing the binding domain GTGGG$^{A}/_{C}$CCGG were 24 bp with A or C and formed by annealing the TCP I binding A F-IRD oligonucleotide with the TCP I binding A R oligonucleotide, or TCP I binding C F-IRD with TCP I binding C R. IRD-labeled RPL24 promoter region was synthesized by PCR, on Arabidopsis Col-0 genomic DNA with IRD-RPL24 promoter F/RPL24 promoter R primers (for full sequence see Table 3). For the binding reaction, TCP20 and TCP22 and their phosphonull (TCP20 S237A, TCP20 S237N, TCP22 S140A, or TCP22 S140N) and phosphomimic (TCP20 S237E or TCP22 S140E) mutants were incubated for 1 h in the dark at room temperature with the double-stranded oligonucleotides in 20 μL binding buffer (for reactions with TCP I binding C or TCP I binding A using a protein concentration from 0-50 mM containing 5 μM DNA in binding reaction buffer (20 mM HEPES, pH 7.5, 50 mM KCl, 2 mM $MgCl_2$, 0.5 mM EDTA, 1 mM DTT, 0.5% Triton-X 100, 22 ng/μL BSA, 0.5 μg/μL polydIdC, and 10% glycerol) and incubated for 1 h at room temperature; for the RPL24 reaction there was 0-15mM protein and 5 μM DNA. The samples from the binding reactions combined with 3μL 10 x Orange Gel Loading Dye (5% Orange G, 60% glycerol, in 50mM EDTA, pH 8) were subjected to

electrophoresis on 1% agarose gels in 1x TBE (0.2M Tris, pH 8.3, 0.2 M borate and 4 mM EDTA) in the dark and imaged with a Li-Cor Odyssey Fluorescent Imager.

Radioactive EMSA

Radiolabeled double stranded DNA was formed by annealing forward primers and reverse primers Rad TCP I Binding C F with Rad TCP I Binding C R or Rad TCP I Binding A F with Rad TCP I Binding A R. DNA was labeled using the protocol for fill-in of 5' overhang ends using DNA Polymerase I, Large (Klenow) Fragment (New England Bioscience) with [α-P^{32}]ATP. TCP20 and TCP22 (0-1.6 μM) and their phosphonull (serine to alanine or asparagine) and phosphomimic (serine to glutamate) mutants were incubated with 0.05 μM labeled double-stranded oligonucleotides in a reaction volume of 20 μL in binding reaction buffer for 1 h at room temperature and analyzed by PAGE using 4% acrylamide gels in 1 x TBE. Gels were dried and radioactivity was determined using a GE Storm 865 imager and Image 069 Snapshot 2 software. Data were plotted using Microsoft Excel 2013 Solver.

Yeast-two Hybrid Studies

Gene constructs for yeast two hybrid assays (except TCP20 S237E) were first cloned into pDONR221 plasmids via PCR (see Table 2 and Table 3 for templates and primers). The TCP20 S237E pDONR221 plasmid was formed via mutagenesis. The plasmid pDONR221 was chosen because it is an entry clone for a variety of expression vectors adapted for the

Gateway® Technology (Thermo. Final Y2H constructs were generated by reactions containing the empty pDEST22 destination vector with the TCP20 or TCP22 entry plasmids using the Clonase II LR kit protocol. The product was used to transform DH5α cells. Plasmids were verified by DNA sequencing (Eton Biosceinces). Yeast two hybrid assays were performed by Soon-Ki Han in Doris Wagner's Lab (University of Pennsylvania).

Quantitative BiFC

Constructs for BIFC (bimolecular fluorescence complementation) were cloned via PCR (see Table 2 and Table 3 for details) in pSPYCE (MR) and pSPYNE (R) 173 plasmids. A single colony was used to inoculate 6 mL LB medium with Carb100. Plasmids were purified with the Qiagen Mini Prep kit and verified by sequencing (Eton Biosciences). Cultures (100 mL LB medium with Carb100) of each plasmid were grown overnight at 37 °C, and the plasmids and purified with the Qiagen Midi Prep Kit. DNAs used for transforming protoplasts by Jun Xiao in Doris Wagner's Lab (University of Pennsylvania) as previously published (*27*). Quantitative BiFC assays were preformed by Jun Xiao.

RESULTS

Functional Analysis of SnRK1 Mutants

SnRK1 must be activated by phosphorylation to be an active protein kinase. Recombinant SnRK1, that is not phosphorylated, must also be activated by its upstream kinase, GRIK (*28*), before it can be used in kinase reactions *in vitro*. Given this, it is

necessary to develop reaction conditions that distinguish between the kinase activities of activated SnRK1 and GRIK. Simply mixing the two kinases in a single reaction will not accomplish this. Hence, we investigated the feasibility of using a constitutively active mutant of SnRK1 or SnRK1 preactivated by GRIK. The synthetic peptide (10 pmol), Ace-KGRMRRISSVEMMK, was incubated with various combinations of 0.5 μg of each kinases (GST-GRIK + His-SnRK1(kd)WT, GST-GRIK + His-SnRK1(kd)S175E, GST-GRIK + His-SnRK1(kd) S175E/T176D, GST-GRIK + GST-SnRK1(fl)WT, GST-GRIK + GST-SnRK1(fl)S175E, GST-GRIK + GST-SnRK1(fl)S175E/T176D, His-SnRK1(kd)WT, His-SnRK1(kd)S175E, His-SnRK1(kd) S175E/T176D, GST-SnRK1(fl)WT, GST-SnRK1(fl)S175E, GST-SnRK1(fl)S175E/T176D, or no kinase) and 1 mM ATP supplemented with 0.5 μCi γ-^{32}P ATP for 20 min at 30°C (Fig. 1). Full-length (fl) and kinase domain (kd) versions of wild-type (WT) SnRK1 and the S175E mutant were more active when incubated in the presence of GRIK. In contrast, incubation with GRIK did not enhance the activity of the S175E/T176D mutant. This result suggested that GRIK could activate SnRK1 by phosphorylating T176 in the S175E mutant. Wild-type SnRK1 (fl) and the S175E (kd) mutant displayed the most kinase activity in the absence of GRIK, but their activities were at least 2-fold less in the absence of GRIK. The activities of wild-type SnRK1 (kd), 175E/T176D (kd), and 175E/T176D (fl), were even lower in the absence of GRIK, and S175E (fl) was inactive. Based on these results, we concluded that SnRK1 activity was not enhanced by the inclusion of phosphomimic mutations in its activation loop in peptide phosphorylation assays.

We also asked if the SnRK1 phosphomimic mutants could phosphorylate recombinant proteins using TCP22 as a model. GST-TCP22 was incubated with His-GRIK, His-GRIK + His-SnRK1(kd), His-SnRK1(kd), His-GRIK + His- SnRK1.1(kd)S175E, GST - GRIK + His- SnRK1.1(kd)S175E, His- SnRK1.1(kd)S175E, or no kinase in the presence of 10 nmol ATP and 0.5 μCi P^{32} γ-ATP for 1 h at 30°C (Fig. 2). TCP22 was only phosphorylated when both GRIK and wild-type SnRK1 were included in the reaction (lane 2). Wild-type GRIK was also phosphorylated in lanes 1, 2 and 4, and wild-type SnRK1 was phosphorylated in lane 2. These results indicated that the SnRK1 phosphomimic mutants are unable to phosphorylate a protein substrate, establishing that they cannot be used to examine SnRK1 kinase activity *in vitro*.

Based on the above results, we devised a method to use GRIK to activate SnRK1 and then to remove it prior to SnRK1 kinase assays. We reasoned that after His-SnRK1 (kd) is phosphorylated by GST-GRIK, GRIK can be removed using glutathione affinity resin and activated SnRK1 purified further by nickel affinity chromatography or vise versa for His-GRIK and GST-SnRK1. To test these strategies, we compared the activities of preactivated His-SnRK1(kd), GST-GRIK + preactivated His-SnRK1(kd), GST-GRIK1, preactivated GST-SnRK1(fl), His-GRIK + preactivated GST-SnRK1(fl), His-GRIK, or no kinase in the peptide kinase assay described above (Fig. 3). Both full-length (fl) and the kinase domain (kd) versions of preactiviated SnRK1 efficiently phosphorylated the Ace-KGRMRRISSVEMMK peptide. No peptide phosphorylation was detected in reactions only containing GRIK, indicating that it did not contribute to any of the observed phosphorylation.

Importantly, the activities of the preactivated SnRK1 in the presence and absence of GRIK were equivalent; indicating that removal of GRIK did not reduce the activity of the preactivated SnRK1.

We then asked if preactivated SnRK1 could also phosphorylate protein substrates. For this analysis, we compared phosphorylation of GST-TCP20 in reactions containing GST-GRIK, preactivated His-SnRK1(kd), GST-GRIK + preactivated His-SnRK1(kd), GST-GRIK K137A + preactivated His-SnRK1(kd), or no kinase, or phosphorylation of GST-TCP22 in reactions containing preactivated His-SnRK(kd), His-GRIK, or His-GRIK + preactivated His-SnRK(kd) as described above (Fig. 4). TCP20 and TCP22 were phosphorylated in all reactions containing preactivated SnRK1 (lanes 3-5, 7 and 9), but not by GRIK alone (lanes 2 and 8). Together, these results indicated that preactivation of SnRK1 by GRIK followed by removal of GRIK can be used to distinguish the activities of the two kinases *in vitro*.

SnRK1 Phosphorylates Some TCP Transcription Factors *in vitro*

Three TCPs were identified as GRIK partners in a yeast 2-hybrid screen of an Arabidopsis cDNA library (Table 1). Based on these results, we reasoned that GRIK might phosphorylate TCPs or that it might activate SnRK1 to phosphorylate TCPs. To address these possibilities, we first cloned cDNAs corresponding to 23 of the 24 Arabidopsis TCPs and used them to construct *E. coli* expression cassettes for the 23 TCPs tagged with GST (Table 2). (We were unable to generate a cDNA for TCP17.) We then tested the recombinant GST-TCPs as substrates in *in vitro* kinase assays containing GRIK alone, preactivated

SnRK1 alone, GRIK + SnRK1, and GRIK K137A+ SnRK1, with the overall results summarized in Table 4 and selected results shown in Fig. 5. Labeled bands (Fig. 5B) corresponding to GST-tagged, full-length TCP9 (lane 1) and a truncation of TCP19 (lane 2) were observed in GRIK kinase reactions. In both cases, the intensities of the radiolabeled bands was not strong. None of the other TCPs, including the three that bound to GRIK in yeast 2-hybrid assays, were phosphorylated by GRIK *in vitro* (representative negative results are shown for GST-tagged TCP20 (lane 3) and TCP22 (lane 4).

Unlike GRIK, preactivated SnRK1 phosphorylated several TCPs *in vitro*. Strong radiolabeled bands (Fig. 5A) were reproducibly detected for full-length or truncated GST-tagged TCP3 (lane 2), TCP13 (lane 5) TCP18 (lane 25) and TCP22 (lanes 8, 16, 23 and 26) (the identities of the full-length and truncated bands were confirmed on immunoblots using GST antibodies in other experiments). SnRK1 phosphorylation products were also readily detected for full-length or truncated TCP1 (lane 9), TCP9 (lane 12), TCP12 (lane 10), TCP19 (lane 13), TCP20 (lane 15), TCP24 (lane 6), while weaker bands were sometimes seen for TCP8 (lane 21), TCP10 (lane 3), TCP14 (lane 24), TCP15 (lane 18), TCP21 (lane 19), and TCP23 (lane 23). Including GRIK in the kinsase reactions with preactivated SnRK1 resulted in a moderate increase in phosphorylation of TCP8 and TCP23, while inclusion of GRIK moderately decreased TCP13 phosphorylation. No SnRK1 phosphorylation was observed for TCP2 (lane 7), TCP5 (lane 4), TCP6 (lane 17), TCP7 (lane 20), TCP11 (lane 14) and TCP16 (lane 11) in any experiments suggesting these TCPs are unlikely to be substrates of the GRIK-SnRK1 cascade. The above results established that four Class I and seven Class 2

TCPs are unambiguously phosphorylated by SnRK1 *in vitro*, while five Class I and one Class II TCPs may be substrates of the kinase.

SnRK1 Does Not Phosphorylate the TCP Domain

Given that only a subset of TCPs are phosphorylated by SnRK1, we hypothesized that the phosphorylation sites occur outside the conserved TCP binding domain. To test this idea, we selected TCP3, TCP18, TCP20 and TCP22, all of which are unambiguously phosphorylated by SnRK1, for phosphorylation domain analysis. TCP20 and TCP22 are members of class I, while TCP3 and TCP18 are members of class II. Unpublished data indicated that TCP20 mRNA is abundant in Arabidopsis cells in log phase, TCP22 and TCP18 mRNAs are high in stationary cells, and TCP3 mRNA levels are equal in log and stationary cells. These four TCPs have been implicated in diverse functions in the literature. TCP20 affects germination, and seedling development (*29*). TCP22 plays a role in gibberellin response (*30*). TCP3 modulates leaf structure (*31*). TCP18 represses growth from axillary buds (*32*).

Their TCP domains (designated D) and C-termini beyond the TCP domain (designated C) were cloned as GST fusions using PCR (see Tables 2 and 3). The 100-amino acid TCP domains were TCP3(G29-N128), TCP18(Q130-G230), TCP20(S67-G166), and TCP22(A40-139). The C-termini, also tagged with GST, corresponded to TCP3(A127-H391), TCP18(R225-Y433), TCP20(H162-R324), and TCP22(R135-K375) and were designed to overlap the final amino acid of the TCP domain and extend to the end of the

protein. Each TCP and its corresponding truncations were incubated with GRIK and SnRK1 in the presence of 10 nmol ATP and 0.5 μCi P^{32} γ-ATP for 1h at 30°C (Fig. 6). Full-length (FL) TCP3 (lane 5), TCP20 (lane 6) and TCP22 (lane 6) were efficiently phosphorylated by SnRK1. The C-termini of TCP3 (lane 6) and TCP20 (lane 5) were also phosphorylated *in vitro*, but not their TCP domains (lane 4). The C-terminus of TCP22 (lane 5) was also phosphorylated, however the TCP domain of TCP22 was weakly phosphorylated (lane 4) although not sufficient to account for the strong phosphorylation of full-length TCP22. It was not as straight forward to assess SnRK1 phosphorylation of the different regions of TCP18 because *E. coli* produces truncated forms of TCP18. However, the truncations produced from the C-terminus of TCP18 were efficiently phosphorylated (lane 5), while the TCP domain was not (lane 4). Together, these results support our hypothesis that SnRK1 does not phosphorylate the TCP domain.

SnRK1 Target Sites in TCPs

To determine the exact locations of the TCP phosphorylation, we used LC/MS/MS analysis. Recombinant TCP3, TCP18, TCP20 and TCP22 proteins were incubated with GRIK and SnRK1, and analyzed via in-gel digestion (data not shown). These aquisitions yielded poor coverage and few sites, and TCP18 was unstable. However, S262 in TCP3 and S336 in TCP18 were implicated as phosphorylation sites in the spectra shown in Fig. 7 and Fig. 8, respectively. The sequence surrounding TCP3 S262 matched a consensus derived from known SnRK1 phosphorylation sites. An S336E mutant of TCP18 appeared to have

slightly lower concentrations of truncations than TCP18 WT. Additionally a phosphomimic mutant will allow for any possible secondary phosphorylations, where the chemical difference of phosphonulls like S336A does not. For these reasons, TCP3 S262E and TCP18 S336E were used for in solution digestions along with wild type TCP20 and TCP22 in subsequent experiments.

The amino acid sequences of the TCPs also provided challenges for mapping SnRK1 phosphorylation sites. Traditional trypsin digestion did not provide significant coverage because of distributions of arginine and lysine residues, which were either highly clustered (less than every 5 AA) or too spread out (more then every 15 AA). As a consequence, the resulting peptide fragments were outside the range of detection of the orbi-trap with a mass range of m/z 200 to 4,000. This is also true of the aromatic amino acids and aspartic acid, such that chymotrypsin and Asp_N were also not good tools for digesting the TCPs. However, the amino acid patterns for the three proteases were different and their combined coverages were sufficient to map the SnRK1 phosphorylation sites.

TCP3 S262E, TCP18 S336E, TCP20, and TCP22 were incubated with GRIK + SnRK1 in the presence of ATP in triplicate. Each reaction was digested with trypsin, chymotrypsin, or Asp_N overnight at 37°C, followed by acidification with the addition of formic acid (FA). Sample aliquots were enriched for phosphopetides via IMAC, producing three samples – unenriched, IMAC-enriched, and IMAC-flow through. The resulting samples were analyzed via LC-MS/MS. An Easy nLC tandem Orbi-trap Elite system was used with CID/ETD and HCD/ETD decision tree acquisition. Files were processed by

Proteome Discoverer and searched against the modified *E. coli* database with added standards and recombinant fusion proteins using MASCOT.

Analysis of TCP3 S262E yielded 90% coverage (Fig 7A) but because the MASCOT scores for the few phosphopeptides were below the accepted threshold no new phosphorylation sites were identified. The coverage of TCP18 S336E was 88% (Fig 8A), and two phosphopeptides corresponding to pS38 and pT233 were identified with MASCOT scores above the threshold (Fig 8B). TCP20 coverage was 98% (Fig 9A) with only two phosphopeptides indicating the same site, pS237 (Fig 9B). TCP22 had 84% coverage (Fig 10A) and one phosphopeptide at pS140 was identified (Fig 10B).

To verify the phosphorylation sites, the various sites were subjected to site-directed mutagenesis (see Tables 2 and 3) and the mutant TCP proteins were expressed in *E. coli*, affinity purified and analyzed in SnRK1 kinase reactions. Wild-type TCP and the mutant proteins were incubated with GRIK and SnRK1 as described above. Wild-type TCP3 (WT) and its S262A and S262E mutants were phosphorylated to equivalent levels by SnRK1, suggesting that S262 is not a phosphorylation site (Fig 7C). The site for TCP3 was not determined.

TCP18 S336E showed two additional phosphorylation sites pS38 and pT233. TCP18 contains serines at positions 36, 37 and 38 that are potential SnRK1 target sites. Hence, we analyzed individual and triple mutants – S36A, S37A, S38A, and S36A/S37A/S38A. We also analyzed the individual TCP18 mutants, S336A and S336E, and the combination mutant, S36A/S37A/S38A/S336E (Fig 11). Wild-type TCP18, S336A and 336E showed no

difference in phosphorylation, indicating that S336 is not a phosphorylation site. In contrast, S36A, S37A, S38A, and S36A/S37A/S38A were not phosphorylated by SnRK1 *in vitro*. In a longer exposure (not shown), a low level phosphorylation can be seen for S37A, reducing the likelihood that it is a phosphorylation site. Because of the proximity of S36 and S38, it is unlikely that both are phosphorylation sites. Based on the sequence contexts of other known SnRK1 phosphorylation sites, we hypothesize that Ser-38 is the phosphorylation site and Ser-36 is necessary for Ser-38 phosphorylation. We also analyzed a series of TCP18 mutants to assess if T233 is a SnRK1 phosphorylation site (Fig 8C). T233A and T233E only showed a slight reduction in phosphorylation relative to wild-type TCP. The combination mutants, S38A/T233D, S36E/T233D and S38E/T233D, had decreased phosphorylation and resembled the single mutants, S36A and S36E. No phosphorylation was seen for S38A, S38E and S36A/T233D. Thus, we were unable to confirm T233 as a SnRK1 target site in TCP18.

Wild-type TCP20, TCP22 and their mutants were also analyzed in SnRK1 kinase assays (Fig. 9C and 10C). High levels of phosphorylation were seen for wild-type TCP20 (Fig 9C, lane 4), and the S237A (lane 5) and S237E (lane 6) mutations resulted in a complete loss of phosphorylation. Similarly, wild-type TCP22 was strongly phosphorylated by SnRK1 *in vitro* (Fig. 10C, lane 4), and the S140A (lane 5) and S140E (lane 6) mutations resulted in a nearly complete loss of phosphorylation. Thus, TCP20 is phosphorylated by SnRK1 only at S237, while the predominant SnRK1 phosphorylation site in TCP22 is S140. Given that LC/MS/MS analysis did not uncover any additional sites in TCP22, we were unable to determine any additional sites.

The SnRK1 phosphorylation sites in TCP18, TCP20 and TCP22 are all located outside of the TCP domains, consistent with the truncation studies. The SnRK1 target sites in TCP20 and TCP22 are located on the C-terminal side of the TCP domain, while the sites in TCP18 are on either side of the TCP domain.

Optimization of TCP DNA Binding

Our next question was does SnRK1 phosphorylation alter the DNA binding properties of TCP20 or TCP22 even though its target sites are outside of their TCP domains. Before we could do this, it was necessary to optimize the DNA binding assays for TCP20 and TCP22. We first replaced the GST tag because it can form homodimers (*33*) and has the potential to alter the DNA binding properties of transcription factors like TCPs that bind to DNA as dimers. Moreover, the large size of the GST tag could interfere with DNA binding. We chose the GB tag, which is derived from IgG-binding-B and is used in NMR studies as a soluble tag (*34*). The GB tag is only 56 amino acids in length and does not dimerize. Wild-type TCP20 was designed as a GB-TCP-His fusion protein with and without an enterokinase cleavable tag and compared to GST-TCP20 on a native gel in the presence and absence of a double-stranded DNA oligonucleotide containing the TCP20 binding site (Fig12). The various TCP20 forms stayed near the top of the gel in the absence of DNA, indicating that they were in large complexes or aggregates (an unknown band was seen for GST-TCP20 that may be a contaminant). In contrast, in the presence of DNA, only GB-TCP20-His formed a unique band indicating the GB tag is the best candidate for TCP/DNA binding studies.

TCPs are believed to interact with dsDNA through helix I that extends from a basic region and helix II and connect by a disordered region (a loop) (*35*). This TCP domain also interacts with another TCP transcription factor froming homo or heterodimers (*21*). Previous studies showed that TCP20 binds to the DNA sequence GTGGGACCGG (*22*), but the DNA sequence bound by TCP22 was not known when we started our studies. Electrophoriesis Moblity Shift Assay (EMSA) were preformed with TCP22 and four variations on the dsDNA: GTGGGACCGG, GTGGGCCCGG, GTGGGGCCGG, and GTGGGTCCGG (data not shown). TCP22 was verified to bind the sequence variation GTGGGCCCGG.

DNA binding was examined using EMSA. Initially, fluorescent IR tags were covalently linked to the DNA oligonucleotides used for binding assays. As seen in Figure 13, as the amount of GB-TCP20-His binding to DNA increases, the total fluorescence in each reaction decreases, indicating a quenching event. One possibility was that quenching was due to the proximity of the protein to the fluorescent label. To circumvent this, we designed fluorescent-labeled primers to amplify an RPL24 promoter region for binding assays (Table 3). These primers were used to clone the RPL24 promoter region from Arabidopsis Col-0 genomic DNA. The product was sequenced to verify that it was a clone of the RPL24 promoter region, before use in EMSAs. Unfortunately, total fluorescence intensity still decreased inversely to protein concentration (Fig. 14), indicating that moving the fluorescent label away from the TCP protein does not reduced quenching. For these reasons, we used radiolabeled double-stranded oligonucleotids for all subsequent EMSA reactions.

SnRK1 Phosphorylation Does Not Alter TCP-DNA Interactions *in vitro*

SnRK1 is a master regulator, and it is likely that SnRK1 phosphorylation of TCPs affects transcription directly or indirectly. To gain insight into the consequences of TCP phosphorylation, we compared a number of characteristics of wild-type TCP20 and TCP22 to their phosphonull and phosphomimic mutants. We first asked if phosphorylation had an effect on TCP DNA binding in EMSAs. The potential impact of SnRK1 phosphorylation on DNA binding specificity was assessed by incubating TCP20 WT, S237A, S237E, and S237N (0.1 μM) with 25 nM of a radiolabeled dsDNA containing the TCP20 DNA binding consensus in the presence of increasing amounts (0-1 mM) of unlabeled competitor dsDNA with a sequence not bound by class I TCPs. The reaction products were resolved on a 4% acrylamide gel in TBE buffer, and the gels were dried, imaged by autoradiograph (not shown), and quantified using Storm 865 and Image 069 Snapshot 2 software (Fig. 15B and 15D). Binding curves were determined for each protein in each gel using Microsoft Excel 2013 Solver.

TCP20 and its mutants required a 3000-4000 fold excess of nonspecific dsDNA to radiolabeled specific dsDNA for 50% loss of binding activity (Fig15B), indicating that the phosphonull and phosphomimic mutants of TCP20 bind to DNA with high specificity like wild-type TCP20. We then asked if SnRK1 phosphorylation has the potential to alter the DNA binding constant of TCP20. TCP20 WT, S237A, S237E, and S237N were incubated in triplicate over a range of concentrations (0-0.8 μM) with 0.05 μM of a radiolabeled dsDNA

containing the TCP20 DNA binding consensus. The binding assays were analyzed as described above. The binding curves of TCP20 and its mutants showed no significant difference (Fig 16), indicating the phosphorylation has no impact on DNA binding affinity *in vitro*.

The equivalent EMSAs were performed for TCP22 and its phosphonull and phosphomimic mutants using the DNA binding consensus identified above. DNA binding specificity was assessed by incubating TCP22 WT, S140A, S140E, and S140N (0.15 μM) with 25 nM radiolabeled dsDNA containing the TCP22 DNA binding consensus in the presence of increasing amounts (0-1.0 mM) of unlabeled, nonspecific competitor dsDNA, and the reaction products were analyzed as described above. TCP22 and its mutants required >7000-fold excess of nonspecific dsDNA to radiolabeled dsDNA for 50% loss of binding activity (Fig15D), indicating that the TCP22 mutants also bind to DNA with high specificity like wild-type TCP22. We also analyzed the effect of protein concentration on the binding activities of TCP22 and its mutants. TCP22 WT, S140A, S140E, and S140N were incubated in triplicate over a range of concentrations (0-1.6 μM) with 0.05 μM of a radiolabeled dsDNA containing the TCP22 DNA binding consensus, the binding reactions were analyzed as described above. The binding curves of TCP22 and its mutants were essentially identical (Fig 17), indicating the phosphorylation has no impact on DNA binding affinity *in vitro*.

Together, our results establish that SnRK1 phosphorylation of TCP20 and TCP22 does not alter their DNA binding properties. An extension of this conclusion is that SnRK1 phosphorylation does not impact TCP dimerization, which is required for DNA binding(*21*).

These results are consistent with the fact that TCP20 S237 and TCP22 S140 are outside of the TCP binding domain.

SnRK1 Phosphorylation Impairs TCP Interaction with a Chromatin Remodeling Protein

The SnRK1 phosphorylation sites in TCP20 and TCP22 might be in regions that interact with other proteins. A yeast two-hybrid (Y2H) study identified TCP20 and TCP22 as potential partners of BRM and SWI-3C, components of the SWI/SNF chromatin-remodeling complex in Arabidopsis (*36*). In collaboration with Dr. Doris Wagner's group (University of Pennsylvania), we asked if SnRK1 phosphorylation impacts TCP20 or TCP22 interactions with BRM and SWI-3C. We constructed Y2H plasmids that expressed wild-type TCP20 or its S237A, S237E and S237N mutants or wild-type TCP22 or its S140A or S140E mutants as fusions to the GAL4 activation domain (AD). The TCP AD plasmids were cotransfected into yeast with plasmids carrying GAL4 DNA binding domain (DBD) fusions to BRM or SWI-3C. The resulting yeast transformants were grown on medium lacking tryptophan and leucine to confirm the presence of the plasmids and that expression of the bait and prey proteins are toxic. The yeast transformants were then grown on medium also lacking histidine and supplemented with 3–Amino-1,2,4–triazole and monitored for growth indicative of protein interaction (these assays were preformed by Soon-Ki Han).

In Y2H assays using the BRM-DBD fusion as bait (Fig18A), growth was detected when the prey were AD-fusions for wild-type TCP20, thereby confirming the earlier study

indicating interaction between TCP20 and BRM. The TCP20 phosphonull mutants S237A and S237N also grew in the absence of histidine to similar levels as wild-type TCP20, establishing that mutation of S237 to alanine or asparigine does not impair interaction. In contrast, very little growth was seen for the phosphomimic mutant S237E, suggesting that SnRK1 phosphorylation of TCP20 interferes with its binding to BRM.

The results with TCP22 were less clear-cut because only the phosophonull S140A mutant grew efficiently in the absence of histidine, indicative of interaction with BRM (Fig. 18A). In contrast, both wild-type TCP22 and its phosphomimic S140E showed minimal growth in the absence of histidine. Although we cannot rule out S140A is a gain-of-function mutant for binding to BRM, a more likely explanation is that wild-type TCP22 is efficiently phosphorylated by SNF1, the endogenous SnRK1 homolog in yeast. According to this scenario, SNF1 phosphorylation of TCP22 interferes with BRM binding, consistent with the inability of S140E to bind to BRM. When S140 is mutated to an alanine, it cannot be phosphorylated by SNF1 and binding to BRM occurs. Unlike BRM, none of the TCP-AD constructs were positive for growth in the absence of histidine in assays using SWI-3C as bait (Fig. 19).

We then examined the interactions between TCP20 or TCP22 with BRM in plants using a quantitative bimolecular fluorescence complementation assay (BiFC) (*27*). We constructed plant expression cassettes in which wild-type TCP20, TCP22 and their phosphorylation mutants were fused to the C-terminus of YFP (Tables 2 and 3). The TCP expression cassettes were DNA-PEG–calcium transfected into Arabidopsis mesophyll

protoplasts along with a plant expression cassette specifying SWI3C or BRM fused to the YFP N-terminus, and the ratio of fluorescent protoplast nuclei to total protoplasts was determined. For each construct, 300-500 nuclei were scored in a bioreplicate, and the average ratio over 3 bioreplicates used as an indirect measure of binding efficiency (the analyses were conducted by Dr. Jun Xiao in the Wagner lab.) Consistent with the Y2H data, no fluorescent protoplasts were observed in agroinfiltrations containing the N-YFP-SWI3C cassette in combination with any of the C-YFP-TCP cassettes. Thus TCP20 and TCP22 do not interact with SWI3C or their interactions are too weak or transient to be detected by BiFC.

Unlike SWI3C, fluorescent protoplasts were observed in agroinfiltrations containing the N-YFP-BRM cassette in combination with all the C-YFP-TCP cassettes. The ratio of fluorescent protoplasts varied between the different C-YFP-TCP fusions, indicating that their relative BRM binding efficiencies differed (Fig. 18B). The TCP22 phosphonull mutants, S140A and S140N, had the highest fractions of fluorescent protoplasts with their ratios two-fold greater than wild-type TCP22 and S140E. The TCP20 S237N phosphonull mutant also showed a moderate but significant increase in the ratio of protoplasts in which binding to BRM occurred relative to wild-type TCP20 and S237E (a corresponding increase was not seen for S237A but analysis of transgenic Arabidopsis cell lines has indicated that the alanine substitution has pleotropic effects and the mutant protein is inactivate *in planta*). The reduced BRM binding of the phosphomimics relative the phosphonull mutants supports the idea that SnRK1 phosphorylation interferes with the binding of both TCP20 and TCP22 to

BRM. The similar BRM binding seen for wild-type TCP20 and TCP22 and their phosphomimics is consistent with the wild-type proteins existing primarily as their phosphoforms at S237 and S140, respectively, *in planta.* In this scenario, removal of the phosphate groups by an unknown protein phosphatase(s) may play a crucial role in regulating TCP20 and TCP22 interactions with BRM and in the recruitment of the SWI/SNF chromatin remodeling complex for transcription. Alternatively, SnRK1 may play a regulatory role in protliferating cell types, whereas in mesophyllic cells TCP20 and TCP22 may be maintained in an inactive state, but further analysis is need to determine if this is probable.

DISCUSSION

We showed that although the activation loop phosphomimic mutant of SnRK1, S175E, can support phosphorylation of a peptide substrate, it is unable to phosphorylate TCP22, a known SnRK1 protein substrate. Thus, it is necessary to use GRIK to activate SnRK1 for kinase assays using protein substrates. We developed a method for preactivating SnRK1 using GRIK and removing the upstream kinase by a two-step affinity purification. We used preactivated SnRK1 to study the phosphorylation of 23 of the 24 TCP family members in Arabidopsis. Phosphorylation was not specific to the entire family or one class of TCPs and we predicted and showed that the phosphorylation sites were outside of the conserved TCP DNA binding domain using TCP protein truncations and mapping of phosphoamino acids by LC/MS/MS. We identified two SnRK1 phosphorylation sites in TCP18 (S36 or S38 and T233) and one each in TCP20 (S237) and TCP22 (S140). EMSA

studies of TCP20, TCP22, and their phosphonull and phosphomimic mutants showed no significant difference in their binding to dsDNA, indicating that SnRK1 phosphorylation has no impact on their DNA binding activity *in vitro*. This observation is consistent with the fact that the SnRK1 phosphorylation sites in TCP20 and TCP22 are outside of the TCP binding domain. The absence of an affect on DNA binding also indicates that phosphorylation dose not alter the formation of homodimers. In contrast, results from Y2H and quantitative BIFC assays support the idea that SnRK1 phosphorylation reduces TCP20 and TCP22 interactions with BRM, a subunit of the SWI/SNF chromatin-remodeling complex. Recruitment of the SWI/SNF chromatin-remodeling complex by transcription factors is vital for function (*37-40*). Our BRM interaction data also suggest that wild-type TCP20 and TCP22 are mostly phosphorylated by SnRK1 *in vivo*. If this is the case, that removal of the phosphate groups by an unknown protein phosphatase(s) may play a crucial role in regulating TCP20 and TCP22 interactions with BRM and in the recruitment of the SWI/SNF chromatin remodeling complex for transcription. Future experiments using mass spectrometry and anti-phosphoserine antibodies will examine the phosphorylation status of TCP20 and TCP22 in plant cells and address this possibility directly.

FIGURES AND TABLES

Table 1. An Arabidopsis cDNA library (4×10^6) was screened in yeast two-hybrid assays under stringent conditions using GRIK1 or GRIK2 as bait. Data provided by Wei Shen and Maria Reyes.

Protein	Locus	GRIK1 interaction	GRIK2 interaction
TCP13	At3g02150	strong	Strong
TCP14	At3g47620	weak	Weak
TCP15	At1g69690	weak	Weak
TIFY2a	At3g21175	strong	Weak
NAC2	At5g04410	weak	None

Table 2. Plasmid for expressing Recombinant Proteins in *E. coli*

Fusion Protein	Method	Accession #	pNSB #	cDNA source	F Primer	R Primer	RE digestion	Vector	Resistence	Expression line
His-GRIK1	In lab	At3g45240	1451	-	-	-	-	-	Amp	BL21 (DE3)
His-SnRK1.1 (fl)	In lab	At3g01090.1	1490	-	-	-	-	-	Amp	BL21 (DE3)
His-SnRK1.1 (kd) M1-Y341	In lab	At3g01090.1	1494	-	-	-	-	-	Amp	BL21 (DE3)
GST-GRIK1	In lab	At3g45240	1554	-	-	-	-	-	Amp	BL21 (DE3)
GST-GRIK1 K137A	In lab	At3g45240	1555	-	-	-	-	-	Amp	BL21 (DE3)
GST-TIFY2b	PCR	At3g21175	1728	U15151	GSTGIP 1 F2	GSTGIP1 R	BglII/XhoI	BamHI/XhoI pGEX-5x3	Amp	BL21 (DE3)
GST-NAC	PCR	At5g04410	1730	U24865	GSTGIP 11 F2	GSTGIP11 R	BglII/XhoI	BamHI/XhoI pGEX-5x3	Amp	BL21 (DE3)
GST-TCP16	PCR	At3g45150	1791	Arabidopsisb young leaf cDNA	TCP16F	TCP16R	BglII/XhoI	BamHI/XhoI pGEX-5x3	Amp	BL21 (DE3)
GST-TCP11	PCR	At2g37000	1759	U63429	TCP11F	TCP11R	BamHI/Not I	BamHI/NotI pGEX-5x3	Amp	BL21 (DE3)
GST-TCP20	PCR	At3g27010	1794	U50934	TCP20F3	TCP20R2	BglII/XhoI	BamHI/XhoI pGEX-5x3	Amp	BL21 (DE3)
GST-TCP6	PCR	At5g41030	1787	Arabidopsisb young leaf cDNA	TCP6F	TCP6R	BamHI/Xh oI	BamHI/XhoI pGEX-5x3	Amp	BL21 (DE3)
GST-TCP15	PCR	At1g69690	1731	U14268	GSTGIP 17 F2	GSTGIP17 R	EcoRV/Xh oI	BamHI/Kleno w/XhoI pGEX-5x3	Amp	BL21 (DE3)
GST-TCP14	PCR	At3g47620	1732	U14172	GSTGIP 38F2	GSTGIP38 R	BglII/XhoI	BamHI/XhoI pGEX-5x3	Amp	BL21 (DE3)

Table 2. Plasmid for expressing Recombinant Proteins in *E. coli* (continued)

Fusion Protein	Method	Accession #	pNSB #	cDNA source	F Primer	R Primer	RE digestion	Vector	Resistence	Expression line
GST-TCP21	PCR	At5g08330	1755	U13511	TCP1F	TCP1R	BamHI/NotI	BamHI/NotI pGEX-5x3	Amp	BL21 (DE3)
GST-TCP7	PCR	At5g23180	1788	Arabidopsisb young leaf cDNA	TCP7F	TCP7R	BamHI/XhoI	BamHI/XhoI pGEX-5x3	Amp	BL21 (DE3)
GST-TCP8	PCR	At1g58100	1756	U24662	TCP8F	TCP8R	BamHI/XhoI	BamHI/XhoI pGEX-5x3	Amp	BL21 (DE3)
GST-TCP23	PCR	AT1G35560	1796	Arabidopsisb young leaf cDNA	TCP23F	TCP23R	EcoRV/XhoI	BamHI/Klenow/XhoI pGEX-5x3	Amp	BL21 (DE3)
GST-TCP22	PCR	AT1G72010	1795	U10497	TCP22F2	TCP22R2	BglII/NotI	BamHI/NotI pGEX-5x3	Amp	BL21 (DE3)
GST-TCP19	PCR	At5g51910	1793	Arabidopsisb young leaf cDNA	TCP19F	TCP19R	BglII/XhoI	BamHI/XhoI pGEX-5x3	Amp	BL21 (DE3)
GST-TCP9	PCR	At2g45680	1789	U10678	TCP9F3	TCP9R3	BamHI/NotI	BamHI/NotI pGEX-5x3	Amp	BL21 (DE3) with pG-Tf2
GST-TCP18	PCR	At3g18550	1792	Arabidopsisb young leaf cDNA	TCP18F	TCP18R	BglII/XhoI	BamHI/XhoI pGEX-5x3	Amp	BL21 (DE3)
GST-TCP12	PCR	At1g68800	1760	U87032	TCP12F	TCP12R	BamHI/XhoI	BamHI/XhoI pGEX-5x3	Amp	BL21 (DE3)
GST-TCP1.1	PCR	At1g67260.1	1817	Columbia-0 Geneomic DNA	TCP1F3	TCP1.1R	BamHI/XhoI	BamHI/XhoI pGEX-5x3	Amp	BL21 (DE3)

Table 2. Plasmid for expressing Recombinant Proteins in *E. coli* (continued)

Fusion Protein	Method	Accession #	pNSB #	cDNA source	F Primer	R Primer	RE digestion	Vector	Resistence	Expression line
GST-TCP10	PCR	At2g31070	1790	U17110	TCP10F2	TCP10R2	BamHI/XhoI	BamHI/XhoI pGEX-5x3	Amp	BL21 (DE3)
GST-TCP4	PCR	At3g15030	1818	Columbia-0 Geneomic DNA	TCP4F	TCP4R	BamHI/XhoI	BamHI/XhoI pGEX-5x3	Amp	BL21 (DE3) with pG-KJE8
GST-TCP3	PCR	At1g53230	1757	U24911	TCP3F	TCP3R	BamHI/XhoI	BamHI/XhoI pGEX-5x3	Amp	BL21 (DE3) with pG-Tf2
GST-TCP13	PCR	At3g02150	1729	U15321	GSTGIP3F2	GSTGIP3R	BglII/XhoI	BamHI/XhoI pGEX-5x3	Amp	BL21 (DE3)
GST-TCP5	PCR	At5g60970	1819	Columbia-0 cDNA	TCP5F2	TCP5R	BamHI/NotI	BamHI/NotI pGEX-5x3	Amp	BL21 (DE3)
GST-TCP24	PCR	At1g30210	1754	U09765	TCP24F	TCP24F	BamHI/XhoI	BamHI/XhoI pGEX-5x3	Amp	BL21 (DE3)
GST-TCP2	PCR	At4g18390	1786	Arabidopsisb young leaf cDNA	TCP2F2	TCP2R2	BamHI/XhoI	BamHI/XhoI pGEX-5x3	Amp	BL21 (DE3) with pG-Tf2
GST-SnRK1.1 (fl)	PCR	At3g01090.1	1833	pNSB1490	SnRK1.1 F2	SnRK1.1 R2	BamHI/XhoI	BamHI/XhoI pGEX-5x3	Amp	BL21 (DE3)
GST-SnRK1.1 (fl) T175E	PCR	At3g01090.1	1834	pNSB1831	SnRK1.1 F2	SnRK1.1 R2	BamHI/XhoI	BamHI/XhoI pGEX-5x3	Amp	BL21 (DE3)
GST-TCP3 domain G29-N128	PCR	At1g53230	1887	pNSB1757	TCP3dF	TCP3dR	BamHI/XhoI	BamHI/XhoI pGEX-5x3	Amp	BL21 (DE3)
GST-TCP18 domain Q130-G230	PCR	At3g18550	1889	pNSB1792	TCP18dF	TCP18dR	BamHI/XhoI	BamHI/XhoI pGEX-5x3	Amp	BL21 (DE3)

Table 2. Plasmid for expressing Recombinant Proteins in *E. coli* (continued)

Fusion Protein	Method	Accession #	pNSB #	cDNA source	F Primer	R Primer	RE digestion	Vector	Resistence	Expression line
GST-TCP20 domain S67-G166	PCR	At3g27010	1891	pNSB1794	TCP20dF3	TCP20dR	BamHI/XhoI	BamHI/XhoI pGEX-5x3	Amp	BL21 (DE3)
GST-TCP22 domain A40-139	PCR	At1g72010	1893	pNSB1795	TCP22dF	TCP22dR	BamHI/XhoI	BamHI/XhoI pGEX-5x3	Amp	BL21 (DE3)
GST-TCP3 C-term A127-H391	PCR	At1g53230	1888	pNSB1757	TCP3A127F	TCP3R	BamHI/XhoI	BamHI/XhoI pGEX-5x3	Amp	BL21 (DE3)
GST-TCP18 C-termR225-Y433	PCR	At3g18550	1890	pNSB1792	GSTTCP18 R453F	TCP18R	BamHI/XhoI	BamHI/XhoI pGEX-5x3	Amp	BL21 (DE3)
GST-TCP20 C-term H162-R324	PCR	At3g27010	1892	pNSB1794	TCP20H153F	TCP20R	BamHI/XhoI	BamHI/XhoI pGEX-5x3	Amp	BL21 (DE3)
GST-TCP22 C-term R135-K375	PCR	At1g72010	1894	pNSB1795	TCP22R135F	TCP22R	BamHI/XhoI	BamHI/XhoI pGEX-5x3	Amp	BL21 (DE3)
GB-TCP20S237A-His	PCR	At3g27010	2014	pNSB1960	GB-TCP20F	GB-TCP20R	BglII/XhoI	BamHI/XhoI pET30A-GB	Kan	BL21 (DE3)
GB-TCP20S237E-His	Mutagenesis-Q5	At3g27010	2015	pNSB2006	TCP20S237E F	TCP20S237E R	-	-	Kan	BL21 (DE3)
GB-TCP22WT-His	PCR	At1g72010	2016	pNSB1795	GB-TCP22 F	GB-TCP22 R	BamHI/XhoI	BamHI/XhoI pET30A-GB	Kan	BL21 (DE3)

Table 2. Plasmid for expressing Recombinant Proteins in *E. coli* (continued)

Fusion Protein	Method	Accession #	pNSB #	cDNA source	F Primer	R Primer	RE digestion	Vector	Resistence	Expression line
GB-TCP22S140A-His	PCR	At1g72010	2017	pNSB1942	GB-TCP22 F	GB-TCP22 R	BamHI/XhoI	BamHI/XhoI pET30A-GB	Kan	BL21 (DE3)
GB-TCP22S140E-His	PCR	At1g72010	2018	pNSB1959	GB-TCP22 F	GB-TCP22 R	BamHI/XhoI	BamHI/XhoI pET30A-GB	Kan	BL21 (DE3)
GST-TCP20(fl) S237N	Mutagenesis-Pfu	At1g72010	2020	pNSB1794					Amp	BL21 (DE3)
TCP20WT in pDONR221	PCR	At1g72010	2023	pNSB1794	Y2H TCP20 F	Y2H TCP20 R	Gateway BP clonase II	pDONR221	Kan	
TCP20 S237A in pDONR221	PCR	At1g72010	2024	pNSB1960	Y2H TCP20 F	Y2H TCP20 R	Gateway BP clonase II	pDONR221	Kan	
TCP20 S237E in pDONR221	Mutagenesis-Pfu	At1g72010	2025	pNSB2023	TCP20S237E F	TCP20S237E R	-	-	Kan	
TCP20 S237N in pDONR221	PCR	At1g72010	2026	pNSB2020	Y2H TCP20 F	Y2H TCP20 R	Gateway BP clonase II	pDONR221	Kan	
TCP22WT in pDONR221	PCR	At1g72010	2027	pNSB1795	Y2H TCP22 F	Y2H TCP22 R	Gateway BP clonase II	pDONR221	Kan	
TCP22 S140A in pDONR221	PCR	At1g72010	2028	pNSB1942	Y2H TCP22 F	Y2H TCP22 R	Gateway BP clonase II	pDONR221	Kan	
TCP22 S140E in pDONR221	PCR	At1g72010	2029	pNSB1959	Y2H TCP22 F	Y2H TCP22 R	Gateway BP clonase II	pDONR221	Kan	
TCP20WT in pDEST22	Gateway ligation	At3g27010	2030	pNSB2023	-	-	Gateway LR clonase II	pDEST22	Kan	yeast
TCP20 S237A in pDEST22	Gateway ligation	At3g27010	2031	pNSB2024				pDEST22	Kan	yeast
TCP20 S237E inpDEST22	Gateway ligation	At3g27010	2032	pNSB2025	-	-	Gateway LR clonase II	pDEST22	Kan	yeast

Table 2. Plasmid for expressing Recombinant Proteins in *E. coli* (continued)

Fusion Protein	Method	Accession #	pNSB #	cDNA source	F Primer	R Primer	RE digestion	Vector	Resistence	Expression line
TCP20 S237N inpDEST22	Gateway ligation	At3g27010	2033	pNSB2026	-	-	Gateway LR clonase II	pDEST22	Kan	yeast
TCP22WT inpDEST22	Gateway ligation	At1g72010	2034	pNSB2027	-	-	Gateway LR clonase II	pDEST22	Kan	yeast
TCP22 S140A inpDEST22	Gateway ligation	At1g72010	2035	pNSB2028	-	-	Gateway LR clonase II	pDEST22	Kan	yeast
TCP22 S140E inpDEST22	Gateway ligation	At1g72010	2036	pNSB2029	-	-	Gateway LR clonase II	pDEST22	Kan	yeast
GST-TCP22(fl) S140N	Mutagenesis-Pfu	At1g72010	2042	pNSB1795	TCP22S140N F	TCP22S140N R	-	-	Amp	BL21 (DE3)
GB-TCP22S140N-His	Mutagenesis-Pfu	At1g72010	2043	pNSB2016	TCP22S140N F	TCP22S140N R	-	-	Kan	BL21 (DE3)
CeYFP-TCP20WT	PCR	At3g27010 At1g72010	2044	pNSB2006	BiFCTCP20F	CeYFPTCP20R	SpeI/XhoI	SpeI/BanI pSPYCE (MR)	Amp	mesophyll protoplasts
CeYFP-TCP20 S237A	PCR	At1g72010	2045	pNSB2014	BiFCTCP20F	CeYFPTCP20R	SpeI/XhoI	SpeI/BanI pSPYCE (MR)	Amp	mesophyll protoplasts
CeYFP-TCP20 S237E	PCR	At1g72010	2046	pNSB2015	BiFCTCP20F	CeYFPTCP20R	SpeI/XhoI	SpeI/BanI pSPYCE (MR)	Amp	mesophyll protoplasts
CeYFP-TCP20 S237N	PCR	At1g72010	2047	pNSB2020	BiFCTCP20F	CeYFPTCP20R	SpeI/XhoI	SpeI/BanI pSPYCE (MR)	Amp	mesophyll protoplasts
CeYFP-TCP22WT	PCR	At1g72010	2048	pSNB2016	BiFCTCP22F	CeYFPTCP22R	SpeI/BamHI	SpeI/BamHI pSPYCE (MR)	Amp	mesophyll protoplasts

Table 2. Plasmid for expressing Recombinant Proteins in *E. coli* (continued)

Fusion Protein	Method	Accession #	pNSB #	cDNA source	F Primer	R Primer	RE digestion	Vector	Resistence	Expression line
CeYFP-TCP22 S140A	PCR	At1g72010	2049	pNSB2017	BiFCTCP 22F	CeYFPTC P22R	SpeI/BamHI	SpeI/BamHI pSPYCE (MR)	Amp	mesophyll protoplasts
CeYFP-TCP22 S140E	PCR	At1g72010	2050	pNSB2018	BiFCTCP 22F	CeYFPTC P22R	SpeI/BamHI	SpeI/BamHI pSPYCE (MR)	Amp	mesophyll protoplasts
CeYFP-TCP22 S140N	PCR	At1g72010	2051	pNSB2043	BiFCTCP 22F	CeYFPTC P22R	SpeI/BamHI	SpeI/BamHI pSPYCE (MR)	Amp	mesophyll protoplasts
NeYFP-TCP20WT	PCR	At3g27010	2052	pNSB2006	BiFCTCP 20F	NeYFPTC P20R	SpeI/XmaI	SpeI/XmaI pSPYNE (R) 173	Amp	mesophyll protoplasts
NeYFP-TCP20 S237A	PCR	At3g27010	2053	pNSB2014	BiFCTCP 20F	NeYFPTC P20R	SpeI/XmaI	SpeI/XmaI pSPYNE (R) 173	Amp	mesophyll protoplasts
NeYFP-TCP20 S237E	PCR	At3g27010	2054	pNSB2015	BiFCTCP 20F	NeYFPTC P20R	SpeI/XmaI	SpeI/XmaI pSPYNE (R) 173	Amp	mesophyll protoplasts
NeYFP-TCP20 S237N	PCR	At3g27010	2055	pNSB2020	BiFCTCP 20F	NeYFPTC P20R	SpeI/XmaI	SpeI/XmaI pSPYNE (R) 173	Amp	mesophyll protoplasts
NeYFP-TCP22WT	PCR	At1g72010	2056	pSNB2016	BiFCTCP 22F	NeYFPTC P22R	SpeI/XmaI	SpeI/XmaI pSPYNE (R) 173	Amp	mesophyll protoplasts
NeYFP-TCP22 S140A	PCR	At1g72010	2057	pNSB2017	BiFCTCP 22F	NeYFPTC P22R	SpeI/XmaI	SpeI/XmaI pSPYNE (R) 173	Amp	mesophyll protoplasts

Table 2. Plasmid for expressing Recombinant Proteins in *E. coli* (continued)

Fusion Protein	Method	Accession #	pNSB #	cDNA source	F Primer	R Primer	RE digestion	Vector	Resistence	Expression line
NeYFP-TCP22 S140E	PCR	At1g72010	2058	pNSB2018	BiFCTCP 22F	NeYFPTC P22R	SpeI/XmaI	SpeI/XmaI pSPYNE (R) 173	Amp	mesophyll protoplasts
NeYFP-TCP22 S140N	PCR	At1g72010	2059	pNSB2043	BiFCTCP 22F	NeYFPTC P22R	SpeI/XmaI	SpeI/XmaI pSPYNE (R) 173	Amp	mesophyll protoplasts
GB-TCP20 S237N-His	PCR	At3g27010	2061	pNSB2020	GB-TCP20F	GB-TCP20R	BamHI/XhoI	BamHI/XhoI pET30A-GB	Kan	BL21 (DE3)
His-SnRK1.1 (kd) T175D	Mutagenesis-Pfu	At3g01090.1	1753	pNSB 1494	SnRK1 1T198D F	SnRK1 1T198D R	-	-	Amp	BL21 (DE3)
His-SnRK1.1 (kd) T175E	Mutagenesis-Pfu	At3g01090.1	1815	pNSB 1753	SnRK1.1T 198E F	SnRK1.1T 198E R	-	-	Amp	BL21 (DE3)
His-SnRK1.1 (fl) T175E	Mutagenesis-Pfu	At3g01090.1	1831	pNSB 1490	SnRK1.1T 198E F	SnRK1.1T 198E R	-	-	Amp	BL21 (DE3)
His-SnRK1.1 (kd) T175E/S176D	Mutagenesis-Pfu	At3g01090.1	1850	pNSB 1494	SnRK1.1 T175E/S1 76D F	SnRK1.1 T175E/S1 76D R	-	-	Amp	BL21 (DE3)
His-SnRK1.1 (fl) T175E/S176D	Mutagenesis-Pfu	At3g01090.1	1853	pNSB 1490	SnRK1.1 T175E/S1 76D F	SnRK1.1 T175E/S1 76D R	-	-	Amp	BL21 (DE3)
GST-TCP22(fl) S140A	Mutagenesis-Pfu	At1g72010	1942	pNSB1975	TCP22S1 40A F	TCP22S1 40A R	-	-	Amp	BL21 (DE3)
GST-TCP18(fl)T233A	Mutagenesis-Pfu	At3g18550	1954	pNSB1792	TCP18T2 33A F	TCP18T2 33A R	-	-	Amp	BL21 (DE3)
GST-TCP22(fl) S140E	Mutagenesis-Pfu	At1g72010	1959	pNSB1795	TCP22S1 40E F	TCP22S1 40E R	-	-	Amp	BL21 (DE3)

Table 2. Plasmid for expressing Recombinant Proteins in *E. coli* (continued)

Fusion Protein	Method	Accession #	pNSB #	cDNA source	F Primer	R Primer	RE digestion	Vector	Resistence	Expression line
GST-TCP20(fl) S237A	Mutagenesis-Pfu	At3g27010	1960	pNSB1794	TCP20S237A F	TCP20S237A R	-	-	Amp	BL21 (DE3)
GST-TCP20(fl) S237E	Mutagenesis-Pfu	At3g27010	1961	pNSB1794	TCP20S237E F	TCP20S237E R	-	-	Amp	BL21 (DE3)
GST-TCP3(fl) S262A	Mutagenesis-Pfu	At1g53230	1925	pNSB1757	TCP3S262AF	TCP3S262A R	-	-	Amp	BL21 (DE3)
GST-TCP3(fl) S262E	Mutagenesis-Pfu	At1g53230	1969	pNSB1757	TCP3S262E F	TCP3S262E R	-	-	Amp	BL21 (DE3)
GST-TCP18(fl) S36A/S37A/S38A	Mutagenesis-Pfu	At3g18550	1970	pNSB1792	TCP18S336AS37AS38A F	TCP18S336AS37AS38A R	-	-	Amp	BL21 (DE3)
GST-TCP18(fl) S336A	Mutagenesis-Pfu	At3g18550	1971	pNSB1792	TCP18S336A F	TCP18S336A R	-	-	Amp	BL21 (DE3)
GST-TCP18(fl) S336E	Mutagenesis-Pfu	At3g18550	1972	pNSB1792	TCP18S336E F	TCP18S336E R	-	-	Amp	BL21 (DE3)
GST-TCP18(fl) S36A	Mutagenesis-Pfu	At3g18550	1982	pNSB1792	TCP18S36A F	TCP18S36A R	-	-	Amp	BL21 (DE3)
GST-TCP18(fl) S37A	Mutagenesis-Q5	At3g18550	1983	pNSB1792	TCP18S37A F	TCP18S37A R	-	-	Amp	BL21 (DE3)
GST-TCP18(fl) S38A	Mutagenesis-Pfu	At3g18550	1984	pNSB1792	TCP18S38A F	TCP18S38A R	-	-	Amp	BL21 (DE3)
GST-TCP18(fl) S36AS37AS38A S336E	Mutagenesis-Q5	At3g18550	1985	pNSB1970	TCP18S336E F	TCP18S336E R	-	-	Amp	BL21 (DE3)
GST-TCP18(Cterm) S336A	Mutagenesis-Q5	At3g18550	1986	pNSB1890	TCP18S336A F	TCP18S336A R	-	-	Amp	BL21 (DE3)

Table 2. Plasmid for expressing Recombinant Proteins in *E. coli* (continued)

Fusion Protein	Method	Accession #	pNSB #	cDNA source	F Primer	R Primer	RE digestion	Vector	Resistence	Expression line
GST-TCP18(Cterm) S336E	Mutagenesis-Pfu	At3g18550	1988	pNSB1890	TCP18S3 36E F	TCP18S3 36E R	-	-	Amp	BL21 (DE3)
GST-TCP18(fl) S36E	Mutagenesis-Q5	At3g18550	1992	pNSB1792	TCP18S3 6E F	TCP18S3 6E R	-	-	Amp	BL21 (DE3)
GST-TCP18(fl) S38E	Mutagenesis-Q5	At3g18550	1993	pNSB1792	TCP18S3 8E F	TCP18S3 8E R	-	-	Amp	BL21 (DE3)
GST-TCP18(fl) T233D	Mutagenesis-Q5	At3g18550	1994	pNSB1792	TCP18T2 33D F2	TCP18T2 33D R2	-	-	Amp	BL21 (DE3)
GST-TCP18(fl) S36ET233A	Mutagenesis-Q5	At3g18550	1995	pNSB1954	TCP18S3 6E F	TCP18S3 6E R	-	-	Amp	BL21 (DE3)
GST-TCP18(fl) S38ET233A	Mutagenesis-Q5	At3g18550	1996	pNSB1954	TCP18S3 8E F	TCP18S3 8E R	-	-	Amp	BL21 (DE3)
GST-TCP18(fl) S36AT233D	Mutagenesis-Q5	At3g18550	1997	pNSB1982	TCP18T2 33D F2	TCP18T2 33D R2	-	-	Amp	BL21 (DE3)
GST-TCP18(fl) S38AT233D	Mutagenesis-Q5	At3g18550	1998	pNSB1984	TCP18T2 33D F2	TCP18T2 33D R2	-	-	Amp	BL21 (DE3)
GB-TCP20WT-His	PCR	At3g27010	2006	pNSB1794	GB-TCP20F	GB-TCP20R	BglII/XhoI	BamHI/XhoI pET30A-GB	Kan	BL21 (DE3)
GB-EntK-TCP20WT-His	PCR	At3g27010	2007	pNSB1794	GB-EntK-TCP20 F	GB-TCP20R	BglII/XhoI	BamHI/XhoI pET30A-GB	Kan	BL21 (DE3)
GST-TCP18(fl) S36ET233D	Mutagenesis-Q5	At3g18550	2011	pNSB1992	TCP18T2 33D F2	TCP18T2 33D R2	-	-	Amp	BL21 (DE3)
GST-TCP18(fl) S38ET233D	Mutagenesis-Q5	At3g18550	2012	pNSB1993	TCP18T2 33D F2	TCP18T2 33D R2	-	-	Amp	BL21 (DE3)

Table 3. Primer Sequences.

Name	Sequence
BiFCTCP20F	GGACTAGTATGGATCCCAAGAACCTAA
BiFCTCP22F	GGACTAGTATGAATCAGAATTCCTCTG
CeYFPTCP20R	GCGGTACCTTAAGCATTACGACCTGAGCCTTGAG
CeYFPTCP22R	CGGGATCCTTACTTTTTGTCATCACCACCA
GB-EntK-TCP20 F	GAAGATCTGATGATGATGATAAAATGGATCCCAAGAACCTAAATCGT
GB-TCP20F	GAAGATCTATGGATCCCAAGAACCTAAATCGT
GB-TCP20R	GAGTTCCTCGAGACGACCTGAGCCTTGAGAATCATC
GB-TCP22F	CGCGGATCCATGAATCAGAATTCCTCTG
GB-TCP22R	GAGTTCCTCGAGCTTTTTGTCATCACCACC
GSTGIP1 F2	GAAGATCTTGATTGGATGATCTTCATGG
GSTGIP1 R	GAGTTCCTCGAGTCACTGTGTGTTGCTAATGT
GSTGIP11 F2	GAAGATCTTGAGGGTCGTGGATCCGGA
GSTGIP11 R	GAGTTCCTCGAGTTACCGAGCAGACACCATG
GSTGIP17 F2	TGCAGGATATCATGGATCCGGATCCGGA
GSTGIP17 R	GAGTTCCTCGAGCTAGGAATGATGACTGGTG
GSTGIP3 F2	GAAGATCTTGATGAATATCGTCTCTTG
GSTGIP3 R	GAGTTCCTCGAGTCACATATGGTGATCACTTC
GSTGIP38 R	GAGTTCCTCGAGCTAATCTTGCTGATCCTCC
GSTGIP38F2	GAAGATCTTGATGCAAAAGCCAACATC
GSTTCP18R453F	GAAGATCTTGCGACCGGTGTTAGGATCCA
NeYFPTCP20R	CCCCCCGGGTTAAGCATTACGACCTGAGCCTTGAG
NeYFPTCP22R	CCCCCCGGGTTACTTTTTGTCATCACCA
SnRK1 1T198D F	GAGATGGTCATTTTTTGAAGGATAGTTGTGGAAGTCCAAATTATG
SnRK1 1T198D R	CATAATTTGGACTTCCACAACTATCCTTCAAAAAATGACCATCTC
SnRK1.1 F2	CGCGGATCCCCATGGATGGATCAGGCAC
SnRK1.1 T175E/S176D F	GAGATGGGTCATTTTTTGAAGGAAGATTGTGGAAGTCCAAATTAATG
SnRK1.1 T175E/S176D R	CATAATTTGGACTTCCACAATCTTCCTTCAAAAAATGACCATCTC
SnRK1.1R2	GAGTTCCTCGAGTTATCAGAGACTCGGAGCT
SnRK1.1T198E F	GAGATGGGTCATTTTTTGAAGGAAAGTTGTGGAAGTCCAAATTAATG
SnRK1.1T198E R	CATAATTTGGACTTCCACAACTTTCCTTCAAAAAATGACCATCTC
TCP1.1R	GAGTTCCTCGAGGTTTACAAAAGAGTCT
TCP10F2	CGCGGATCCCCATGGGACTTAAAGGATATAGCGT
TCP10R2	GAGTTCTCGAGTCATTAGAGGTGTGAGTTACCCT
TCP11F	CGCGGATCCCCATGATTTTTCAGAATGTGT
TCP11R	TCTAGAGCGGCCGTCATCAATTAGGGTTTTTTAGTT
TCP12F	CGCGGATCCCCATGTTTCCTTCTTTCATTA
TCP12R	AGTTCCTCGATCATCAATTAGGGTTTTAGTT
TCP16F	GAAGATCTTGATGGATTAGAAAATGGAATT
TCP16R	GAGTTCCTCGAGTCATCAAACTGTGGTTGTGGCTGT
TCP18dF	CGCGGATCCCCGGTGGTGGTGGTGGTGGTCAGAGAATCTCAACTTCT

Table 3. Primer Sequences (continued).

Name	Sequence
TCP18dR	GAGTTCCTCGAGTCATCCTAACACCGGTCGGA
TCP18F	GAAGATCTTGATGAACAACTTTTCA
TCP18R	GAGTTCCTCGAGTCATCAATACATGTTTTGATAGTT
TCP18S336A F	GTGAGATAATAAAAGAATAATAATAGTAGCCCAGTGAATCGGAGTTC
TCP18S336A R	GAACTCCGATTCACTTGGGCTCTATTATTATTCTTTATTATCTCAC
TCP18S336A R	GAACTCCGATTCACTTGTTCTCTATTATTCTTTATTATCTCAC
TCP18S336E F	GTGAGATAATAAAGAATAATAATAGTGAACAAGTGAATCGGAGTTC
TCP18S36A F	CATTGCTCCCTTTTAGCCCTGCTTCTTCCATTAACGACATCTTG
TCP18S36A R	CAAGATGTCGTTAATGGAAGAAGCAGGGCTAAAAGGGAGCAATG
TCP18S36A R	CAAGATGTCGTTAATGGAAGCAGAAGGGCTAAAAGGGAGC
TCP18S36AS37AS38A F	CATTGCTCCCTTTTAGCCCTGCTGCTGCCATTAACGACATCTTGATTC
TCP18S36AS37AS38A R	GAATCAAGATGTCGTTAATGGCAGCAGCAGGGCTAAAAGGGAGCAATG
TCP18S36E F	CATTGCTCCCTTTTAGCCCTGAATCTTCCATTAACGACATCTTG
TCP18S36E R	CAAGATGTCGTTAATAATGGAAGATTCAGGGCTAAAAGGGAGCAATG
TCP18S37A F	GCTCCCTTTTAGCCCTTCTGCTTCCATTAACGACATCTTG
TCP18S38A F	CCCTTTTAGCCCTTCTTCTGCATTAACGACATCTTGATTC
TCP18S38A R	GAATCAAGATGTCGTTAATGGCAGAAGAAGGGCTAAAAGGG
TCP18S38E F	CCCTTTTAGCCCTTCTTCTGAAATTAACGACATCTTGATTC
TCP18S38E R	GAATCAAGATGTCGTTAATTTCAGAAGAAGGGCTAAAAGGG
TCP18T233A F	GTTAGGATCCATGGACGCATCTTCTGATCTATGTG
TCP18T233A R	CACATAGATCAGAAGATGCGTCCATGGATCCTAAC
TCP18T233D F2	GCAAGTTCACATAGATCAGAAGAGTCGTCCATGGATCCTAAGACC
TCP18T233D R2	GCAAGTTCACATAGATCAGAAGAGTCGTCCATGGATCCTAACACC
TCP19F	GAAGATCTTGATGGAATCGAATCAGAA
TCP19R	GAGTTCTCGAGTCATTAAGTCTCATGCCATGAA
TCP1F	CGCGGATCCCCATGGCCGACAACGACGGAG
TCP1F3	CGCGGATCCCCATGTCGTCTTCCACCAA
TCP1R	TCTAGAGCGGCCGTCATCAACGTGGTTCGTGTCGTGGTCG
TCP20dF3	CGCGGATCCCCGGTGGTGGTGGTGGTGGTTCCGACAAAGAACCAAACAAGAAAG
TCP20dR	GAGTTCCTCGAGTCACCCACCTTGCTATGATGGT
TCP20F3	GAAGATCTTGATGGATCCCAAGAACCTAAAT
TCP20H153F	CGCGGATCCCCATCATCAAGGTGGGTCT
TCP20R2	GAGTTCTCGAGTCAGAGTTCCTCGAGTCA
TCP20S237A F	CTGGTGTTGGTCATATGGCTTTTGCATCTATTTTGGG
TCP20S237A R	CCCAAAATAGATGCAAAAGCCATATGACCAACACCAG

Table 3. Primer Sequences (continued).

Name	Sequence
TCP20S237E F	CTGGCTGTTGGTCATC]AGGAATTTGCATCTATTTTGGG
TCP20S237E R	CCCAAAATAGATGCAAATTCCATATGACCAACACCAG
TCP22dF	CGCGGATCCCCGGTGGTGGTGGTGGTGGTGGTGCGACGAGTTCGACAA
TCP22dR	GAGTTCCTCGAGTCAGCCACCACCACTGCGTA
TCP22F2	GAAGATTCTTGATGAATCAGAATTCCTCT
TCP22R135F	CGCGGATCCCCGCAGTGGTGGTGGCTCCA
TCP22R2	TCTAGAGCGGCCGTCATCACTTTTTGTCATCACCA
TCP22S140A F	CTTTACGCAGTGGTGGTGGCGCTACCTTGTTTTCTCAGGC
TCP22S140A R	GCCTGAGAAAACAAGGTAGCGCGCCACCACCACTGCGTAAAG
TCP22S140E F	CTTTACGCAGTGGTGGTGGCGAAACCTTGTTTTCTCAGGC
TCP22S140E R	GCCTGAGAAAACAAGGTTTCGCCACCACCACTGCGTAAAG
TCP22S140N F	CTTTACGCAGTGGTGGTGGCAACACCTTGTTTTCTCAGGC
TCP22S140N R	GCCTGAGAAAACAAGGTGTTGCCACCACCACTGCGTAAAG
TCP22S316A F	GTAACTGCACCAATGGGGGCAATGATGTTGGGAGGTCAAC
TCP22S316A R	GTTGACCTCCCAACATCATTGCCCCCATTGGTGCAGTTAC
TCP23F	TGCAGGATATCATGGATCCCACAACAA
TCP23R	GAGTTCCTCGAGTCATCAAGGAGAACCATCTATA
TCP23S132A R2	CAGTGGAGCTGAAAGAGTAGCGCCACTGCTTCGAAGAG
TCP24F	CGCGGATCCCCATGGAGGTTGACGAAGACA
TCP24F	GAGTTCCTCGAGTCACTATCTCCTTTCCTTTGCC
TCP2F2	CGCGGATCCCCAAAGAAATTCCAATTTT
TCP2R2	GAGTTCCTCGAGTCATCAGTTCTTTACCCT
TCP3A127F	CGCGGARCCCCGCTAACGCTAAACCCAGAA
TCP3dF	CGCGGATCCCCGGTGGTGGTGGTGGTGGTGGTGGTTGCGGCG
TCP3dR	GAGTTCTCGAGTCAGTTAGCAGCAGCGGCGGCGT
TCP3F	CGCGGATCCCCATGGCACCAGATAACGACC
TCP3R	GAGTTCTCGAGTCAAGTGGGGTTAAAGGTTTCC
TCP3S262A R	GTTCTGTGTATTGCCTCGCGCCGGTGGCTGATGATGATAG
TCP3S262AF	CTATCATCATCAGCCACCGGCGCGAGGCAATACACAGAAC
TCP3S262E F	GATACAGAGACTAGTGGAATGGAACAACGTCG
TCP3S262E R	CGACGTTGTTCCATTCCACTAGTCTCTGTATC
TCP4F	CGCGGATCCCCATGTCTGACGACCAA
TCP4R	GAGTTCCTCGAGTCATCAATGGCGAGAAATAGA
TCP5F2	CGCGGATCCCCATGAGATCAGGAGAATGTGA
TCP5R	GAGTTCGCGGCCGCTCATCAAGAATCTGATTCATTA
TCP6F	CGCGGATCCCCATGGTCATGGAGCCCA
TCP6R	GAGTTCCTCGAGTCATTATGAACCATTTTCCTCT
TCP7F	CGCGGATCCCCATGTATATTAACAACAA
TCP7R	GAGTTCTCGAGTCATTAACGTGGAATCTTCCTCT
TCP8F	CGCGGATCCCCATGGATCTCCTCCGACATCC
TCP8R	GAGTTCCTCGAGTCACTCAGACTATTTGAGT

Table 3. Primer Sequences (continued).

Name	Sequence
TCP9F3	CGCGGATCCCCATGGCGACAATTCAGAAGC
TCP9R3	TCTAGAGCGGCCGTCATCAGTGGTTCGATGACCGT
TCPS132A F2	CTCTTCGAAGCAGTGGCGCTACTCTTTCAGCTCCACTG
Y2H TCP20 F	ACAAGTTTGTACAAAAAAGCAGGCTCGATGGATCCCAAGAACCTAAAAT
Y2H TCP20 R	ACCACTTTGTACAAGAAAGCTGGGTGAGTTCCTCGAGTCA
Y2H TCP22 F	ACAAGTTTGTACAAAAAAGCAGGCTCGATGAATCAGAATTCCTCT
Y2H TCP22 R	ACCACTTTGTACAAGAAAGCTGGGTCTTTTTGTCATCACCA
Rad TCP I Binding A F	AATTCAGATCTGTGGGACCGGGAG
Rad TCP I Binding A R	GATCCTCCCGGTCCCACAGATCTG
Rad TCP I Binding C F	AATTCAGATCTGTGGGCCCGGGAG
Rad TCP I Binding C R	GATCCTCCCGGGCCCACAGATCTG
RPL24 promoter F IRD	/5IRD700/-CATTTCACCCAATGCCATTTTCGTC
RPL24 promoter R	GAGAGCTTAGCTACTTGTTCAAAC
TCP nonbinding F	GTCCGAGGGG
TCP nonbinding R	CCCCTCGGAC
TCP I binding C F IRD	/5IRD700/-ATTTCAAGTGGGCCCGGAACTATT
TCP I binding C R	AATAGTTCCGGGCCCACTTGAAAT
TCP I binding A F IRD	/5IRD700/-ATTTCAAGTGGGACCGGAACTATT
TCP I binding A R	ATTAGTTCCGGTCCCACTTGAAAT

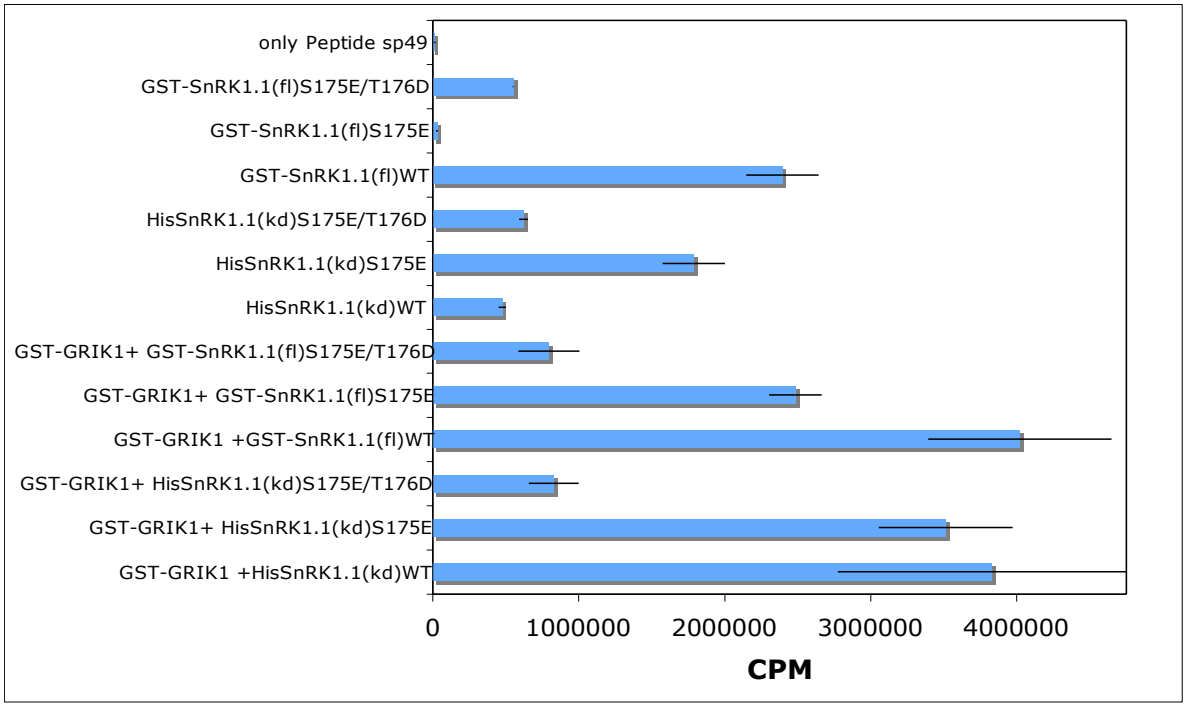

Figure 1. Phosphopeptide assay with various forms of SnRK1. GST-GRIK and His-SnRK1(kd)WT, GST-GRIK and His-SnRK1(kd)S175E, GST-GRIK and His-SnRK1(kd) S175E/T176D, GST-GRIK and GST-SnRK1(fl)WT, GST-GRIK and GST-SnRK1(fl)S175E, GST-GRIK and GST-SnRK1(fl)S175E/T176D, His-SnRK1(kd)WT, His-SnRK1(kd)S175E, His-SnRK1(kd) S175E/T176D, GST-SnRK1(fl)WT, GST-SnRK1(fl)S175E, GST-SnRK1(fl)S175E/T176D, or no kinase were reacted in the presence of [γ-^{32}P]ATP with synthetic peptide SP49 (Ace-KGRMRRISSVEMMK) corresponding to the SnRK1 phopsporylation site of the spinach sucrose-phosphate synthase *(41)*. CPM, count per minute, indicates the intensity of radioactivity from phosphorylation.

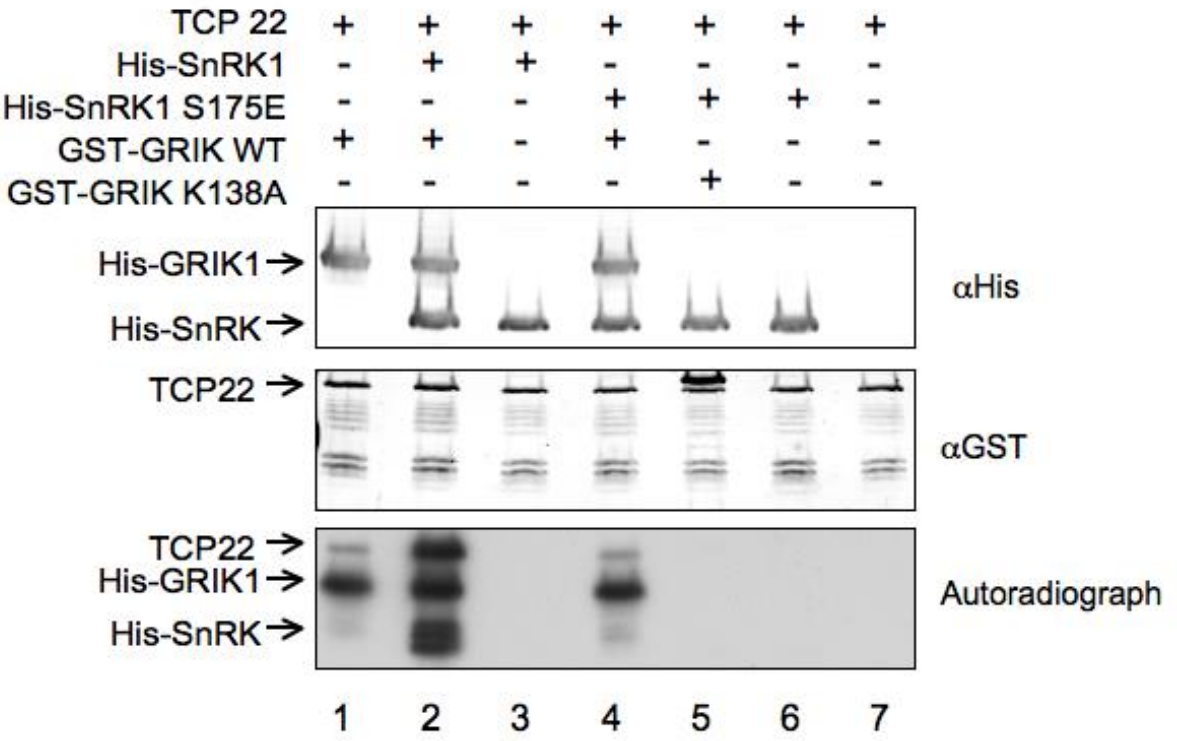

Figure 2. Kinase Assay of TCP22 with the SnRK1 S175E Mutant. Top, Immunoblot with His antibodies. Arrows indicates His-GRIK or His-SnRK1(kd). Middle, Immunoblot with GST antibodies. Arrow indicates GST-TCP22 and astericks indicated GST-GRIK K137A. Bottom, Kinase assay of full length GST-TCP22. Arrows indicates His-GRIK or His-SnRK1(kd). Lane 2 shows strong phosphorylation of TCP22 in the presence of both His-GRIK and His-SnRK1.

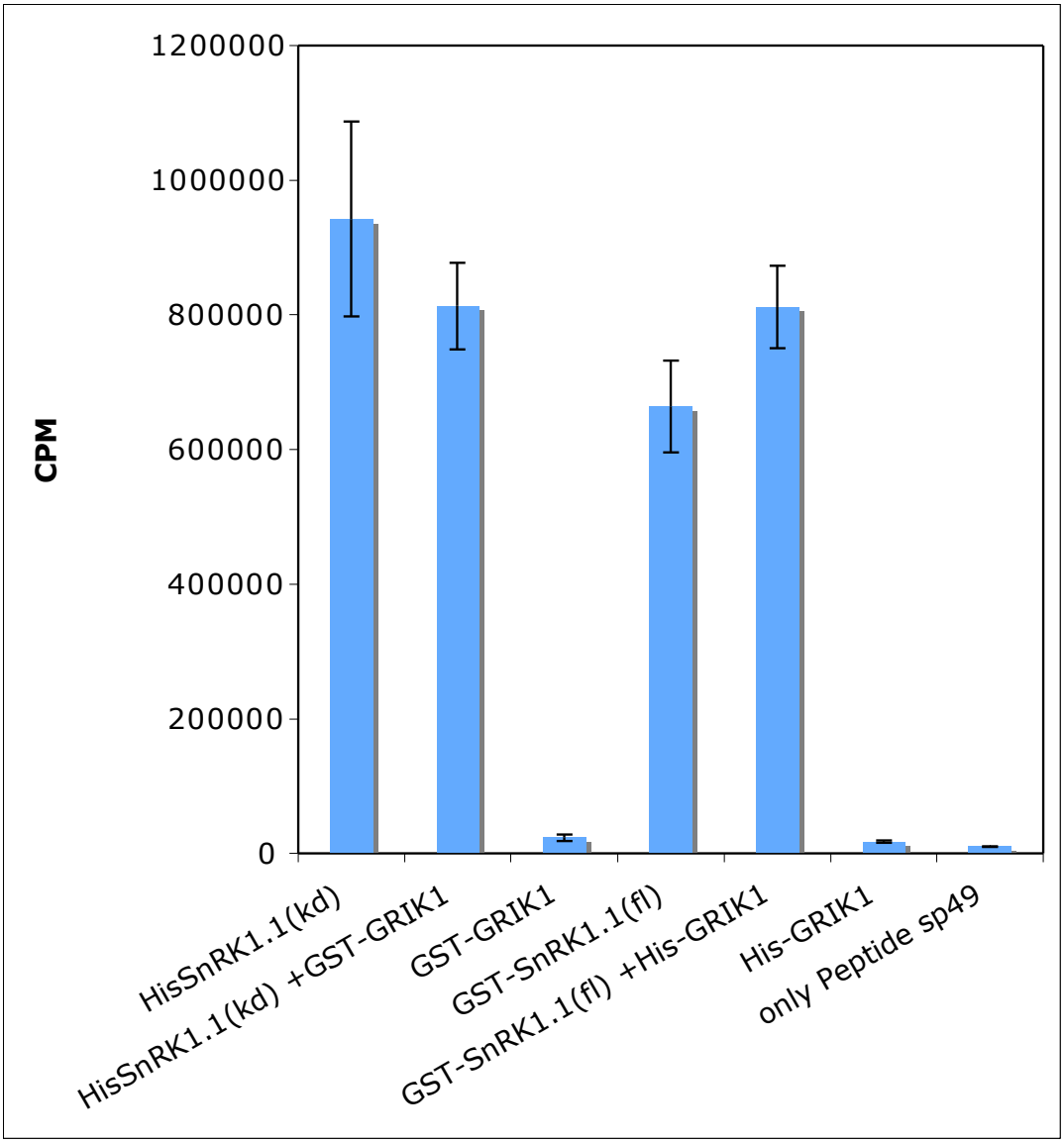

Figure 3. Phophopeptide Assay with Preactivated SnRK1. Preactivated His-SnRK1(kd), GST-GRIK1 and preactivated His-SnRK1(kd), GST-GRIK1, preactivated GST-SnRK1(fl), His-GRIK1 and preactivated GST-SnRK1(fl), His-GRIK1, or no kinase were reacted with synthetic peptide Ace-KGRMRRISSVEMMK . CPM indicates the intensity of radioactivity from phosphorylation.

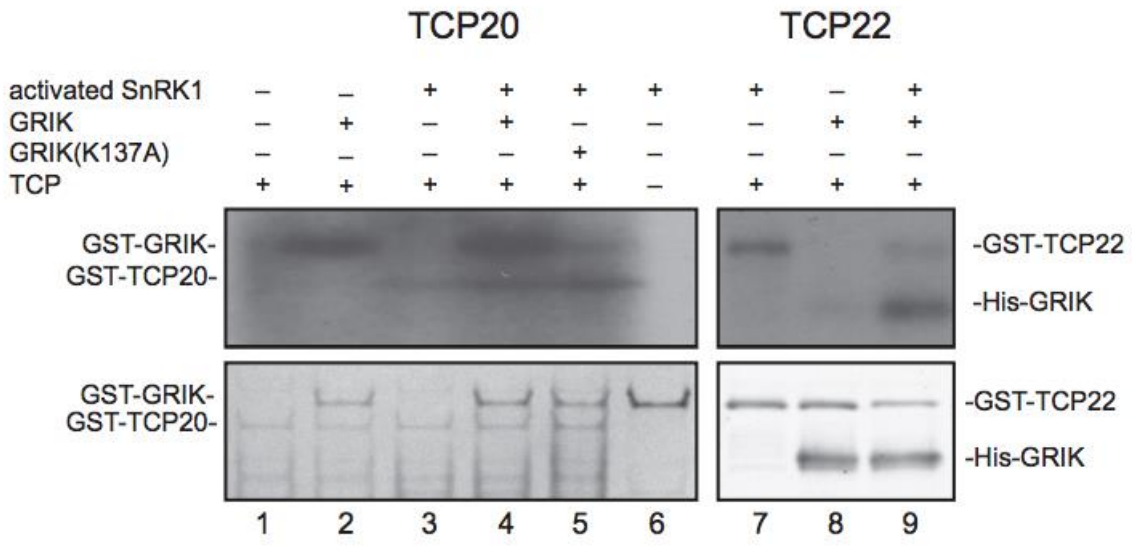

Figure 4. Kinase assay of TCP20 and TCP22 by GRIK and preactivated SnRK1. Images of Coomassie blue stained 10% SDS-PAGE gel with bands indicated for GST-TCP20 and GST-GRIK recombinant proteins (bottom left) and autoradiograph (top left). Images of Coomassie blue stained 10% SDS-PAGE gel with bands indicated for GST-TCP22 and His-GRIK recombinant proteins (bottom right) and autoradiograph (top right). TCP20 and TCP22 bands are only visulaized on X-ray film in reactions containing preactivated SnRK1.

Table 4. TCP phosphorylation by GRIK, SnRK1, GRIK+SnRK1 and GRIK(K137A) +SnRK1

	GRIK	preactivated SnRK1	GRIK + preactivated SnRK1	GRIK(K137A) + preactivated SnRK1
TCP16	–	–	–	–
TCP11	–	–	–	–
TCP20	–	+	+	+
TCP6	–	–	–	–
TCP15	–	(+)	+	+
TCP14	–	(+)	(+)	(+)
TCP21	–	(+)*	(+)*	(+)*
TCP7	–	–	–	–
TCP8	–	(+)	+	+
TCP23	–	(+)	+	(+)
TCP22	–	++	++	++
TCP19	+*	+	+	+
TCP9	+	+	+	+
TCP18	–	++	++	++
TCP12	–	+	+	+
TCP1	–	+	+	+
TCP10	–	(+)	(+)	(+)
TCP4	–	+	+	+
TCP3	–	++	++	++
TCP13	–	++	+	+
TCP17	nd	nd	nd	Nd
TCP5	–	–	–	–
TCP24	–	+*	+*	+*
TCP2	–	–	–	–

* indicates TCP phosphorylation observed in truncations, not full length

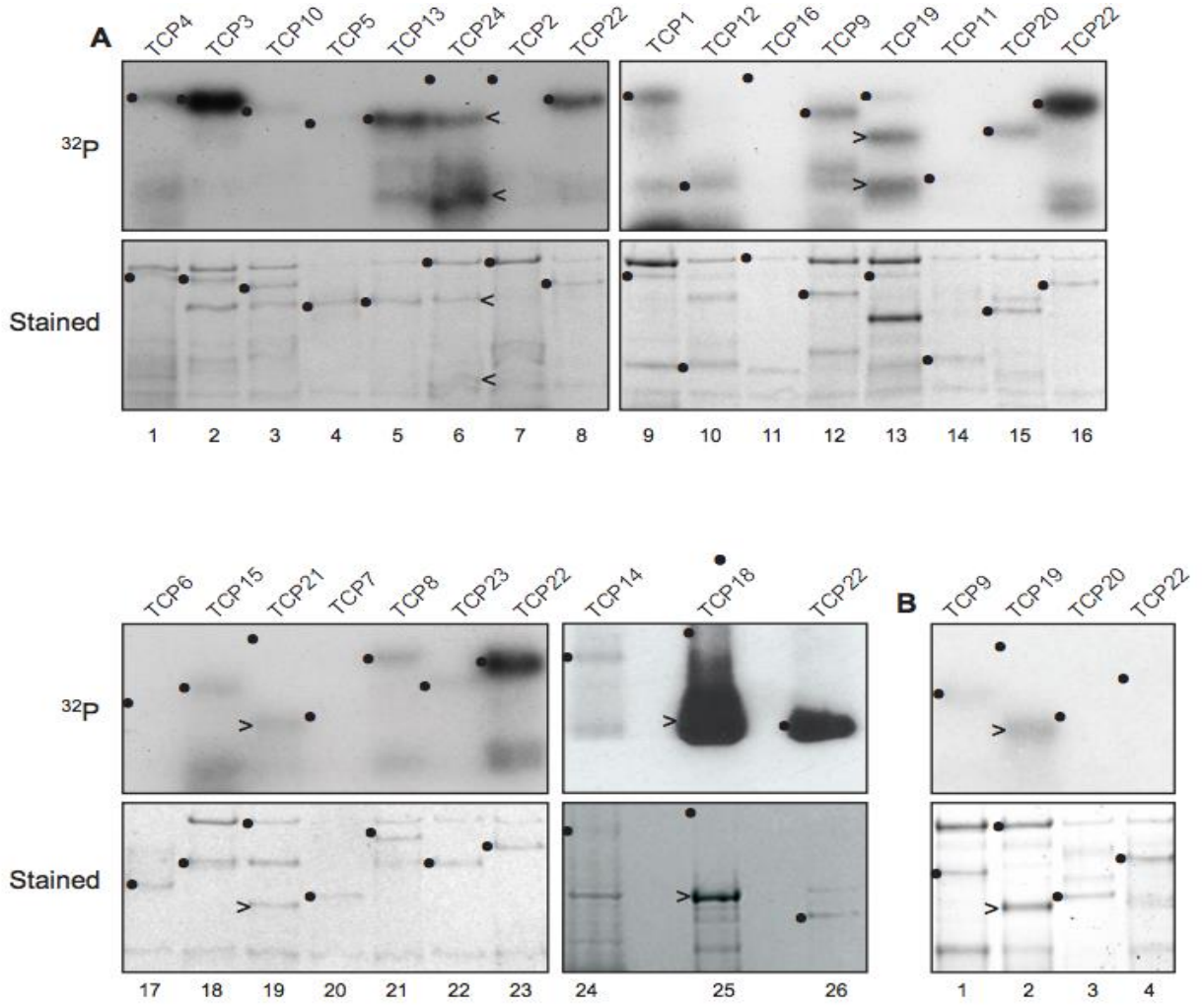

Figure 5. Kinase assay of GST-TCPs by preactivated SnRK1 or GRIK. A) Images of Coomassie blue stained 10% SDS-PAGE gel (bottom image of lanes 1-26) and autoradiograph (top image of lanes 1-26) of all recombinant GST-TCP family members (excluding TCP17) by preactivated His-SnRK1 (kd). Each TCP is indicated with black dot and phosphorylated trunctions indicated by an arrow. Intensity of TCP phosphorylation is indicated in Table 4. B) Images of Coomassie blue stained 10% SDS-PAGE gel (bottom) and autoradiograph (top) GST-TCP9, GST-TCP19, GST-TCP20, and GST-TCP22 by GRIK. Each TCP is indicated with black dot and phosphorylated trunctions indicated by an arrow.

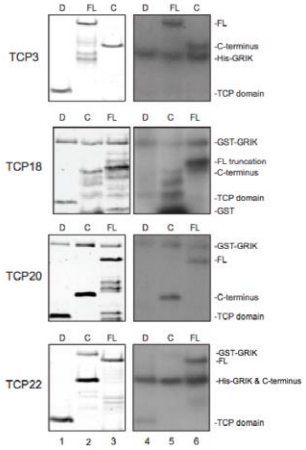

Figure 6. Kinase assay of full length GST-TCP3, GST-TCP18, GST-TCP20, GST-TCP22 and truncations of each TCP domain and C-terminal end by GRIK and SnRK1. Shown are images of Coomassie blue stained 10% SDS-PAGE gel (left panels) and autoradiograph (right panels) of GST-TCP3, GST-TCP18, GST-TCP20, GST-TCP22 and truncations after phosphorylation by GST-GRIK or His-GRIK (for TCP3s and TCP22 C only) and preactivated His-SnRK1 (kd). Variation of GRIK protein was due to conflicts of size with TCP22 and its truncations. Lanes D, GST-TCP domain fusions of TCP3 G29-N128, TCP18 Q130-G230, TCP20 S67-G166 and TCP22 A40-G139; Lanes C, GST fusions with the C-termini of TCP3 (A127-H391), TCP18 (R255-Y433), TCP20 (H162-R324) and TCP22 (R135-K375); Lanes FL, GST fusions with the full-length TCP proteins. GST-TCP3 (fl), GST-TCP3 C-terminus, GST-TCP18 (fl), GST-TCP22 (fl),GST-TCP22 C-terminus show strong phosphorylation. GST-TCP18 C-terminus, GST-TCP20 (fl), GST-TCP18 TCP domain, GST-TCP20 C-terminus, and GST-TCP22 TCP domain show weak phosphorylation. GST-TCP3 TCP domain and GST-TCP20 TCP domain are not phosphorylated.

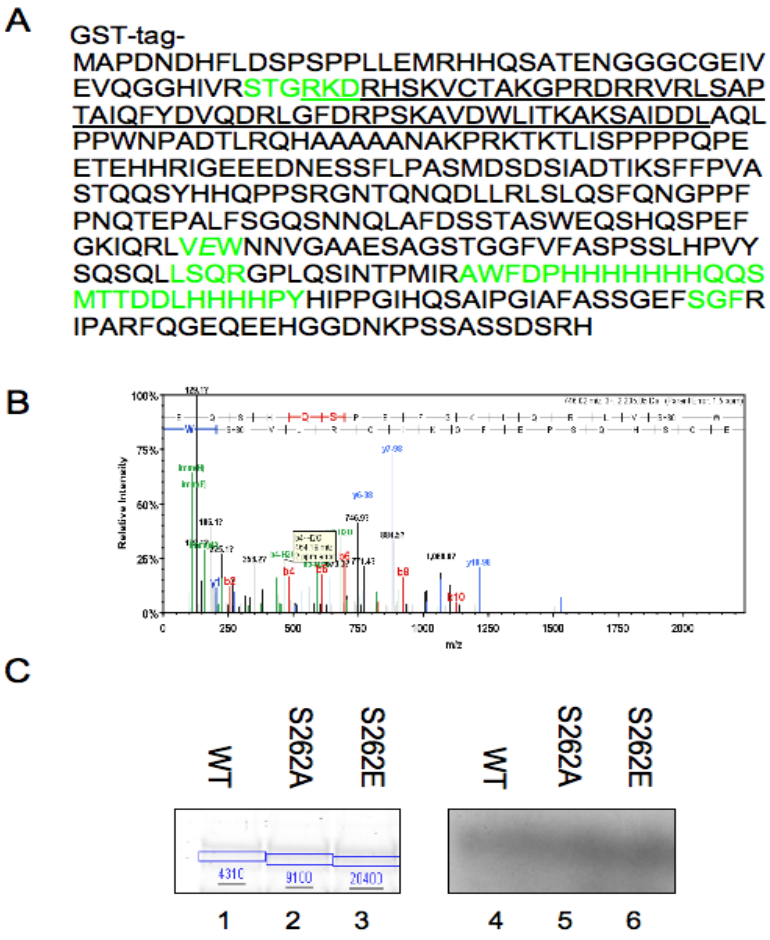

Figure 7. GRIK-SnRK1 cascade phosphorylation site of TCP3. A) TCP3 S262E coverage map via peptides identified with LC/MS/MS showing a 90% coverage of TCP3. Diagram indicates the TCP domain (Underlined), uncovered amino acids (green), identified peptides (black). B) Spectrum of TCP3 phosphopeptides pS262 The image was generated by Scaffold. C) Kinase assay of full length GST-TCP3 and mutants by His-GRIK and His-SnRK1 (kd). Left panel, Coomassie stain; Right panel, autoradiograph. The visualized intensely between lanes 4, 5 and 6 on X-ray film do not appear to vary.

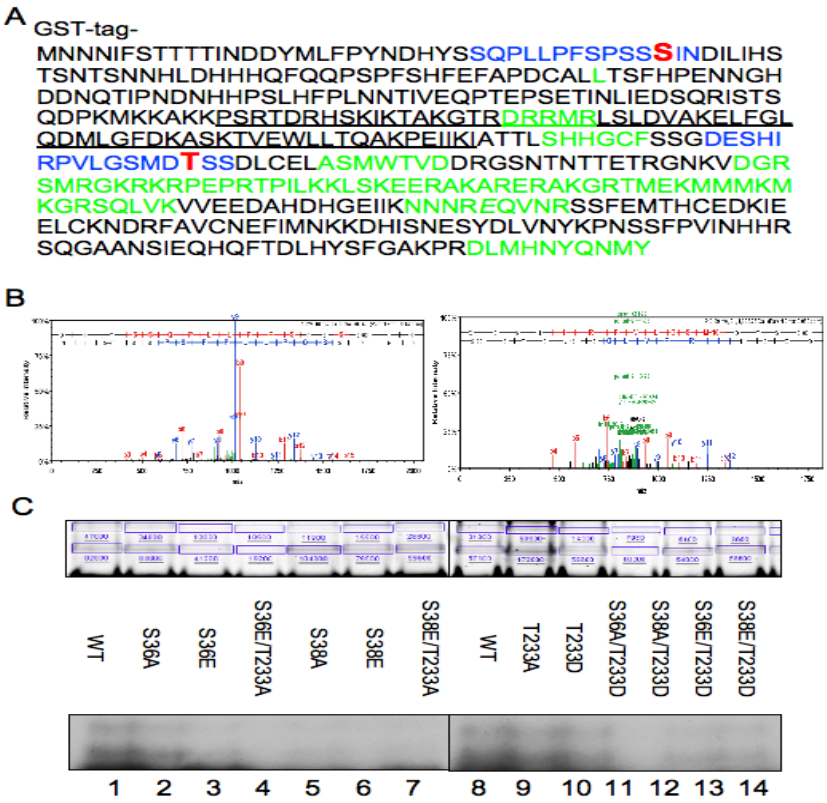

Figure 8. GRIK-SnRK1 cascade phosphorylation site of TCP18. A) TCP18 S336E coverage map via peptides identified with LC/MS/MS showing an 88% coverage of TCP18. Diagram indicates the TCP domain (Underlined), uncovered amino acids (green), identified peptides (black), phosphopeptides (blue), phosphoserine (Red). B) Spectrum of TCP18 S336E phosphopeptides pS38 and pT233. The images were generated by Scaffold. C) Kinase assay of full length GST-TCP18 and mutants by His-GRIK and His-SnRK1 (kd). Upper panels, Coomassie stain; Lower panels, autoradiography. The visualized intensety of lanes 2, 3 9 and 10 are slightly lower compared to lanes 1 and 8. Lanes 4, 5, 6, 7 11,12,13,14 are very light.

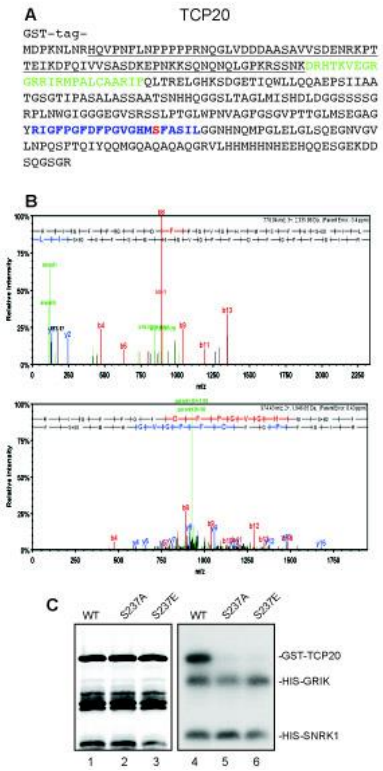

Figure 9. GRIK-SnRK1 cascade phosphorylation site of TCP20. A) TCP20 Coverage Map via peptides identified with LC/MS/MS showing a 98% coverage of TCP20. Diagram indicates the TCP domain (Underlined), uncovered amino acids (green), identified peptides (black), phosphopeptides (blue), phosphoserine (Red). B) Spectrum of TCP20 phosphopeptides pS237. The image were generated by Scaffold. C) Kinase assay of full length GST-TCP20 and mutants His-GRIK and His-SnRK1 (kd). Left panel, Anti-GST immunoblot; Right panel, autoradiography. Each protein indicated with a dash. TCP20 WT is visualized intensely on X-ray film but TCP20 S237A and TCP20 S237E are not visualized. The visualized intensity of lanes 1, 2, and 3 were similar. The visualized intensity TCP20 of lanes 5 and 6 appears to be zero.

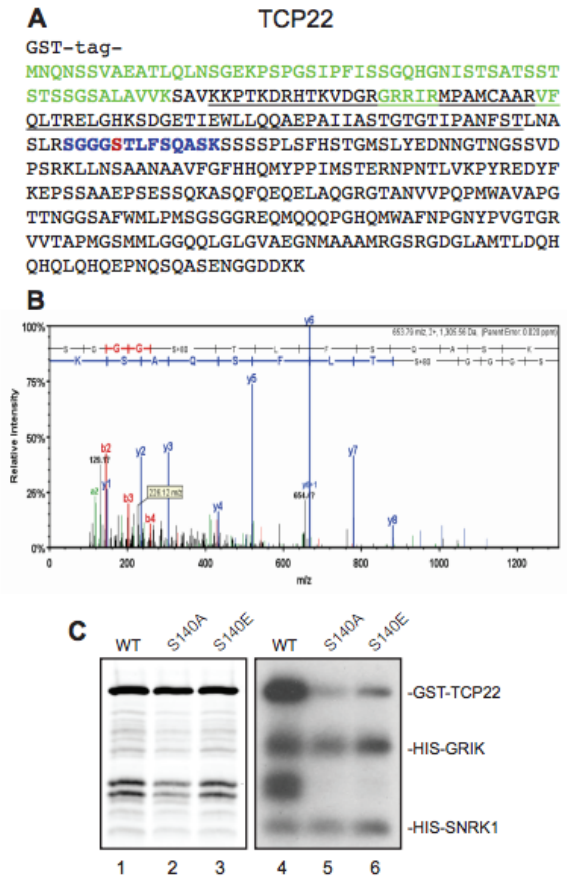

Figure 10. GRIK-SnRK1 cascade phosphorylation site of TCP22. A) TCP22 Coverage Map via peptides identified with LC/MS/MS showing an 84% coverage of TCP22. Diagram indicates the TCP domain (Underlined), uncovered amino acids (green), identified peptides (black), phosphopeptides (blue), phosphoserine (red). B) Spectrum of TCP22 phosphopeptide. The image generated by Scaffold. C) Kinase assay of full length GST-TCP22, and mutants by His-GRIK and His-SnRK1 (kd). Left panel, Anti-GST immunoblot; Right panel, autoradiography. Each protein indicated with a dash. The visualized intensity of lanes 1, 2, and 3 were similar. The visualized intensity TCP22 of lanes 5 and 6 appears weak compared to lane 4.

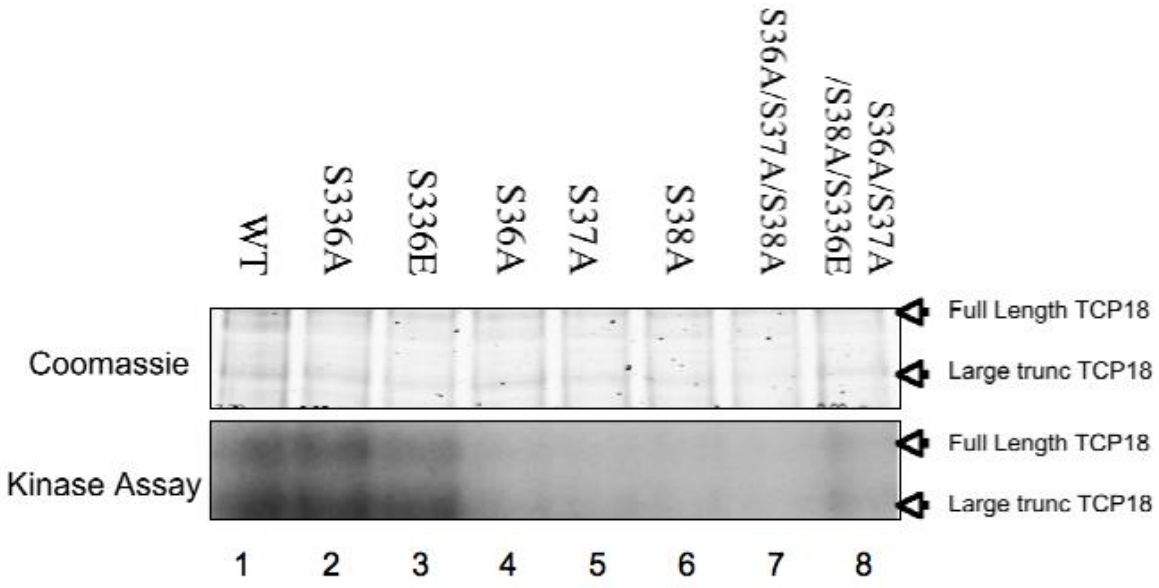

Figure 11. Kinase Assay of TCP18 mutants.by His-GRIK and His-SnRK1 (kd). Upper panel, Coomassie staining of the SDS-PAGE gel; Lower panel, autoradiograph. The visualized intensetiy on X-ray film of wild-type TCP18 (lane 1), TCP18 S336A (lane 2), and TCP18 S336E (lane 3) does not appear to vary. TCP18 S36A (lane 4), TCP18 S37A (lane 5), TCP18S 38A (lane 6), and TCP18 S36AS37AS38A (lane 7) do not appear to visualize on X-ray film. TCP18 S36AS37AS38AS336E (lane 8) has slight phosphorylation.

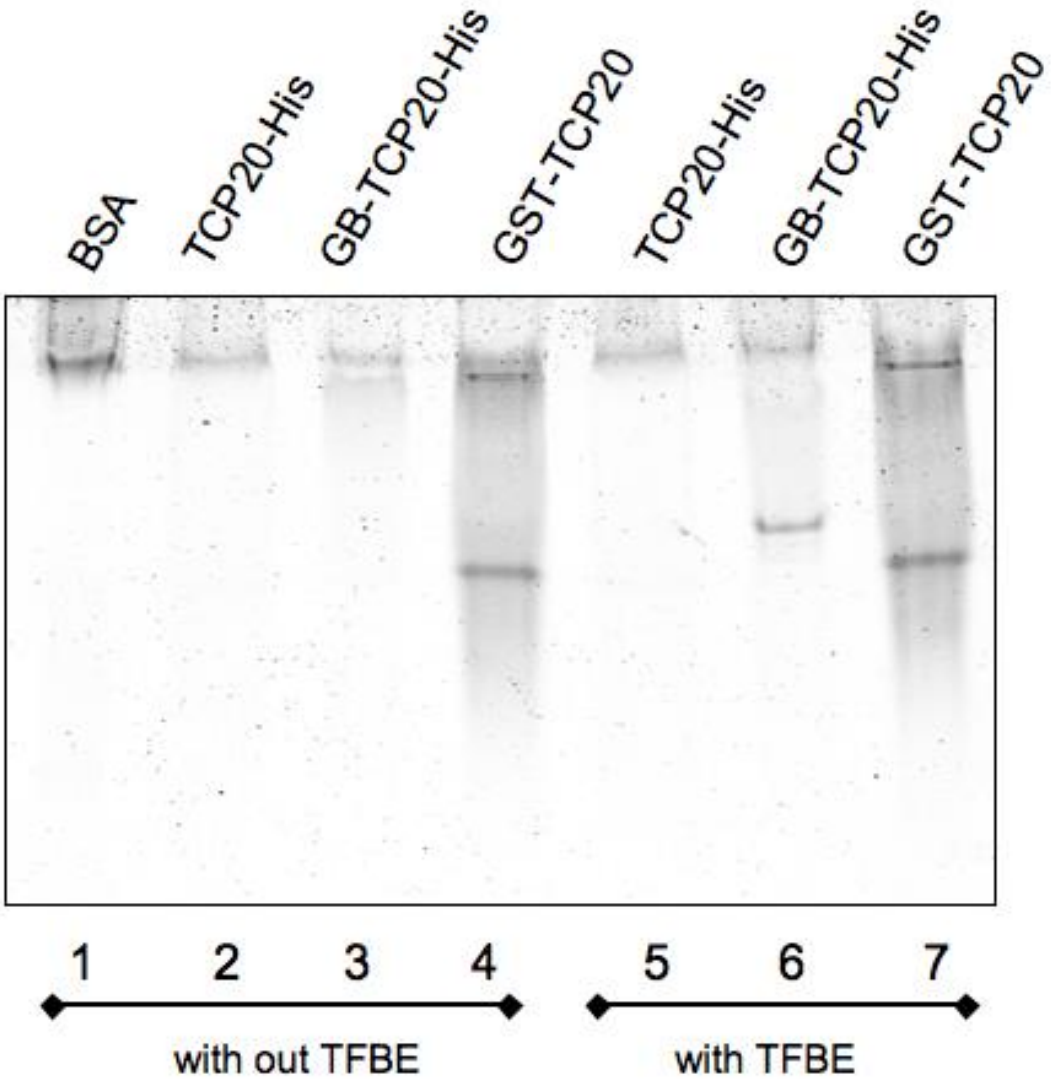

Figure 12. Coomassie blue stained 10% Native PAGE gel of GB-TCP20-His, and GST-TCP20 after enterokinase cleavage to remove the tags and incubation with or without a fragment of dsDNA containing Transcription Factor Binding Element (TFBE). All proteins remain at the top of the gel with the exception of GST-TCP20 and GB-TCP20-His in the presence of dsDNA.

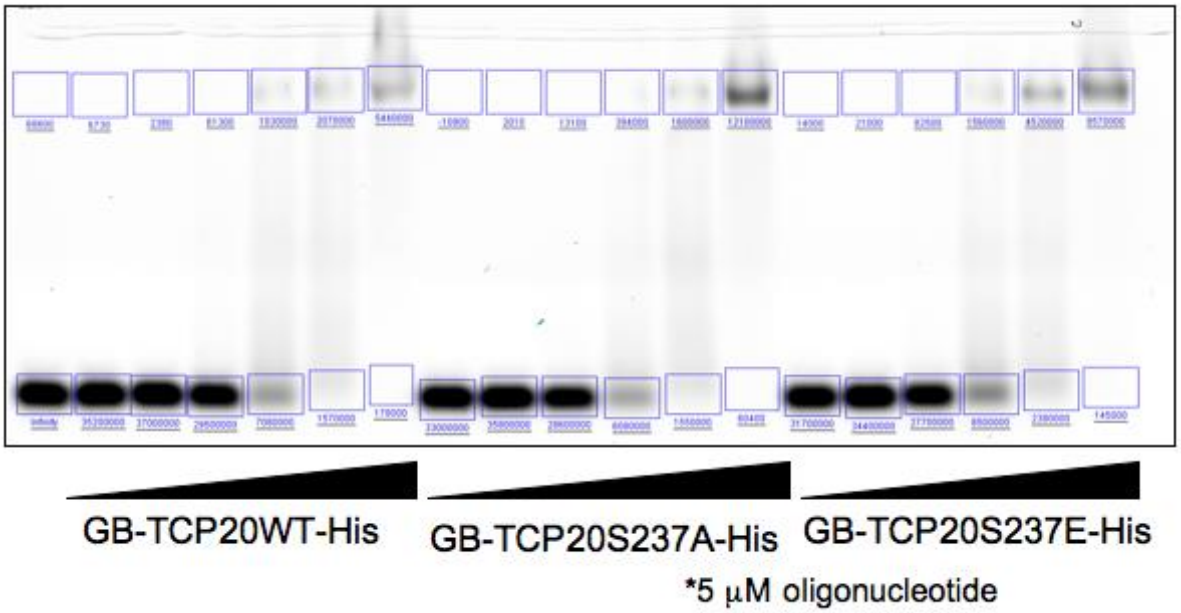

Figure 13. Fluorescent EMSA assay of GB-TCP20-His binding to a dsDNA probe. TCP20WT, TCP20S237A, and TCP20S237E with concentrations ranging from 0 to 50 nM were incubated with 5 μM of a fluorescent dsDNA probe /5IRD700/-ATTTCAAGTGGGCCCGGAACTATT, and applied to a 1 % agarose gel after incubation. Total intensity of fluorescence within each lane decreases inversely to protein concentration.

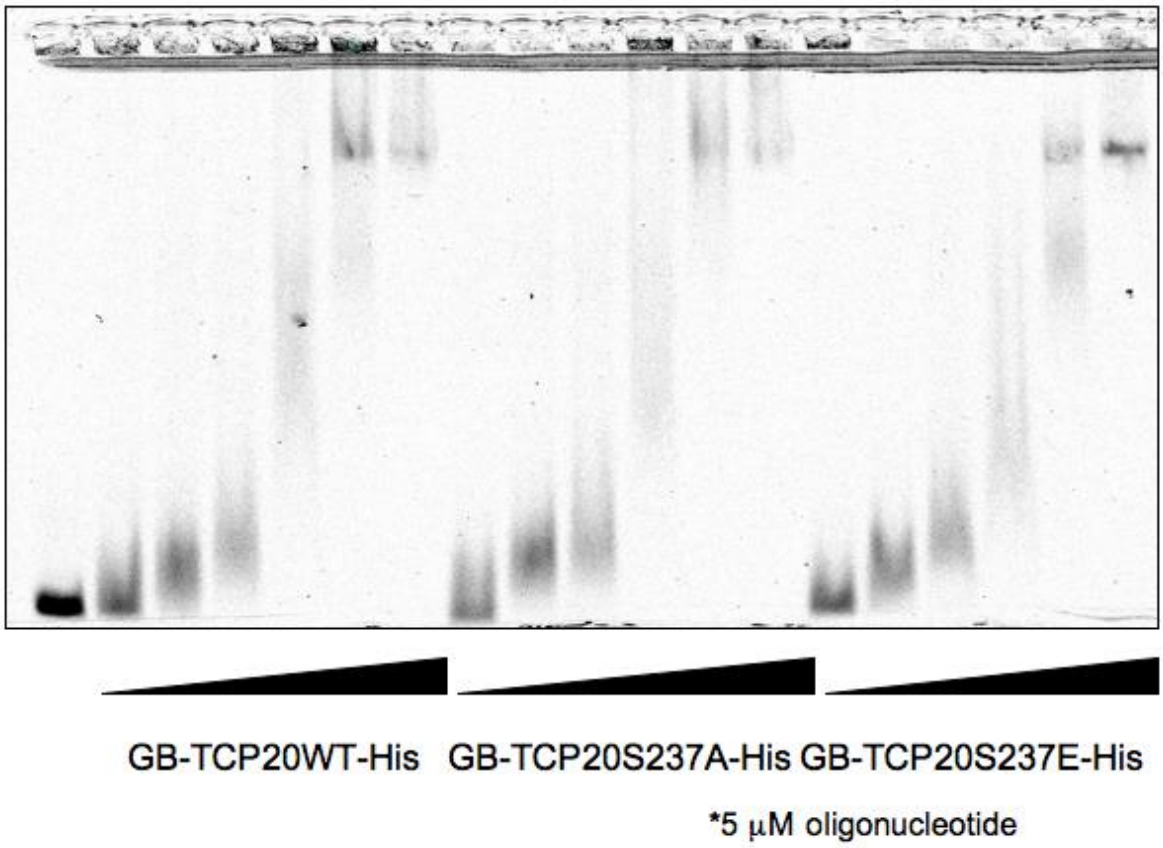

Figure 14. Fluorescent EMSA assay of GB-TCP20-His binding to the RPL24 promoter region. TCP20WT, TCP20S237A, and TCP20S237E with concentrations ranging from 0 to 50 mM were incubated with 5 μM of a /5IRD700/-labled dsDNA corresponding to the RPL24 promoter region and applied to a 1 % agarose gel after incubation. Total intensity of fluorescence within each lane decreases inversely to protein concentration.

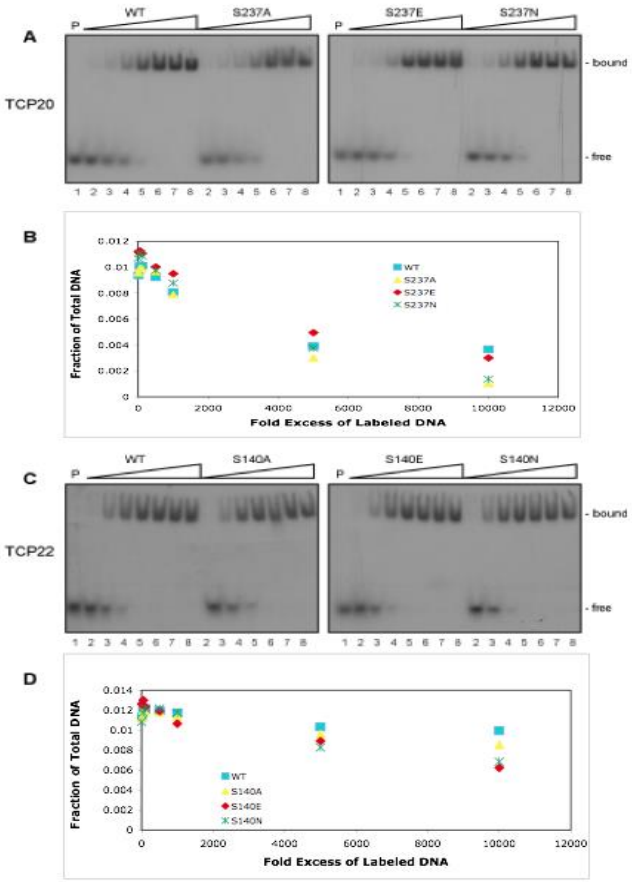

Figure 15. EMSA assay on binding of TCP20 SnRK1 phosphorylation mutants to TCP20 target DNA. A) Autoradiograph of protein titration EMSA assay for wild-type TCP20 or its S237A, S237E and S237N mutants with radiolabeld dsDNA probe. B) Binding curve of competition from unlabeled nonspecific DNA sequence EMSA assay for TCP20 WT, S237A, S237E and S237N based on Storm intensity ratio of bound:total radioactivity. C) Autoradio graph of protein titration EMSA assay for TCP22 WT, S140A, S140E and S140N with radiolabeld dsDNA. D) Binding curve of competition from unlabeled nonspecific DNA sequence EMSA assay for TCP22 WT, S140A, S140E and S140N based on Storm intensity ratio of bound:total radioactivity.

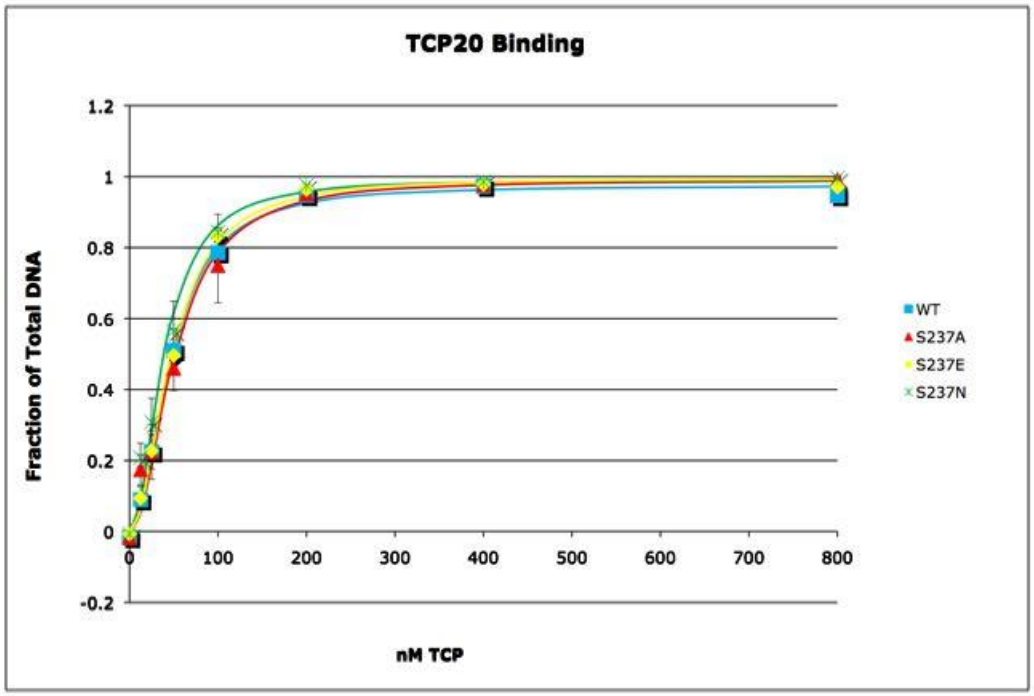

Figure 16. Tritraion curve of EMSA for TCP20 WT, S237A, S237E and S237N with radiolabeled dsDNA. Numerical data based on Storm intensity ratio of bound:total radioactive-label dsDNA of triplicate experiment show in Fig.15 A.

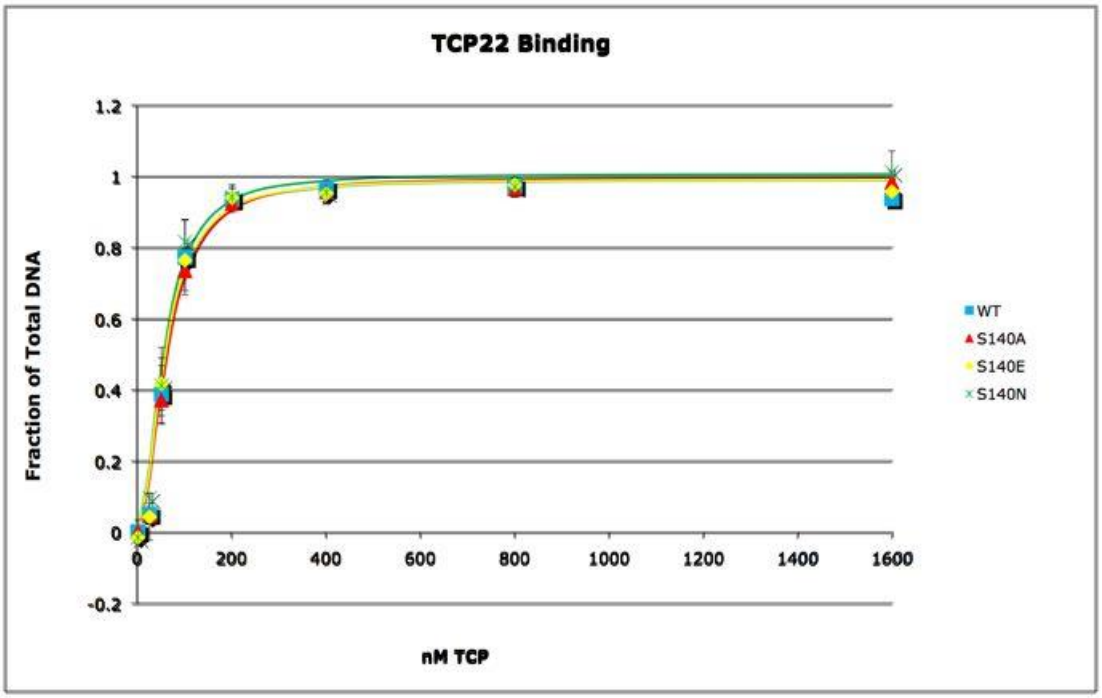

Figure 17. Tritraion curve of EMSA assay for TCP22 WT, S140A, S140E and S140N with radiolabeled dsDNA. Numerical data based on Storm intensity ratio of bound:total radioactive-label dsDNA of triplicate experiment show in Fig.15 AC

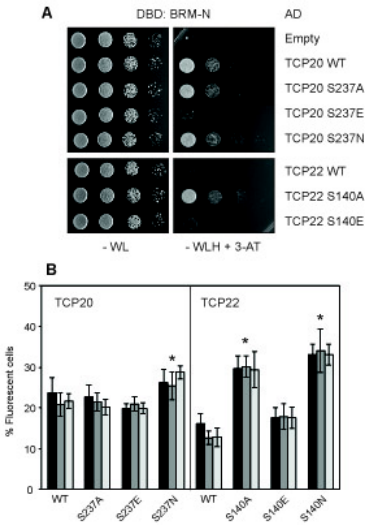

Figure 18. Effect of phosphorylation of TCP20 and TCP22 by SnRK1 on their interaction with BRM. A) Yeast two Hybrid assay of BRM and TCP20 (top) or TCP22 (bottom). Image of yeast colonies on selection medium without Trp and Leu (-WL) show that all transformed yeast lines grow in the presence of histidine. Image of yeast colonies on selection medium without Trp, Leu and His (-WLH) show little to no growth for yeast transformed with an empty vector, little growth in yeast transformed with TCP20 S237E, TCP22 WT, or TCP22 S140E and moderate growth of yeast transformed with TCP20 WT, TCP20 S237A, TCP20 S237N and TCP22 S140A. B) Quantitative BiFC assay for BRM-TCP20 interaction. Left panel, bar graph of percent of TCP20-transformed protoplasts that fluoresce (black and greys indicate bioreplicates). Only TCP20 S237N displays significant difference in fluorescence when compare to other samples via T-test (* indicated p-Value of <0.05). Right panel, bar graph of percent of TCP22-transformed protoplasts that fluoresce. TCP22 S140A and TCP20 S140N display significant difference in fluorescence when compare to other samples via T-test.

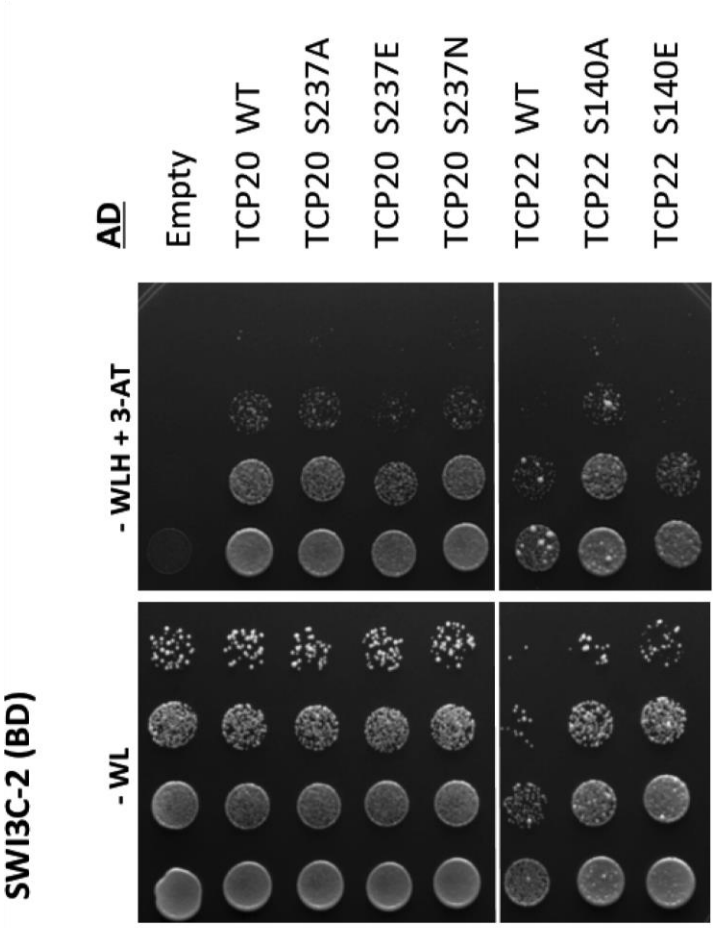

Figure 19. Yeast two Hybrid assay of SWI3c and TCP20 (top) or TCP22 (bottom). Image of yeast colonies -WL show that all transformed yeast lines grow in the presence of histidine. Image of yeast colonies -WLH show little to no growth for yeast transformed with an empty vector and moderate growth of yeast lines transformed by TCP20 WT, TCP 20 S237A, TCP 20S237N and TCP22 S140A. , A slight retardation in growth of yeast transformed with TCP20 S237E TCP22 WT, or TCP22 S140E. compared to TCP20 WT.

REFERENCES

1. Vlad, F., Turk, B. E., Peynot, P., Leung, J., and Merlot, S. (2008) A versatile strategy to define the phosphorylation preferences of plant protein kinases and screen for putative substrates, *Plant J 55*, 104-117.

2. Hrabak, E. M., Chan, C. W., Gribskov, M., Harper, J. F., Choi, J. H., Halford, N., Kudla, J., Luan, S., Nimmo, H. G., Sussman, M. R., Thomas, M., Walker-Simmons, K., Zhu, J. K., and Harmon, A. C. (2003) The Arabidopsis CDPK-SnRK superfamily of protein kinases, *Plant Physiol 132*, 666-680.

3. Nelson, D. L. (2005) *Lehninger Principles of Biochemistry*, 4th ed., W. H. Freeman and Company, New York, New York.

4. Wang, D., Harper, J. F., and Gribskov, M. (2003) Systematic trans-genomic comparison of protein kinases between Arabidopsis and *Saccharomyces cerevisiae*, *Plant Physiol 132*, 2152-2165.

5. Ghillebert, R., Swinnen, E., Wen, J., Vandesteene, L., Ramon, M., Norga, K., Rolland, F., and Winderickx, J. (2011) The AMPK/SNF1/SnRK1 fuel gauge and energy regulator: structure, function and regulation, *FEBS J 278*, 3978-3990.

6. Polge, C., and Thomas, M. (2007) SNF1/AMPK/SnRK1 kinases, global regulators at the heart of energy control?, *Trends Plant Sci 12*, 20-28.

7. Shen, W., Reyes, M. I., and Hanley-Bowdoin, L. (2009) Arabidopsis protein kinases GRIK1 and GRIK2 specifically activate SnRK1 by phosphorylating its activation loop, *Plant Physiol 150*, 996-1005.

8. Baena-Gonzalez, E., Rolland, F., Thevelein, J. M., and Sheen, J. (2007) A central integrator of transcription networks in plant stress and energy signalling, *Nature 448*, 938-942.

9. Nunes, C., Primavesi, L. F., Patel, M. K., Martinez-Barajas, E., Powers, S. J., Sagar, R., Fevereiro, P. S., Davis, B. G., and Paul, M. J. (2013) Inhibition of SnRK1 by metabolites: tissue-dependent effects and cooperative inhibition by glucose 1-phosphate in combination with trehalose 6-phosphate, *Plant Physiol Biochem 63*, 89-98.

10. Alberts, B. (2002) *Molecular biology of the cell*, 4th ed., Garland Science, New York.

11. Hawley, S. A., Pan, D. A., Mustard, K. J., Ross, L., Bain, J., Edelman, A. M., Frenguelli, B. G., and Hardie, D. G. (2005) Calmodulin-dependent protein kinase kinase-beta is an alternative upstream kinase for AMP-activated protein kinase, *Cell Metab 2*, 9-19.

12. Hong, S. P., Momcilovic, M., and Carlson, M. (2005) Function of mammalian LKB1 and Ca2+/calmodulin-dependent protein kinase kinase alpha as Snf1-activating kinases in yeast, *J Biol Chem 280*, 21804-21809.

13. Shen, W., and Hanley-Bowdoin, L. (2006) Geminivirus infection up-regulates the expression of two Arabidopsis protein kinases related to yeast SNF1- and mammalian AMPK-activating kinases, *Plant Physiol 142*, 1642-1655.

14. Crozet, P., Margalha, L., Confraria, A., Rodrigues, A., Martinho, C., Adamo, M., Elias, C. A., and Baena-Gonzalez, E. (2010) Mechanisms of regulation of SNF1/AMPK/SnRK1 protein kinases, *Front Plant Sci 5*, 190.

15. Halford, N. G., and Hey, S. J. (2009) Snf1-related protein kinases (SnRKs) act within an intricate network that links metabolic and stress signalling in plants, *Biochem J 419*, 247-259.

16. Shen, Q., Liu, Z., Song, F., Xie, Q., Hanley-Bowdoin, L., and Zhou, X. (2011) Tomato SlSnRK1 protein interacts with and phosphorylates betaC1, a pathogenesis protein encoded by a geminivirus beta-satellite, *Plant Physiol 157*, 1394-1406.

17. Masuda, H. P., Cabral, L. M., De Veylder, L., Tanurdzic, M., de Almeida Engler, J., Geelen, D., Inze, D., Martienssen, R. A., Ferreira, P. C., and Hemerly, A. S. (2008) ABAP1 is a novel plant Armadillo BTB protein involved in DNA replication and transcription, *EMBO J 27*, 2746-2756.

18. Navaud, O., Dabos, P., Carnus, E., Tremousaygue, D., and Herve, C. (2007) TCP transcription factors predate the emergence of land plants, *J Mol Evol 65*, 23-33.

19. Cubas, P., Lauter, N., Doebley, J., and Coen, E. (1999) The TCP domain: a motif found in proteins regulating plant growth and development, *Plant J 18*, 215-222.

20. Kosugi, S., and Ohashi, Y. (1997) PCF1 and PCF2 specifically bind to cis elements in the rice proliferating cell nuclear antigen gene, *Plant Cell 9*, 1607-1619.

21. Jonsson, Z. O., and Hubscher, U. (1997) Proliferating cell nuclear antigen: more than a clamp for DNA polymerases, *Bioessays 19*, 967-975.

22. Kosugi, S., and Ohashi, Y. (2002) DNA binding and dimerization specificity and potential targets for the TCP protein family, *Plant J 30*, 337-348.

23. Martin-Trillo, M., and Cubas, P. (2010) TCP genes: a family snapshot ten years later, *Trends Plant Sci 15*, 31-39.

24. Cubas, P., Coen, E., and Zapater, J. M. (2001) Ancient asymmetries in the evolution of flowers, *Curr Biol 11*, 1050-1052.

25. Valsecchi, I., Guittard-Crilat, E., Maldiney, R., Habricot, Y., Lignon, S., Lebrun, R., Miginiac, E., Ruelland, E., Jeannette, E., and Lebreton, S. (2013) The intrinsically disordered C-terminal region of *Arabidopsis thaliana* TCP8 transcription factor acts both as a transactivation and self-assembly domain, *Mol Biosyst 9*, 2282-2295.

26. Nag, A., King, S., and Jack, T. (2009) miR319a targeting of TCP4 is critical for petal growth and development in Arabidopsis, *Proc Natl Acad Sci U S A 106*, 22534-22539.

27. Yoo, S. D., Cho, Y. H., and Sheen, J. (2007) Arabidopsis mesophyll protoplasts: a versatile cell system for transient gene expression analysis, *Nat Protoc 2*, 1565-1572.

28. Crozet, P., Jammes, F., Valot, B., Ambard-Bretteville, F., Nessler, S., Hodges, M., Vidal, J., and Thomas, M. (2010) Cross-phosphorylation between *Arabidopsis thaliana* sucrose nonfermenting 1-related protein kinase 1 (AtSnRK1) and its activating kinase (AtSnAK) determines their catalytic activities, *J Biol Chem 285*, 12071-12077.

29. Herve, C., Dabos, P., Bardet, C., Jauneau, A., Auriac, M. C., Ramboer, A., Lacout, F., and Tremousaygue, D. (2009) *In vivo* interference with AtTCP20 function induces severe plant growth alterations and deregulates the expression of many genes important for development, *Plant Physiol 149*, 1462-1477.

30. Daviere, J. M., Wild, M., Regnault, T., Baumberger, N., Eisler, H., Genschik, P., and Achard, P. (2014) Class I TCP-DELLA interactions in inflorescence shoot apex determine plant height, *Curr Biol 24*, 1923-1928.

31. Koyama, T., Furutani, M., Tasaka, M., and Ohme-Takagi, M. (2007) TCP transcription factors control the morphology of shoot lateral organs via negative regulation of the expression of boundary-specific genes in Arabidopsis, *Plant Cell 19*, 473-484.

32. Aguilar-Martinez, J. A., Poza-Carrion, C., and Cubas, P. (2007) Arabidopsis BRANCHED1 acts as an integrator of branching signals within axillary buds, *Plant Cell 19*, 458-472.

33. Mathieu, Y., Prosper, P., Buee, M., Dumarcay, S., Favier, F., Gelhaye, E., Gerardin, P., Harvengt, L., Jacquot, J. P., Lamant, T., Meux, E., Mathiot, S., Didierjean, C., and Morel, M. (2012) Characterization of a Phanerochaete chrysosporium glutathione transferase reveals a novel structural and functional class with ligandin properties, *J Biol Chem 287*, 39001-39011.

34. Kobashigawa, Y., Kumeta, H., Ogura, K., and Inagaki, F. (2009) Attachment of an NMR-invisible solubility enhancement tag using a sortase-mediated protein ligation method, *J Biomol NMR 43*, 145-150.

35. Aggarwal, P., Das Gupta, M., Joseph, A. P., Chatterjee, N., Srinivasan, N., and Nath, U. (2010) Identification of specific DNA binding residues in the TCP family of transcription factors in Arabidopsis, *Plant Cell 22*, 1174-1189.

36. Wu, M. F., Sang, Y., Bezhani, S., Yamaguchi, N., Han, S. K., Li, Z., Su, Y., Slewinski, T. L., and Wagner, D. (2012) SWI2/SNF2 chromatin remodeling ATPases overcome polycomb repression and control floral organ identity with the LEAFY and SEPALLATA3 transcription factors, *Proc Natl Acad Sci U S A 109*, 3576-3581.

37. Archacki, R., Buszewicz, D., Sarnowski, T. J., Sarnowska, E., Rolicka, A. T., Tohge, T., Fernie, A. R., Jikumaru, Y., Kotlinski, M., Iwanicka-Nowicka, R., Kalisiak, K., Patryn, J., Halibart-Puzio, J., Kamiya, Y., Davis, S. J., Koblowska, M. K., and Jerzmanowski, A. (2009) BRAHMA ATPase of the SWI/SNF chromatin remodeling complex acts as a positive regulator of gibberellin-mediated responses in arabidopsis, *PLoS One 8*, e58588.

38. Efroni, I., Han, S. K., Kim, H. J., Wu, M. F., Steiner, E., Birnbaum, K. D., Hong, J. C., Eshed, Y., and Wagner, D. (2013) Regulation of leaf maturation by chromatin-mediated modulation of cytokinin responses, *Developmental cell 24*, 438-445.

39. Farrona, S., Hurtado, L., March-Diaz, R., Schmitz, R. J., Florencio, F. J., Turck, F., Amasino, R. M., and Reyes, J. C. (2011) Brahma is required for proper expression of the floral repressor FLC in Arabidopsis, *PLoS One 6*, e17997.

40. Vercruyssen, L., Verkest, A., Gonzalez, N., Heyndrickx, K. S., Eeckhout, D., Han, S. K., Jegu, T., Archacki, R., Van Leene, J., Andriankaja, M., De Bodt, S., Abeel, T., Coppens, F., Dhondt, S., De Milde, L., Vermeersch, M., Maleux, K., Gevaert, K., Jerzmanowski, A., Benhamed, M., Wagner, D., Vandepoele, K., De Jaeger, G., and

Inze, D. (2014) ANGUSTIFOLIA3 Binds to SWI/SNF Chromatin Remodeling Complexes to Regulate Transcription during Arabidopsis Leaf Development, *Plant Cell 26*, 210-229.

41. Shen, W., Dallas, M. B., Goshe, M. B., and Hanley-Bowdoin, L. (2014) SnRK1 phosphorylation of AL2 delays Cabbage leaf curl virus infection in Arabidopsis, *J Virol 88*, 10598-10612.

CHAPTER IV

Determining SnRK1 Phosphorylation Consensus Motifs via LC/MS/MS Analysis of Proteins from Arabidopsis Cell Lysates

INTRODUCTION

Phosphorylation is a dynamic, reversible post-translational modification (PTM) that covalently attaches a phosphophate group to a specific tryrosine, serine, or threonine of a target protein (*1*). The phosphate group is added by protein kinases and can be removed by protein phosphatases (*2*). Protein phosphorylation plays a central role in the regulation of cellular processes (*3, 4*). One important kinase in plants is SNF1-related kinase 1(SnRK1), which is the homologue of SNF1 (Sucrose Nonfermenting−1) from yeast and AMPK (AMP-activated protein kinase) from animals (*4*). As discussed in chapter I, SnRK1 is a heterotrimeric complex that regulates several pathways involved in the environmental stress response, global regulation of metabolism, energy conservation, antiviral defense, and development (*5*). Many signaling pathways contain kinases that are themselves phosphorylated as parts of kinase cascades (*1*). In these cascades, kinases act in series with an upstream kinase phosphorylating and activating a downstream kinase, which can in turn phosphorylates other targets (*1*). One such cascade is the GRIK-SnRK1 cascade, in which GRIK (Geminivirus Rep Interacting Kinase) is activated by autophosphorlyation and then phosphorylates the activation loop of SnRK1(*6, 7*). SnRK1 is then able to phosphorylate its substrates.

The phosphorylation sites in a target protein is part of a primary structure known as the consensus sequence (*2*). Regulation of phosphorylation is complex involving the target protein's structure and other phosphorylation events that affect this PTM. The amino acid context of the target residue also plays a key role in kinase recognition and phosphorylation,

and kinases display strong sequence preferences yielding phosphorylation consensus motifs (*2*). These motifs confer kinase specificity (*3*). A study using semi-degenerate peptide array screening to determine putative SnRK1 substrates identified a consensus motif of -LxRxxSxxxL- (*3*), where x is any amino acid. Metaanalysis of known SnRK1 phosphorylation sites uncovered another consensus motif -xxxxxxSxx(D/E)xx- (*8*). However, the SnRK1 phosphorylation sites in TGMV AL1 (*9*), CaLCuV AL2 (*10*), GRIK1 (*11*) and the sites determined in Chapter III do not always conform strongly to these motifs as shown in Table 1. This table shows the amino acid sequence surrounding experimentally determined SnRK1 phosphorylation sites. The intensities listed are calculated that is equal to the sum of the amino acid position weights (*3*) excluding the phosphorylation site and divided by 20. The percent intensity is the percent of that intensity adjusted to the poorest sequence and optimal sequence purposed by this method (*3*).

This does not indicate that either the literature or our experimental sites are incorrect. Prior to June 2011, training sets used to develop prediction algorithms were largely limited to nonplant species, and no dedicated plant-specific computational prediction algorithms were available (*12, 13*). As a consequence, previous computational software missed 40% of experimentally determined sites in the plant Arabidopsis (*14*). Additionally, because the consensus motif is not the only factor affecting phosphorylation, peptide assays may create an incomplete picture. Although these other factors would be accounted for in a meta-analysis, this method is limited to known correlations between kinases and phosphorylation sites. With the predicted rate of phosphorylated proteins of approximately 30% (*15*), there

are potentially dozens or hundreds of unknown phosphorylation sites. Therefore, a high throughput, biologically relevant method is needed to develop a clearer analysis for the SnRK1 consensus sequence.

One instrumentation that provides the greatest advances in phosphoproteomics is mass spectrometry (MS). In the last decade, MS has been used to study plant-based phophoproteomics (*16*). A great deal of the success of plant phosphopeptide identification by MS-based proteomics is due to methods that selectively enrich for phosphopeptides (*17*). Electrostatic repulsion-hydrophilic interaction chromatography (ERLIC) chromatography is a method developed specifically for phosphopeptides (*18*). In addition to hydrophilic characteristics, this system has a weak anion-exchange that favors retention and separation of relatively hydrophilic and negatively charged analytes, such as phosphopeptides (*18*). The majority of peptides collected are often acidic, which can preclude the identification of phosphopeptides in each fraction, such that further enrichment is often necessary (*18*). Several approaches use further enrichment for phosphopeptides, such as immobilized metal affinity chromatography (IMAC) and metal oxides (*17*). IMAC utilizes bound metal ions, such as Fe^{3+}, and the affinity of phosphate groups for these ions. Titanium oxide (TiO_2) is one of the most common metal oxides utilized and is often used as a second enrichment method (*17*). Although both methods enrich for phosphopeptides, IMAC tends to enrich more for basophilic kinase substrates while TiO_2 enriches for acidophilic kinase substrates, suggesting a method utilizing both enrichments is necessary to capture the full complement of kinase substrates (*19*).

Recently, phosphoproteomics has refined existing enrichment methods by advances in nano-LC and HPLC chip technologies, facilitating 'high-throughput' phosphoproteomics research. Advance in the abilities of the instrument to perform electron transfer dissociation (ETD) have been introduced as alternative peptide fragmentation methods. ETD primarily produces c'-type and z-type ions by cleaving peptides at the N–Cα bond (*20*). Because ETD prefers larger and more basic peptides and leaves PTMs largely intact, it is used as a complementary technique to CID or HCD methods (*21*).

Several plant phosphopeptide studies also included prediction of consensus motifs, based on experimental data using the predictor Motif-x and pLOGO software (*22, 23*). Although these methods provide large amounts of data, most of these studies are limited by the fact that the kinase that creates the phosphorylation is unknown. However, using these methods comparing samples treated with a known kinase or in the absence of a key kinase have been preformed to determine new motifs of specific kinases. Huber et al. (*24*) determined specificity of recombinant protein kinases, BAK1, PEPR1, FLS2, and CDPKb, expressed in *E. coli* (*24*). These kinases are catalytically active after autophosphorylations and transphosphorylations. Using IMAC and TiO_2 with LC/MS/MS (*24*) and Motif-x analysis software (*25*), Zhu et al. (*25*)determined motifs for SnRK2 during ABA treatment by comparing wild-type Arabidopsis with a SnRK2 triple knockout mutant. Although this method is more biologically relevant, this approach is not feasible for SnRK1 because double knockout mutants are not viable (*26*). Additionally SnRK1 is not active without being phosphorylated by an upstream kinase. Therefore we designed an alternative method to

examine biological samples to ask if additional motifs or a greater specificity in predicted motifs of SnRK1 can be identified.

MATERIALS AND METHODS

Recombinant SnRK1 Activation

Recombinant His-SnRK1.1 (expressed by the plasmid pNSB 1494), GST-GRIK1 (pNSB 1554), and GST-GRIK1 K137A (pNSB 1555) (*27, 28*) were expressed as previously described (see chapter III). Recombinant SnRK1.1 (5.0 mg) was preactivated with recombinant GRIK (2.5 mg) and purified as described in chapter III but with 10 ml washes and 400 μL elution. The preactivated SnRK1 concentration was determined using the Bradford assay (BioRad).

Preparation of *E. coli* BL21 (DE3) Cell Lysate

E. coli BL21 (DE3) containing the recombinant protein expression plasmids was grown in one flask of 25 ml (or multiples for lines with low expression) Luria broth (LB) medium (Fisher) with Carb100 or Kan50 (dependent on plasmid resistance) at 37°C for 1-3 hours to an OD of 0.8-1.0 and induced with 0.5-1.0 mM IPTG. Cells were pelleted by centrifugation at 3620 ×g for 15 min and frozen at -20 °C overnight. Cell pellets were resuspended in PBS (10 ml 10 mM Na_2HPO_4, 1.8 mM KH_2PO_4, pH 7.4, 140 mM NaCl, 2.7 mM KCl) with Protease Inhibitors for bacterial cells (Sigma, catalog # P8465) and lysed on ice via 12 sonicating pulses of 10 s at a setting of 30% intensity. Lysates were centrifuged at

38,500 ×g for 30 min to remove all insoluble material. Supernatant was collected and its protein concentration determined using the Bradford assay (BioRad).

Preparation of Arabidopsis Cell Lysate

In triplicate, *Arabidopsis thaliana* Columbia-0 cell line (*29*) were grown in suspension under constant dim light in 50 mL Gamborg's B5 basal medium with minor salt (Sigma-Aldrich, catalog #5893) pH 5.8 supplemented with 2.3 µM 2,4-Dichlorophenoxyacetic acid, 2.5 mM MES, 3% Suc, at 23 °C with 160 rpm. Cells were harvested from 4-day old split cultures by centrifugation at 193xg for 10 min. Cell pellets (~10 g, wet weight) were frozen in liquid nitrogen and immediately ground with a mortar and pestle under liquid nitrogen. The powders were suspended to a concentration of 0.5 g/ml in extraction buffer (50mM MOPS, pH 7.5, 150 mM NaCl, 10 mM $MgCl_2$, 2.5 mM DTT, 1.0 mM EDTA, 1.0 mM $MnCl_2$, 1.0 mM dodecyl maltoside (DM), 0.1 mM EGTA, 1 x protease inhibitor for plants (Sigma, catalog # P9599) and incubated for 10 min at 4 °C with rotation at 20 rpm. Debris was removed by filtration using 2 layers of mircloth by centrifuging the flow-through at 32,500 xg for 15min. The supernatant was collected and its protein concentration determined using the Bradford assay (BioRad).

Cell Lysate Kinase Assay

Soluble *E. coli* or Arabidopsis cell lysate (400 µg protein) was incubated in a 50 µl volume in kinase buffer (50mM Tris, pH 7.4, 10 mM $MgCl_2$, 1 mM EGTA, 1 mM DTT) with

the addition of 1 unit of microcystine, 50 mM NaF, 0.1 mM ATP with 0.25 μCi/μl [γ-^{32}P]ATP, and 1 μg of one of the following kinases: no added kinase, GRIK, preactivated SnRK1, GRIK and preactivated SnRK1, GRIK K137A and preactivated SnRK1. Each reaction was incubated for 16 h at 30°. Reactions were quenched by adding 50 μL SDS loading buffer (0.125 mM Tris-HCl, pH 6.8, 20% (v/v) glycerol, 4% (w/v) SDS, 10% (v/v) β-mercaptoethanol, 0.02 mg/ml bromophenol blue) and then separated by SDS-PAGE using NuPAGE 4-12% Bis-Tris Gels (Novex) with 1x NuPAGE MOPS SDS running buffer (Novex). The gel was fixed for 15 min with 40% methanol, 10% acetic acid and stained for 1 h with 0.25g/L Brilliant Blue R-250 (Fisher). Gel was destained overnight in 20% methanol, 10% acetic acid, equilibrated in 3% glycerol, 20% methanol, 10% acetic acid for 1 h, and dried. Radioactivity was visualized by autoradiography.

Sample Preparation for Peptide Fractionation or LC/MS/MS Analysis

Soluble *E. coli* or Arabidopsis cell lysate (1.0 mg protein) was subjected to the kinase reactions describe above except they were incubated with cold ATP for 20 h at 30°C using a total reaction volume of 1.0 mL. Reactions were quenched by precipitation with -20°C acetone at a 6:1 (v:v) ratio acetone to sample. Samples were centrifuged at 54 ×g at 4 °C, supernatants were decanted, and the pellets were washed with 1 mL cold acetone (-20°C) three times. The protein pellet was dried and resuspended in 200 ml 6 M guanidine in 50 mM ammonium bicarbonate, pH 8. The solution was reduced with 10 mM dithiothreitol for 30 min at 57°C, alkylated with 50 mM iodoacetamide for 30 min at room temperature in the

dark, followed by 6-fold dilution with 50 mM ammonium bicarbonate and digestion with trypsin (1:100, w/w) overnight at 37°C. These digested samples were acidified with the addition of 2 μL formic acid and then desalted using Clean™ Prevail C18 100mg/1.5ml solid-phase extraction (SPE) columns (Grace). For SPE, columns were conditioned with 0.5 mL methanol, equilibrated with 0.5 mL 0.1% formic acid, before protein digests are loaded onto the column. After sample loading, the column was washed with 0.5 mL 0.1% formic and peptides were eluted with 0.5 mL 0.1% formic, 80% acetonitrile.

Electrostatic Repulsion-Hydrophilic Interaction Chromatography (ERLIC)

Arabiodpsis samples were dried via vacuum centrifugation and resuspended in 100 μL mobile phase 1 (20 mM ammonium formate, pH 2.0/75% acetonitrile). Each ERLIC separation was performed using an Agilent 1100 series HPLC system (www.agilent.com) and 2.1 x 200 mm, 5 μm particle size, 300 Å pore size PolyWAX LP column (www.polylc.com). The mobile phases consisted of mobile phase 1 and mobile phase 2 (250 mM ammonium formate, pH 2.0, 20% acetonitrile). Resuspended peptides were injected on the mobile phase 1 pre-equilibrated column. Peptides were eluted with a multistep gradient: 100% mobile phase 1 wash for 15 min followed by 0-50% mobile phase 2 linear gradient over 10 min, then 50-95% mobile phase 2 gradient over 20 min, which was subsequently held at 95% mobile phase 2 for 15 min. Peptides were monitored at 245 and 280 nm with spectra from 190 to 400 nm acquired every second using a diode array detector. The first three fractions were collected for 0.8 min each, the fourth for 1.4 min, and the remaining 28

fractions were collected every 2.0 min. Fractions were combined into four ERLIC samples as follows: fractions 1-9, 10-19, 20-26, and 27-32. Each ERLIC sample was dried via vacuum centrifugation and stored at -20 °C until additional enrichment could be performed.

Enrichment of Phosphopeptides using IMAC-TiO_2

IMAC resin was prepared by washing 400 µL of suspended volume of NTA Agarose (Qiagen) twice with 1.0 mL water, before adding 1.0 mL 40 mM EDTA (pH 7.4). The resin was washed twice with 1.0 mL water before acidifying with 1.0 mL 1% acetic acid. Acidified resin was incubated 4-16 h with 1.0 mL 100 mM $FeCl_3$ in 1% acetic acid in the dark at room temperature and stored at 4°C until phosphopeptide enrichment could be performed. To serve as an internal standard, ß-casein digest (5 µg) was added to each ERLIC sample prior to IMAC enrichment.

For phosphopeptide enrichment of the *E. coli* sample or the ERLIC fraction, each dried-down sample was solubilized in 100 µL 1% acetic acid and enriched via IMAC as seen in chapter III.

Further enrichment of the IMAC flow-through was preformed using TiO_2 p200 spin columns (GL) as previously described (*30*), with the following modifications. Samples utilized for this protocol were dried flow-through samples from IMAC enrichment load and wash steps that were pooled together. This sample was loaded onto the TiO_2 spin column, twice washed with 20 µL 80% MeCN, 1% TFA and twice with 20 µL 80% MeCN, 1% TFA, 1M glycolic acid.

LC/MS/MS Analysis

Easy nLC 1000 coupled to an ETD-enabled Orbitrap Elite (Thermo Scientific) was used for nano-LC/MS/MS analyses. An Acclaim PepMap100 C18 5 µm trapping column (100 µm i.d.; length 20 mm) is attached inline to a Self-Pack PicoFrit® capillary (OD/ID 360/75, Tip ID 10 Å, New Objective) that was packed with either HALO C18 , 2.7 µm particles (Mac-Mod Analytical, Inc.), or Magic C18, 3 µm particles (Microbiosciences) and used as the analytical column. Samples were solubilized in 0.1% formic acid and 18 µl was injected onto the trap column and desalted. Reversed-phase LC was performed at a flow rate of 300 nL/min with the mobile phases of 0.5% formic acid (A) and 0.5% formic acid and 80% acetonitrile (B). For peptide separation a three-step linear gradient of 0% to 5% B in 1 min, 5% to 40% B in 59 min, 40% to 90% B in 1 min, and 90% B for 15 min was used with electrospray performed in the positive ion mode with a voltage of 3.8 kV. The MS precursor scan range was *m/z* 400 to 2,000 with a resolving power of 60,000 at *m/z* 400. The top 5 precursor ions were selected for either ETD or HCD fragmentation. Scan events had a minimum signal intensity of 2,000, a default charge state of +2 or greater, isolation width of *m/z* 3.0, and a normalized collision energy setting of 27. MS/MS acquisitions utilized Decision Tree software with the FTMS analyzer using mass charge cut-offs of +3 at *m/z* 650, +4 at *m/z* 900, and +5 at *m/z* 950.

Post LC/MS/MS Data Processing and Analysis

Raw data were processed with Proteome Discover 1.4 (ThermoScientific) and spectra were databased searched using Mascot (Matrix Science). Spectra were filtered for HCD and ETD events. *E. coli* lysate sample peptides were searched against a protein database containing *E. coli* protein sequences with added standards, such as the proteases used in sample preparation, BSA, β-casein, and recombinant fusion proteins; Arabidopsis sample peptides were searched against the TAIR10 Arabidopsis database containing the same standards as the *E. coli* protein database. The peptide precursor mass and fragment ion masses were determined monoisotopically with a precursor mass tolerance of 10 ppm, a fragment ion mass tolerance of 0.01 Da, and strict trypsin specificity allowing for up to two missed cleavages. Carbamidomethylation of Cys was set as a fixed modification, and oxidation of Met and phosphorylation of Ser, Thr, and Tyr were allowed as variable modifications. Peptides were considered identified if the Mascot score was over 20 and had a p-value < 0.05.

Phosphorylation Site Localization

All unique phosphopeptides within a reaction type with >50% phosphorylation site probabilities (PSR) were analyzed with Motif-X (motif-x.med.havard.edu) (*22*) or pLOGO (https://plogo.uconn.edu) (*23*). Motif-X analysis was performed with the following settings: foreground format of MS/MS IPI Arabidopsis Proteome, width of 13, occurrences of 20, and significance 1×10^{-7}. Peptides were processed with peptidexetender (schwartzlab.uconn.edu)

with the following settings: "*" to the right of modified residue, target sequence width of 15, and the proteome of Arabidopsis. The peptidexetender list was then processed via pLOGO, with the parameters set for Protein and Arabidopsis, and all amino acids with p-values <0.05 were selected for further pLOGO analysis to determine if there were more specific motifs. Finalized motifs were used to design synthetic peptides (see Table 3) for phosphopeptide assays.

Bioinformatics

Assession numbers of identified phosophopeptides form each triplicate were combined into groups by reaction type (no kinase, GRIK, preactivated SnRK1, GRIK and preactivated SnRK1, and GRIK K137A and preactivated SnRK1) and compared using Venny 2.0 *(31)*. All assession numbers unique to preactivated SnRK1, GRIK and preactivated SnRK1, GRIK K137A and preactivated SnRK1, and any combination were combined. Assession numbers were analyzed with Mapman via Classification SuperViewer w/ Bootstrap (*32*) and also analyzed by BinGO (*33*) via Cytoscape (*34*). Parameters for Cytoscape included, assess: overrepresentation and visualization, statistical test: Hypergeometric test, Benjamini & Hochberg False Discovery Rate, significance = 0.05, overrepresentation after correction, reference set: whole annotation, ontology file: GO_Biological_Process, organinsm: *Arabidopsis thaliana*.

Synthetic Phosphopeptide Analysis

All synthetic peptides were obtained from Genscript with purities > 95% as confirmed by LC/MS/MS analysis (see Table 3). Phosphorylation of synthetic peptides was assessed by reacting 0.25 μg kinase (GRIK, preactivated SnRK1, GRIK and preactivated SnRK1, and GRIK K137A and preactivated SnRK1) with 2.5 pmol synthetic peptide and 2.5 μL of 1.0 mM ATP and 0.5 μCi γ[^{32}P]-ATP in kinase buffer (50 mM Tris, pH 7.4, 10 mM $MgCl_2$, 1 mM EGTA, 1 mM DTT) overnight at room temperature in a total volume of 30 μL. Reactions were quenched by adding total reaction volume to p81 filter discs (Whatman) and rinsed four times with 250 mL 75 mM H_3PO_4 before the discs were air-dried and submerged in EcoLume Sintillation Fluid. Samples were analyzed with a scintillation counter (Packard Tri-Carb Model 2900 TR).

RESULTS

Kinase Reaction Optimization for Motif Analysis

To determine if additional motifs for SnRK1 phosphorylation exist, initially the soluble proteins of *E. coli* lysates were used as a population of random amino acid sequences. The lysate was reacted with ^{32}P γATP in the presence of GRIK, preactivitated SnRK, GRIK and preactivated SnRK1, GRIK K137A and preactivated SnRK1, or no added kinase (Fig. 1). SnRK1 containing samples showed an elevated level of phosphorylation, indicating that this may be a suitable background for motif analysis via LC/MS/MS. Lysate (1.0 mg) was reacted with ATP and GRIK and SnRK1 with ratios to total lysate protein (μg:μg) being 0:1,

1:10, 1:40, and 1:200, and the phosphorylated proteins were then analyzed with LC/MS/MS (Fig. 2A). The ratio of 1:40 preactivated SnRK1 to total protein lysate had the highest number of identified phosphopeptides and thereby was the best choice for the kinase reaction ratio. This ratio was then used to determine best duration with kinase reactions of 1, 4 and 20 h (Fig 2B). The highest phosphopeptide identification was obtained with the 20-hour samples.

Reactions were performed using a 1:40 ratio of kinase to total protein for 20 h with no added kinase, GRIK, preactivated SnRK1, and GRIK + preactivated SnRK1 and each sample was analyzed by LC/MS/MS. No phosphopeptides were identified in the GRIK and preactivated SnRK1 sample and very few in remaining samples. Overall, not enough phosphopeptides were identified to perform motif analysis; therefore, the *E. coli* lysate is not a suitable background for motif analysis of SnRK1.

LC/MS/MS analysis of Arabidopsis protein Phosphorylation by SnRK1

To determine if an alternative protein population is suitable for SnRK1 phosphorylation motif analysis, the soluble proteins of Arabidopsis cell culture lysate were used in the kinase reactions. A total of 0.40 mg of lysate proteins was reacted with ^{32}P γATP in the presence of GRIK, preactivitated SnRK, GRIK + preactivated SnRK1, GRIK K137A +preactivated SnRK1, or no added kinase (Fig. 3). SnRK1 containing samples showed an elevated level of phosphorylation, evenly distributed through the sample, indicating multiple

phosphorylation events and potentially a suitable background for motif analysis via LC/MS/MS analysis.

Arabidopsis cell cultures were grown and lysed in triplicate. Soluble Arabidopsis cell lysate (1.0 mg protein) was reacted with phosphatase inhibitors, 0.1 mM ATP, and a 40:1 ratio of lysate to kinase with each of the kinase conditions mentioned above and quenched by acetone precipitation, then prepared for LC/MS/MS as described in the Materials and Methods section. A partial list (21 of a total of 18,089) of identified phosphopetpides appears in Table 2.

To determine if quantitative analysis was possible, all peptides of each reaction type within an Arabidopsis lysate replicate were combined and compared (Fig 4). Overall, more than 30% of the phosphopeptides identified were unique for each lysate replicate, about 40% of peptides were shared with only one of the remaining bioreplicates, and only about 30% were shared with all three. This could be due to high degree of fractionation and/or variation of DT selection of peptides for fractionation. Additionally, because many identified peptides were near the limit of detection, it is likely that the same peptide was present but not identified in the other replicates due to that low intensity. Therefore these reaction sets could not be rigorously analyzed as biological replicates and thus label-free quantitative analysis would be inappropriate.

As a compromise identified phosphopeptides of biological sample sets were combined for comparisons between reaction types (Fig5). Based on this comparison, there

were a sufficient number of phosphopeptides unique to each reaction type to justify a phosphorylation site motif analysis.

Identifying Kinase Substrate Phosphorylation Motifs

All unique peptides with >50% phosphorylation site probabilities of each reaction condition (biological replicates were combined) were analyzed with Motif-X (motif-x.med.havard.edu) (Fig. 6). Motifs generated by Motif-X only revealed one or two amino acids beyond the phosphoserine residue. Phosphopetides from all five reaction conditions produced the motif –xxxxxxSPxxxxx- indicating that this may be part of the phosphorylation background as phosphorylation of serine residues adjacent to proline residues are common to many kinase substrates (*8*). GRIK, preactivated SnRK1, GRIK and preactivated SnRK1, and GRIK K137A and preactivated SnRK1 revealed the motif –xxxRxxSxxxxxx-, and GRIK K137A and preactivated SnRK1 also identified –xxxRxxSPxxxxx-. These two sequences are likely SnRK1 motifs but do not offer enough amino acid specificity to test using a phosphopeptide assay.

To further explore kinase substrate motifs, the datasets were also analyzed by pLOGO (https://plogo.uconn.edu). pLOGO revealed more specificity for the motifs produced when compared to Motif-X. The merging of phosphopeptides unique to preactivated SnRK1, GRIK and preactivated SnRK1, GRIK K137A and preactivated SnRK1, and any combination identified multiple motifs, SnRK1 –xxxRxxSFxxxxx-, –xxxRxxSPxxxxx-, –xxxRSxSxxxxxx-, –xxxxxxSPxxxxR-, –xxxxSxSPxxxxx-, –xxxxxLSPxxxxx-, and –

xxSxxxSPxxxxx- (Fig. 7). These pLOGO-derived motifs provide more amino acid specificity, but those amino acids are below the limit for statistical significance as determined by the pLOGO algothrium. The motifs, including patterns observed in amino acids below statistical significance, were use to design synthetic peptides for further analysis (Table 3). These amino acids, although not statically significant, could indicate trends and thereby were considered when designing synthetic peptides.

Assessing Biological Insights of SnRK Phosphorylation using Bioinformatic Analysis

Phosphopeptides unique to preactivated SnRK1, GRIK and preactivated SnRK1, GRIK K137A and preactivated SnRK1, and any combination used for motif analysis were also used to determine any correlation between the annotated functions of the proteins that contain these novel motifs and SnRK1 function and localization.

In previous studies, SnRK1 was found in the cytoplasm in ring-shaped structures around the nuclei (*35*), as well as plasma membranes of cells of hypocotyls, leaves and sepals of flowers, (*35*). In this study, Cytoscape identified possible SnRK1 targets in nearly every cell compartment, with the strongest representation in plasma membranes, membrane bound organelles, and cytoplasm (Fig. 8). Correlating with observations in the literature, Mapman favored target localization in ribosomes, cytosol and cell wall components in the data normalized by Mapman's algorithm (Fig. 9). Mapman also heavily favored targets localized in the nucleus, in agreement with the documented evidence regarding the interaction of SnRK1 with transcription factors (*36*).

SnRK1 is functionally responsible for the regulation of several pathways. It plays a key role in environmental stress response, global regulation of metabolism, energy conservation, antiviral defense, and fundamental development (*5*). SnRK1 is also implicated in playing transcriptional reprogramming, likely through modulating transcription factors (*9, 26*). Cytoscape analysis of the data revealed molecular functions of SnRK1 phosphorylation targets are of structural molecular activity (in particular of the ribosome), binding of nucleotides and their components, and catalytic activity in metabolites or ATP synthesis (Fig 9). These assignments correlate with known SnRK1 functions. Cytoscape highlights the biological processes of these targets as chromatin remodeling, osmotic stress response, metabolism, and inorganic response, in particular cadmium ions (Fig 10). Osmotic stress response and metabolism regulation are known functions of SnRK1 and the research described in Chapter III implicates SnRK1 in regulation of chromatin remodeling. A function in the regulation of cadmium response maybe an unknown function of SnRK1 revealed by this phosphoproteomic study. Mapman indicated molecular functions in structural molecule activity, nucleotide activity, transporter activity, and kinase activity and shows the strongest correlation of biological function with DNA or RNA metabolism, electron transport or energy pathways, cell organization and biogenesis, developmental processes, and response to abiotic or biotic stimulus (Fig 11). Again, most of these are known functions regulated by SnRK1.

The correlation between the function of the phosphoproteins identified by LC/MS/MS analysis by adding preactivated SnRK1 to Arabidopsis soluble protein lysates and the

previously documented role SnRK1 plays in regulating such functions strongly indicates that the identified phosphopeptides are SnRK1 substrates and that the motif analysis provides insightful data relevant to potential kinase substrate specificity.

GRIK-SnRK1 Phosphorylation of Motif-containing Peptides

To determine if motifs discovered by LC/MS/MS analysis are targets for GRIK-SnRK1 cascade phosphorylation, synthetic peptides designed based on these motifs (Table 3) were incubated with ^{32}P γATP in the presence of GRIK, preactivitated SnRK, GRIK and preactivated SnRK1, or GRIK K137A and preactivated SnRK1(Fig. 12). The only peptide that is an obvious substrate of preactivated SnRK1 is Ace-GRVGRSISFGKNRK. This peptide scores 0.805 intensity by Vald et. al. 2008 (see Table 1 for calculation), which meant their system predicted that it would be phosphorylated. But it appears that a point mutation of the +1 Phe to a Pro or -2 Ser to Met is all that is necessary to disrupt phosphorylation, despite a score of 0.715 for both. This indicates that Phe at the +1 position and Ser at -2 may be vital to phosphorylation by SnRK1. Also, the motif –xxxRSxSFxxxxx- which is represented by this peptide is very similar to two of the motifs identified in our study (xxxRxxSFxxxxx and xxxRSxSxxxxxx). The motifs identified by pLOGO with +1 Pro may have been background that was not accounted for in the MS/MS analysis of no added kinase or GRIK only samples, or they may have been a phosphorylation event due more to target tertiary structure instead of the contiguous amino acid sequence. Further study of phosphorylation of the full-length protein containing the –xxxRSxSPxxxxx- motif by GRIK-

SnRK1 cascade would have to be performed to determine if this motif in particular, and the other putative motifs, are indeed SnRK1 targets.

DISCUSSION

Utilizing Arabidopsis cell lysates to determine activated SnRK1phosphorylation target sequence consensus motifs appears to have confirmed a secondary motif, –xxxRSxSFxxxxx-. *E. coli* lysate was insufficient for this type of phosphoproteomic analysis to determine motifs in this system but may remain useful for other kinases that are more reactive and less dependent on being activated by another kinase. Due to the limitations by the amount of preactivated SnRK1 that could be recovered, larger protein lysate concentrations could not be used. Because many of the phosphopeptides identified were near the limit of detection, we believe that higher concentrations may have yielded a more definitive dataset to enable a better assessment of the kinase background or enable using biological replicates for quantitative analysis, thus leading to more conclusive results. However, despite the limitations of this phosphoproteomic study, several motifs were identified and one was confirmed *in vitro* via a kinase assay using a synthetic peptide. Just as important, the proteins that were detected by the identified phosphopeptides agree well with their biological role as targets for SnRK1 phosphorylation, indicating a basis of the phosphoproteomic approach for revealing biologically relevant kinase substrate motifs. Further study regarding the phosphorylation of a full-length protein containing the identified

motifs by GRIK-SnRK1 cascade would have to be performed to determine these are truly GRIK-SnRK cascade substrates.

FIGURES AND TABLES

Table 1. SnRK1 phosphoryltion sites *in vitro* Compared to Literature Based Consensus Motifs

Source	AA sequence	Score *	% Intensity
TCP22 S140	-IRSGGGsTLFST-	0.385	18.05
TCP20 S237	-PGVGHMsFASIL-	0.415	20.21
TCP18 S38	-PFSPSSsINDIL-	0.63	35.74
TCP18 T233	-VLGSMDtSSDLC-	0.69	40.07
TGMV AL1 S97	-NIQRAKsSSDVK-	0.89	54.51
CaLCuV AL2 S109	-SIGSPQsLLQLP-	0.66	37.90
GRIK1 S261	-IGDFSVsQVFKD-	0.455	23.10
Poor consensus	-xGDVGIsPGGGx-	0.135	0.00
Consensus Opt.	-xLKRVKsFWWLx-	1.52	100.0
	-xLxRxxsxxxLx-	NA	NA
Meta-analysis	-xxxxxxsxx(D/E)xx-	NA	NA

*Score was calculated using values for amino acid position weights by Vald et. al. 2008 (Score=(Sum(AA position weights))/20)

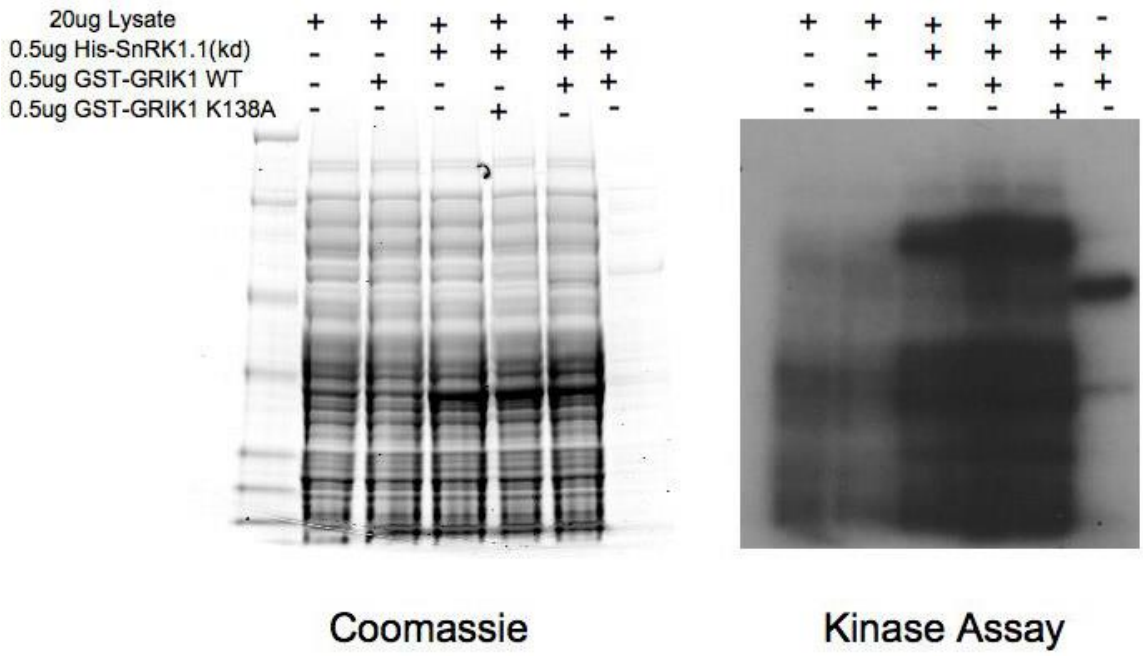

Figure 1. Kinase assay of E. coli BL21 (DE3) lysate by the GRIK-SnRK1 cascade. Images of Coomassie blue stained 10% SDS-PAGE gel (left) and autoradiograph (right) of the soluble component of E. coli BL21 (DE3) lysate subjected to various combinations of active and inactive kinases: no added kinase, GRIK, preactivated SnRK1(kd), GRIK and preactivated SnRK1(kd), and GRIK K137A and preactivated SnRK1(kd). The visualized intensity on X-ray film of preactivated SnRK1, GRIK and preactivated SnRK1(kd), and GRIK K137A and preactivated SnRK1(kd) appears greater than those reactions containing no added kinase or GRIK.

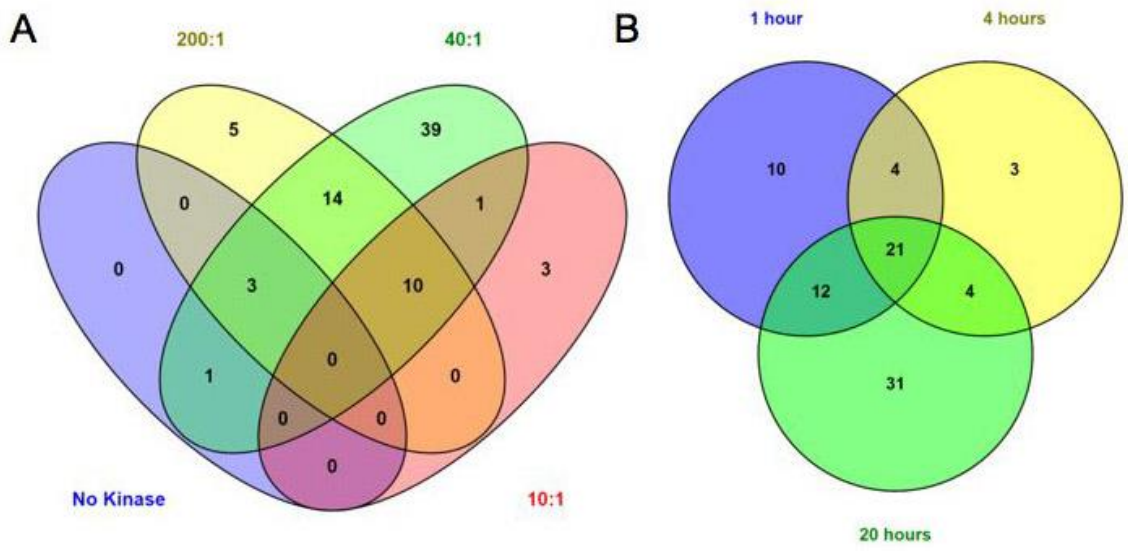

Figure 2. Venn diagrams of lyaste to kinase ratios and incubation times. A) Venn f4 diagram of identified phosphopeptides from E. coli lysates reacted with ATP and ratios of GRIK and SnRK1 to total protein lysate (µg:µg) of 0:1, 1:200, 1:40, and 1:10. B) Venn f3 diagram of identified phosphopeptides from protein lysate reacted with ATP and ratios of GRIK and SnRK1 to total protein lysate protein (µg:µg) 1:40 for 1 h, 4 h, or 20 h.

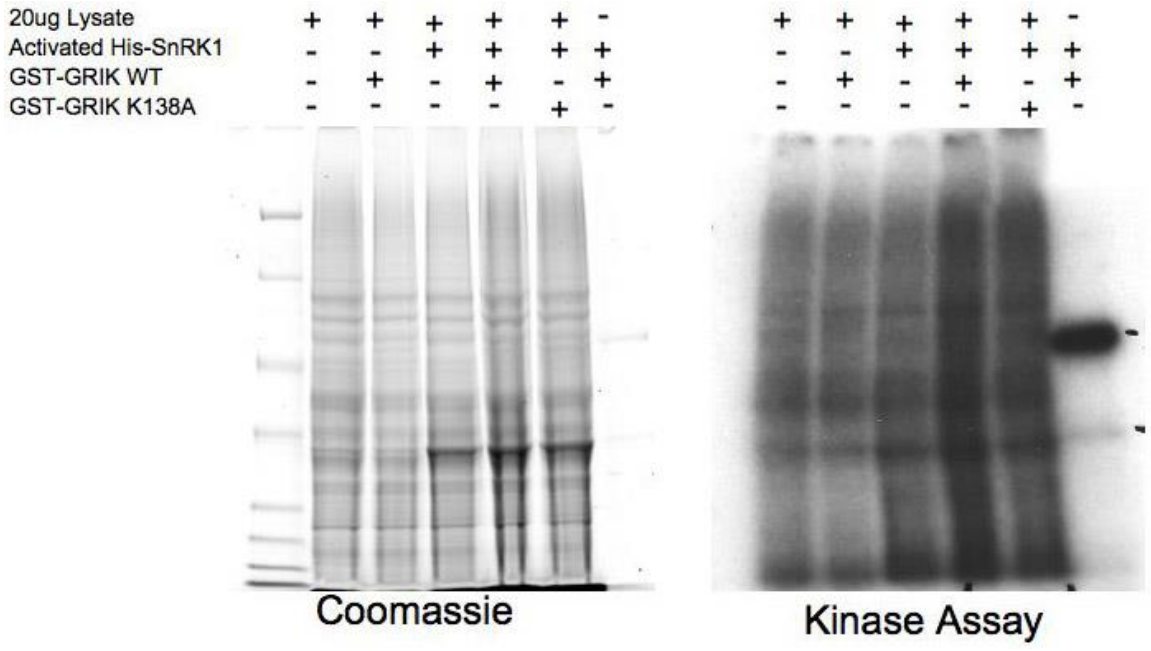

Figure 3. Kinase assay of Arabidopsis lysate by the GRIK-SnRK1 cascade. Images of Coomassie blue stained 10% SDS PAGE gel (left) and autoradiograph (right) of the soluble component of Arabidopsis lysate subjected to various combinations of active and inactive kinases: no added kinase, GRIK, preactivated SnRK1(kd), GRIK and preactivated SnRK1(kd), and GRIK K137A and preactivated SnRK1(kd). The visualized intensely on X-ray film of GRIK and preactivated SnRK1(kd) is significantly greater and preactivated SnRK1 and GRIK K137A and preactivated SnRK1(kd) appear slightly greater than that of no added kinase or GRIK. The increase in intensity does not appear in a few discrete bands but is distributed throughout the lane.

Table 2. Example of phosphopeptides with a q-value < 0.05 using ERLIC fractionation with tandem affinity IMAC/TiO2 and DT LC/MS/MS analysis.

Tair AC	Protien Group	Sequence	Modifications	Kinase(s)	Rep.	ERLIC Fraction	IMAC/ TiO2	q-Value
AT2G32730 AT1G01100	26S proteasome regulatory complex	ASTEKEGDSmQVDsPAAVEK	M10(Oxidation) S14(Phospho)	GRIK K137A + SnRK1	1	F2	IMAC	0.000
AT5G47700 AT1G01100	60S acidic ribosomal protein family	KKDEPAEEsDGDLGFGLFD	S9(Phospho)	GRIK	1	F3	IMAC-TiO2	0.000
AT5G47700	60S acidic ribosomal protein family	KKDEPAEEsDGDLGFGLFD	S9(Phospho)	GRIK K137A + SnRK1	1	F2	IMAC-TiO2	0.002
AT1G04780	Ankyrin repeat family protein	VSDLLGDDDsPSR	S10(Phospho)	no recombinate kinase	3	F3	IMAC-TiO2	0.003
AT5G04430	binding to TOMV RNA 1L (long form)	RSPEPHDSSEADsAEKPTHIR	S13(Phospho)	preactivated SnRK1	3	F1	IMAC-TiO2	0.000
AT3G20410	calmodulin-domain protein kinase 9	AAAAAPGLsPK	S9(Phospho)	GRIK K137A + SnRK1	2	F1	IMAC	0.022
AT5G49890	chloride channel C	TTFGsQILR	S5(Phospho)	preactivated SnRK1	1	F1	IMAC	0.005
AT1G69190	Dihydropterin pyrophosphokinase / Dihydropteroate synthase	ISsQEELDR	S3(Phospho)	preactivated SnRK1	1	F2	IMAC	0.038
AT1G54270 AT3G13920	eif4a-2 |eukaryotic translation initiation factor 4A1	VHAcVGGtSVR	C4(Carbamidomethyl) T8(Phospho)	GRIK K137A + SnRK1	3	F1	IMAC	0.025
AT5G42950	GYF domain-containing protein	SPsSDLLSILQGVTDR	S3(Phospho)	GRIK K137A + SnRK1	2	F2	IMAC-TiO2	0.000
AT5G47210	Hyaluronan / mRNA binding family	AsLNPFDLLGDDAEDPSQLA VALSQK	S2(Phospho)	GRIK	3	F2	IMAC-TiO2	0.000
AT5G03040	IQ-domain 2	QSSSsPPPALAPR	S5(Phospho)	no recombinate kinase	3	F1	IMAC-TiO2	0.000
AT5G03040	IQ-domain 2	QSSSsPPPALAPR	S5(Phospho)	preactivated SnRK1	3	F1	IMAC-TiO2	0.000
AT5G20490	Myosin family protein with Dil domain	ENsGFGFLLTR	S3(Phospho)	preactiv- ated SnRK1	1	F1	IMAC	0.004
AT1G48920	nucleolin like 1	GFDASLsEDDIKNTLR	S7(Phospho)	GRIK K137A + SnRK1	2	F2	IMAC	0.000
AT5G64100	Peroxidase superfamily protein	TVscADILTLAAR	S3(Phospho) C4(Carbamidomethyl)	preactiv- ated SnRK1	1	F1	IMAC	0.004

Table 2. Example of phosphopeptides with a q-value < 0.05 using ERLIC fractionation with tandem affinity IMAC/TiO_2 and DT LC/MS/MS analysis. (Continued)

pRS Probability	pRS Site Probabilities	# Missed Cleavages	Charge	m/z [Da]	MH+ [Da]	ΔM [ppm]	Activation Type
100.0%	S(2); 0.0; T(3); 0.0; S(9); 0.0; S(14); 100.0	1	3	725.6646	2174.9793	29.09	HCD
100.0%	S(9); 100.0	2	2	1074.955	2148.9036	1.21	HCD
100.0%	S(9); 100.0	2	3	716.9714	2148.8996	-0.68	HCD
99.8%	S(2); 0.0; S(10); 99.8; S(12); 0.2	0	2	728.304	1455.6006	0.45	HCD
100.0%	S(2); 0.0; S(8); 0.0; S(9); 0.0; S(13); 100.0; T(18); 0.0	1	3	809.3635	2426.0758	1.04	HCD
100.0%	S(9); 100.0	0	2	517.2707	1033.5341	25.4	HCD
100.0%	T(1); 0.0; T(2); 0.0; S(5); 100.0	0	2	551.7929	1102.5784	44.55	HCD
99.9%	S(2); 0.1; S(3); 99.9	0	2	578.7728	1156.5383	43.26	HCD
90.3%	T(8); 90.3; S(9); 9.7	0	2	611.7924	1222.5776	30.82	HCD
100.0%	S(1); 0.0; S(3); 100.0; S(4); 0.0; S(8); 0.0; T(14); 0.0	0	2	884.4309	1767.8544	1.08	HCD
100.0%	S(2); 100.0; S(17); 0.0; S(24); 0.0	0	3	932.108	2794.3094	-3.24	HCD
100.0%	S(2); 0.0; S(3); 0.0; S(4); 0.0; S(5); 100.0	0	2	687.8244	1374.6415	0.11	HCD
100.0%	S(2); 0.0; S(3); 0.0; S(4); 0.0; S(5); 100.0	0	2	687.8239	1374.6404	-0.69	HCD
100.0%	S(3); 100.0; T(10); 0.0	0	2	660.8316	1320.6559	43.52	HCD
100.0%	S(5); 0.0; S(7); 100.0; T(14); 0.0	1	2	930.942	1860.8768	21.04	HCD
100.0%	T(1); 0.0; S(3); 100.0; T(9); 0.0	0	2	735.8876	1470.768	44.68	HCD
100.0%	S(1); 0.0; S(3); 100.0; S(10); 0.0; S(11); 0.0	0	2	636.3014	1271.5955	25.73	HCD

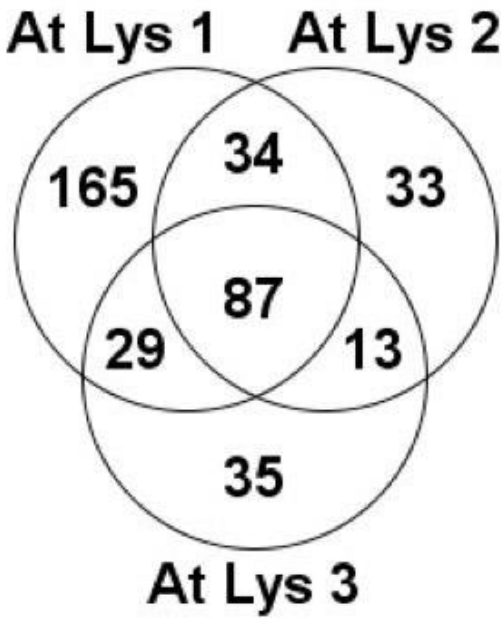

Figure 4. Venn F3 diagram of total unique phosphopeptides identified for all reactions of each Arabidopsis lysate biological replicate.

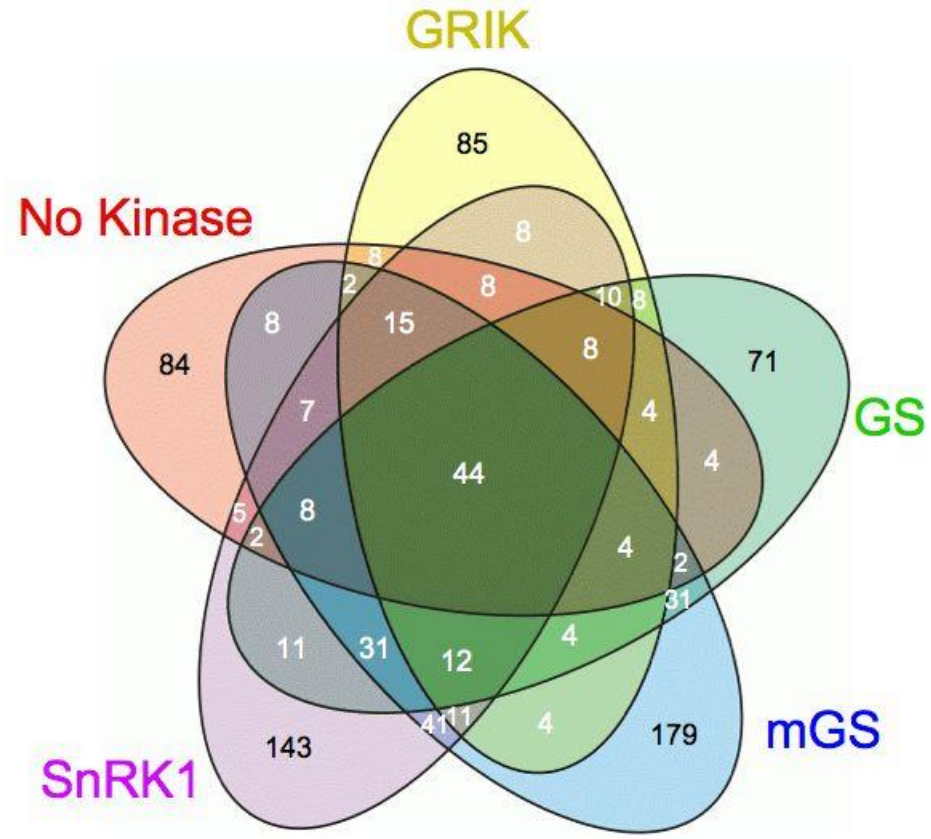

Figure 5. Venn F5 diagram of the total combined sets of peptides for each reaction type. No added kinase (red), GRIK (yellow), preactivated SnRK1 (purple), GRIK and preactivated SnRK1 (GS)(green), and GRIK K137A and preactivated SnRK1 (mGS)(blue).

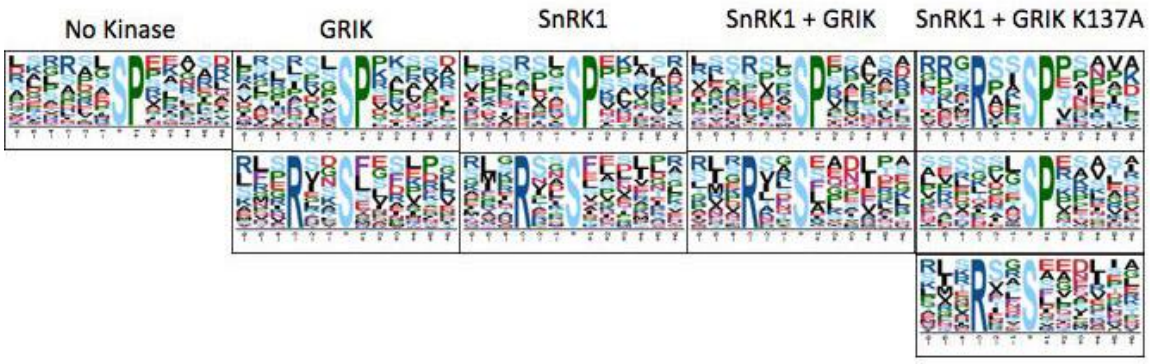

Figure 6. Motif logos generated by Motif-X analysis. Motif logos generated for each reaction type are indicated above each column. The height of the font for each amino acid correlates wth the significance of that amino acid to the motif.

Figure 7. Motif logos by pLOGO analysis. Motif logos generated by combining phosphopeptides unique to preactivated SnRK1, GRIK + Preactivated SnRK1, GRIK K137A + preactivated SnRK1, preactivated SnRK1 and GRIK + Preactivated SnRK1, preactivated SnRK1 and GRIK K137A + Preactivated SnRK1, GRIK + Preactivated SnRK1, GRIK K137A + preactivated SnRK1, and the combination of all three. The height of the font for each amino acid correlates with the significance of that amino acid to the motif.

Table 3. Synthetic Peptides.

Peptide Name	**peptide seq**
SnRK1 control 1	Ace-GNVGGDESANKNRK
SnRK1 motif 12	Ace-GRVSRDLSPEKNRK
SnRK1 motif 11	Ace-GNVGGSISPGKNRK
SnRK1 motif 10	Ace-GNVGRSISPGKNRK
SnRK1 motif 09	Ace-GRVGGDISPEKNRK
SnRK1 motif 08	Ace-GRVGGDLSPEKNRK
SnRK1 motif 07	Ace-GRVGRMISFGKNRK
SnRK1 motif 06	Ace-GRVGRDISPGKNRK
SnRK1 motif 05	Ace-GRVGRDISPEKNRK
SnRK1 motif 04	Ace-GRVGRSISPEKNRK
SnRK1 motif 03	Ace-GRVGRSISAGKNRK
SnRK1 motif 02	Ace-GRVGRSISFGKNRK
SnRK1 motif 01	Ace-GRVGRSISPGKNRK
sp49- posstive control	Ace-KGRMRRISSVEMMK

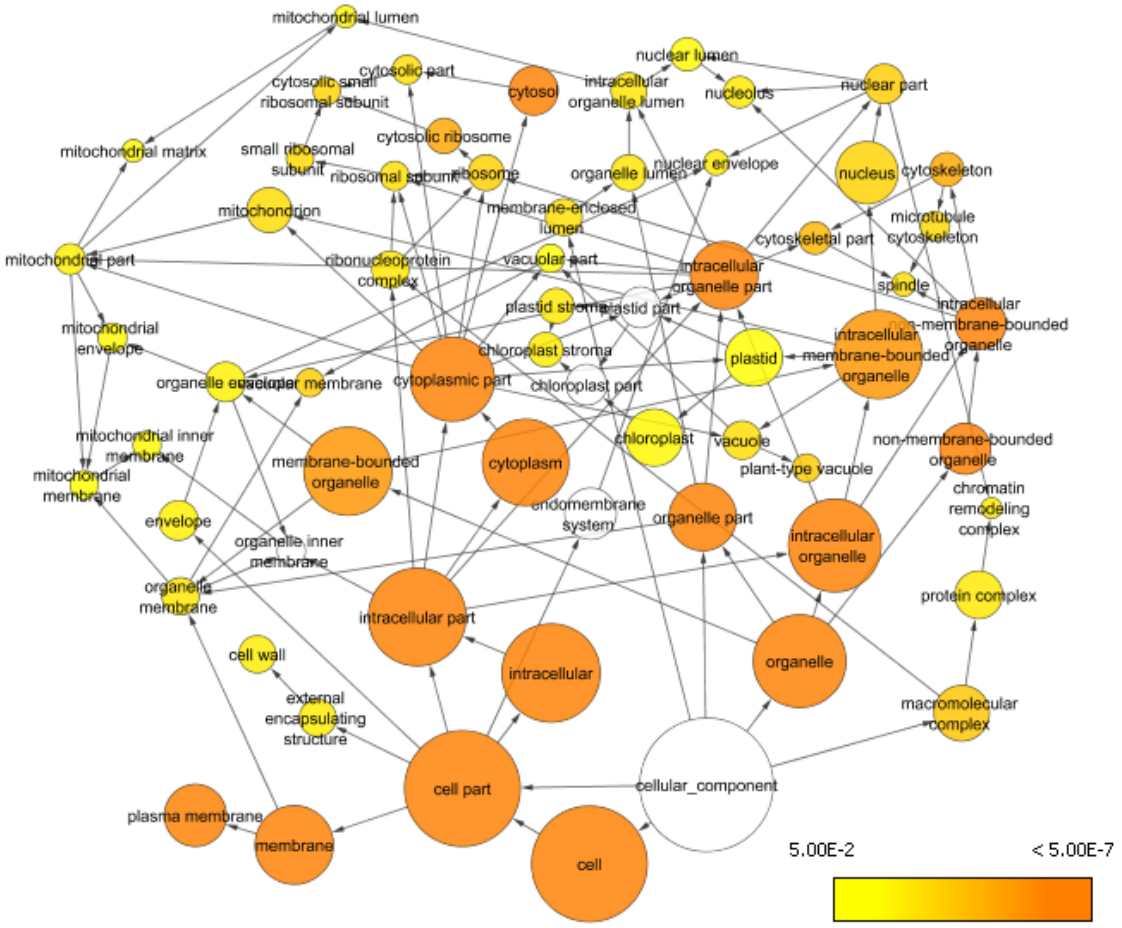

Figure 8. GOterm map from Cytoscape of over-represented cellular components of phosphoproteins as targets of SnRK1. Circles indicate the biological process and arrows indicate the nodes. Colors that fill the circles indicate statistical significance as p-values shown in gradient bar (bottom right).

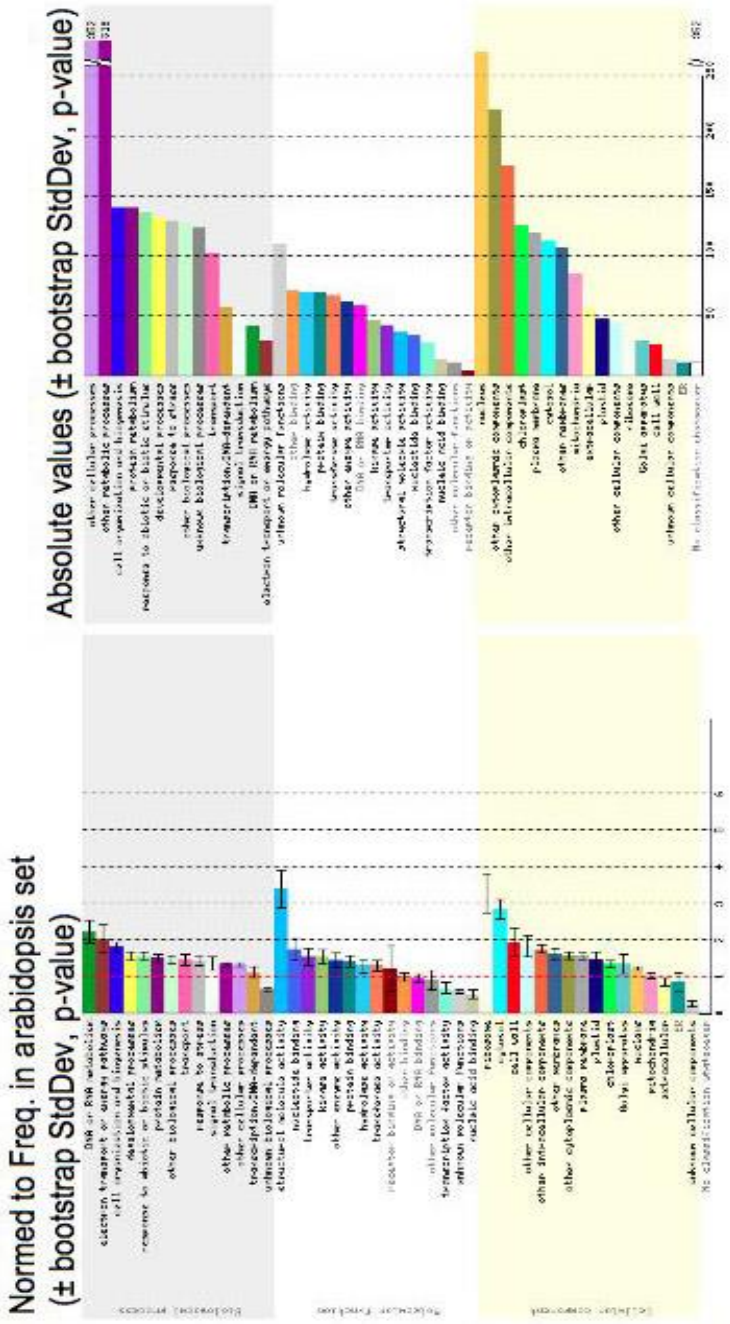

Figure 9. GOterm bar graphs by Mapman analysis of the phosphoproteins as targets of SnRK1.

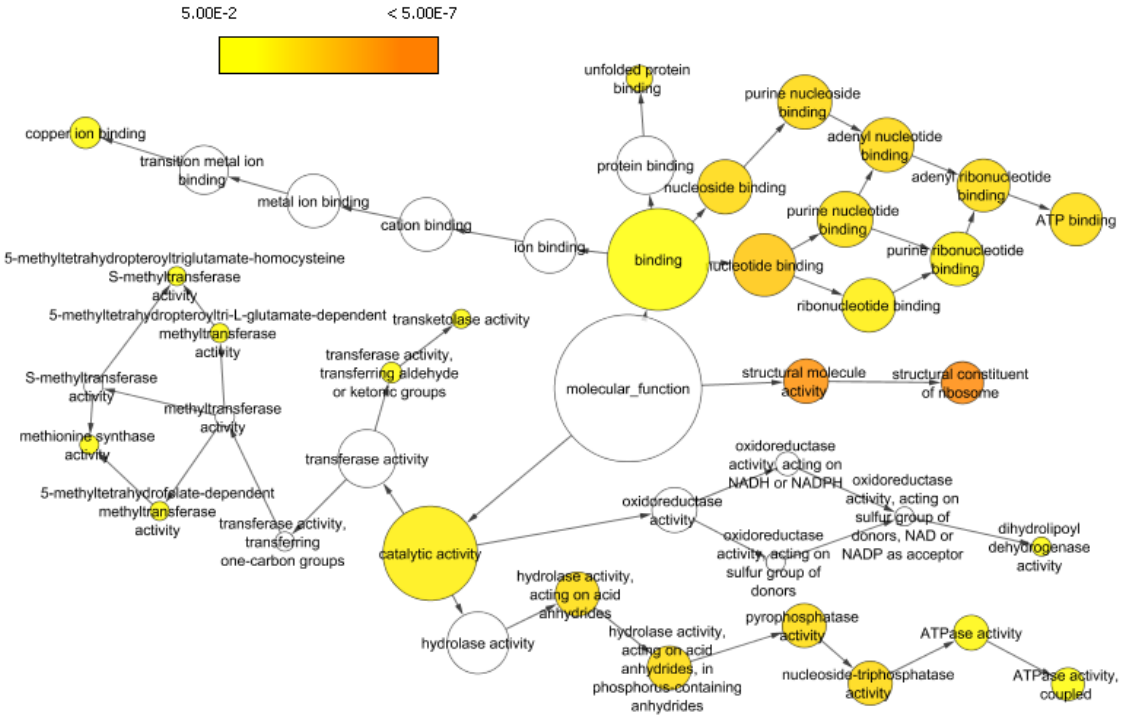

Figure 10. GOterm map from Cytoscape of over-represented molecular function of phosphoproteins as targets of SnRK1. Circles indicate the nodes and arrows indicate the molecular function. Colors that fill the circles indicate statistical significance as p-values shown in the gradient bar (top left).

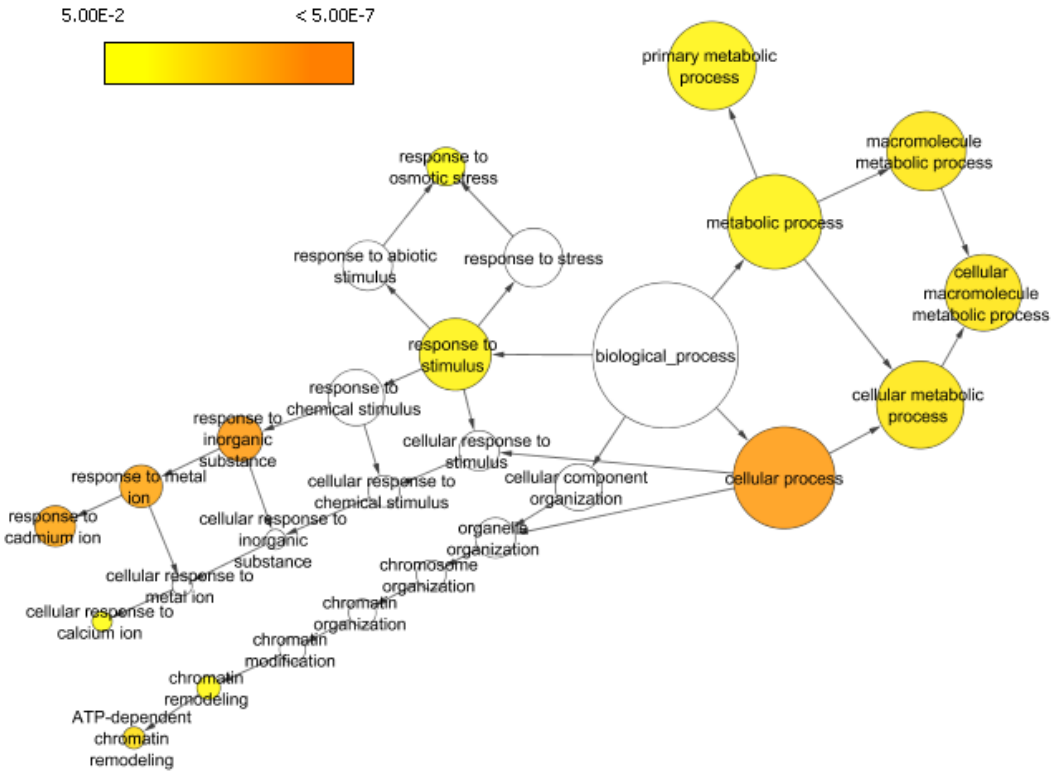

Figure 11. GOterm map from Cytoscape of over-represented biological processes of phosphoproteins as targets of SnRK1. Circles indicate the nodes and arrows indicate the biological process. Colors that fill the circles indicate statistical significance as p-values shown in the gradient bar (top left).

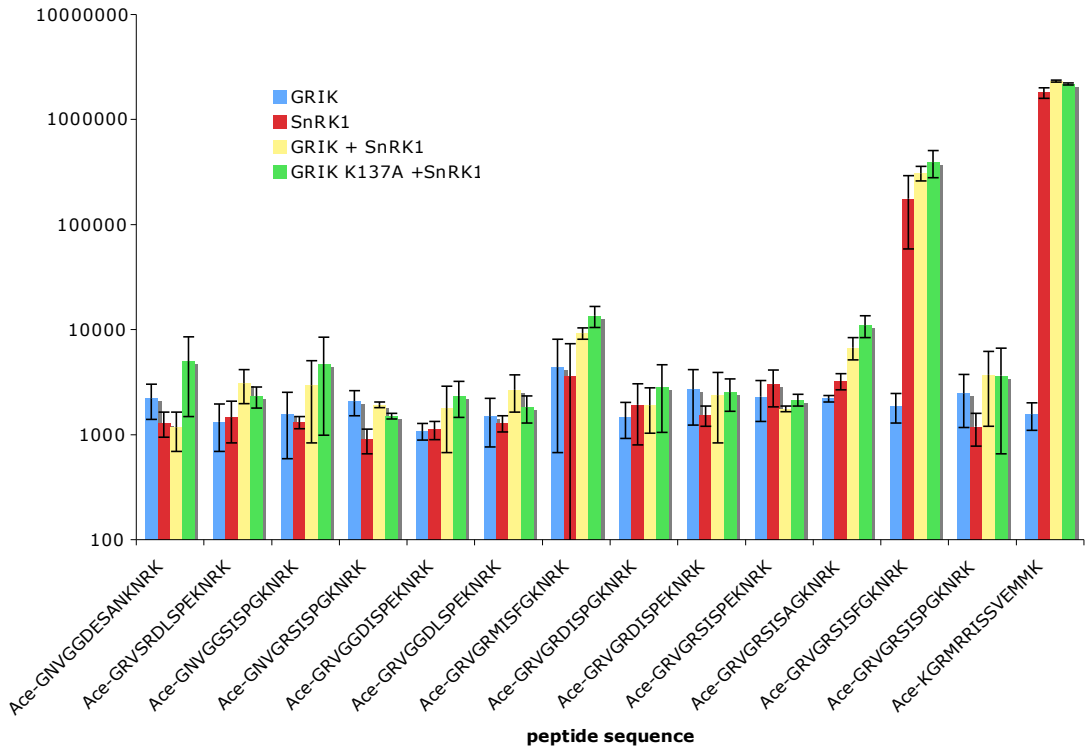

Figure 12. Phosphopeptide Assay of SnRK1 Motif Synthetic Peptides. In triplicate, Each synthetic peptide was incubated with GRIK, preactivated SnRK1, GRIK and preactivated SnRK1, or GRIK K137A and preactivated SnRK1 in triplicate. CPM indicates the intensity of average radioactivity from phosphorylation. Ace-GNVGGDESANKNRK was used as a negative control and Ace-KGRMRRISSVEMMK represented a positive control.

REFERENCES

1. **Alberts, B. (2002) *Molecular biology of the cell*, 4th ed., Garland Science, New York.**

2. **Nelson, D. L. (2005) *Lehninger Principles of Biochemistry*, 4th ed., W. H. Freeman and Company, New York, New York.**

3. **Vlad, F., Turk, B. E., Peynot, P., Leung, J., and Merlot, S. (2008) A versatile strategy to define the phosphorylation preferences of plant protein kinases and screen for putative substrates, *Plant J 55*, 104-117.**

4. **Hrabak, E. M., Chan, C. W., Gribskov, M., Harper, J. F., Choi, J. H., Halford, N., Kudla, J., Luan, S., Nimmo, H. G., Sussman, M. R., Thomas, M., Walker-Simmons, K., Zhu, J. K., and Harmon, A. C. (2003) The Arabidopsis CDPK-SnRK superfamily of protein kinases, *Plant Physiol 132*, 666-680.**

5. **Ghillebert, R., Swinnen, E., Wen, J., Vandesteene, L., Ramon, M., Norga, K., Rolland, F., and Winderickx, J. (2011) The AMPK/SNF1/SnRK1 fuel gauge and energy regulator: structure, function and regulation, *FEBS J 278*, 3978-3990.**

6. **Crozet, P., Margalha, L., Confraria, A., Rodrigues, A., Martinho, C., Adamo, M., Elias, C. A., and Baena-Gonzalez, E. (2010) Mechanisms of regulation of SNF1/AMPK/SnRK1 protein kinases, *Front Plant Sci 5*, 190.**

7. **Halford, N. G., and Hey, S. J. (2009) Snf1-related protein kinases (SnRKs) act within an intricate network that links metabolic and stress signalling in plants, *Biochem J 419*, 247-259.**

8. **van Wijk, K. J., Friso, G., Walther, D., and Schulze, W. X. (2014) Meta-Analysis of Arabidopsis thaliana Phospho-Proteomics Data Reveals Compartmentalization of Phosphorylation Motifs, *Plant Cell 26*, 2367-2389.**

9. **Shen, Q., Liu, Z., Song, F., Xie, Q., Hanley-Bowdoin, L., and Zhou, X. (2011) Tomato SlSnRK1 protein interacts with and phosphorylates betaC1, a pathogenesis protein encoded by a geminivirus beta-satellite, *Plant Physiol 157*, 1394-1406.**

10. **Shen, W., Dallas, M. B., Goshe, M. B., and Hanley-Bowdoin, L. (2014) SnRK1 phosphorylation of AL2 delays Cabbage leaf curl virus infection in Arabidopsis, *J Virol 88*, 10598-10612.**

11. Shen, W., Reyes, M. I., and Hanley-Bowdoin, L. (2009) Arabidopsis protein kinases GRIK1 and GRIK2 specifically activate SnRK1 by phosphorylating its activation loop, *Plant Physiol 150*, 996-1005.

12. Kersten, B., Agrawal, G. K., Durek, P., Neigenfind, J., Schulze, W., Walther, D., and Rakwal, R. (2009) Plant phosphoproteomics: an update, *Proteomics 9*, 964-988.

13. Lee, T. Y., Bretana, N. A., and Lu, C. T. (2011) PlantPhos: using maximal dependence decomposition to identify plant phosphorylation sites with substrate site specificity, *BMC Bioinformatics 12*, 261.

14. Peck, S. C. (2006) Phosphoproteomics in Arabidopsis: moving from empirical to predictive science, *J Exp Bot 57*, 1523-1527.

15. Cohen, P. (2000) The regulation of protein function by multisite phosphorylation--a 25 year update, *Trends Biochem Sci 25*, 596-601.

16. Nakagami, H., Sugiyama, N., Ishihama, Y., and Shirasu, K. (2012) Shotguns in the front line: phosphoproteomics in plants, *Plant Cell Physiol 53*, 118-124.

17. Lemeer, S., and Heck, A. J. (2009) The phosphoproteomics data explosion, *Curr Opin Chem Biol 13*, 414-420.

18. Chien, K. Y., Liu, H. C., and Goshe, M. B. (2011) Development and application of a phosphoproteomic method using electrostatic repulsion-hydrophilic interaction chromatography (ERLIC), IMAC, and LC-MS/MS analysis to study Marek's Disease Virus infection, *J Proteome Res 10*, 4041-4053.

19. Herring, L. E., Grant, K. G., Blackburn, K., Haugh, J. M., and Goshe, M. B. (2015) Development of a tandem affinity phosphoproteomic method with motif selectivity and its application in analysis of signal transduction networks, *J Chromatogr B Analyt Technol Biomed Life Sci 988*, 166-174.

20. Syka, J. E., Coon, J. J., Schroeder, M. J., Shabanowitz, J., and Hunt, D. F. (2004) Peptide and protein sequence analysis by electron transfer dissociation mass spectrometry, *Proc Natl Acad Sci U S A 101*, 9528-9533.

21. Swaney, D. L., McAlister, G. C., and Coon, J. J. (2008) Decision tree-driven tandem mass spectrometry for shotgun proteomics, *Nat Methods 5*, 959-964.

22. Chou, M. F., and Schwartz, D. (2011) Biological sequence motif discovery using motif-x, *Curr Protoc Bioinformatics Chapter 13*, Unit 13 15-24.

23. O'Shea, J. P., Chou, M. F., Quader, S. A., Ryan, J. K., Church, G. M., and Schwartz, D. (2013) pLogo: a probabilistic approach to visualizing sequence motifs, *Nat Methods 10*, 1211-1212.

24. Wu, X., Oh, M. H., Kim, H. S., Schwartz, D., Imai, B. S., Yau, P. M., Clouse, S. D., and Huber, S. C. (2012) Transphosphorylation of E. coli Proteins during Production of Recombinant Protein Kinases Provides a Robust System to Characterize Kinase Specificity, *Front Plant Sci 3*, 262.

25. Wang, P., Xue, L., Batelli, G., Lee, S., Hou, Y. J., Van Oosten, M. J., Zhang, H., Tao, W. A., and Zhu, J. K. (2014) Quantitative phosphoproteomics identifies SnRK2 protein kinase substrates and reveals the effectors of abscisic acid action, *Proc Natl Acad Sci U S A 110*, 11205-11210.

26. Baena-Gonzalez, E., Rolland, F., Thevelein, J. M., and Sheen, J. (2007) A central integrator of transcription networks in plant stress and energy signalling, *Nature 448*, 938-942.

27. Shen, W., and Hanley-Bowdoin, L. (2006) Geminivirus infection up-regulates the expression of two Arabidopsis protein kinases related to yeast SNF1- and mammalian AMPK-activating kinases, *Plant Physiol 142*, 1642-1655.

28. Kong, L. J., and Hanley-Bowdoin, L. (2002) A geminivirus replication protein interacts with a protein kinase and a motor protein that display different expression patterns during plant development and infection, *Plant Cell 14*, 1817-1832.

29. Calikowski, T. T., Meulia, T., and Meier, I. (2003) A proteomic study of the arabidopsis nuclear matrix, *J Cell Biochem 90*, 361-378.

30. Turner, M., Richardson, B., and Soderblom, E. (2013) Protocol for GL spin columns

31. Oliveros, J. C. (2007-2015) Venny. An interactive tool for comparing lists with Venn's diagrams.

32. Provart, N., Zhu, T. (2003) A Browser-based Functional Classification SuperViewer for Arabidopsis Genomics, *Currents in Computational Molecular Biology*, 271-272.

33. Maere S, Heymans K, and M, K. (2005) BiNGO: a Cytoscape plugin to assess overrepresentation of gene ontology categories in biological networks., *Bioinformatics 21*, 3448-3449.

34. Shannon P, Markiel A, Ozier O, Baliga NS, Wang JT, Ramage D, Amin N, Schwikowski B, and T, I. (2003) Cytoscape: a software environment for integrated models of biomolecular interaction networks, *Genome Res 13*, 2498-2504.

35. Bitrian, M., Roodbarkelari, F., Horvath, M., and Koncz, C. (2011) BAC-recombineering for studying plant gene regulation: developmental control and cellular localization of SnRK1 kinase subunits, *Plant J 65*, 829-842.

36. Damerval, C., Le Guilloux, M., Jager, M., and Charon, C. (2007) Diversity and evolution of CYCLOIDEA-like TCP genes in relation to flower development in Papaveraceae, *Plant Physiol 143*, 759-772.

CHAPTER V

Prospectus

PROSPECTUS

Abiotic and biotic stresses often significantly reduce yields of economically important crop plants. Due to their sessile natures, plants have evolved complicated response pathways to react to environmental stresses and signals. SNF1-related kinase 1 (SnRK1) is the plant homolog of AMPK and SNF1. The primary function of the SNF1/AMPK/SnRK1 family is to regulate metabolic and energy homeostasis pathways *(1)*. SnRK1 is functionally responsible for the regulation of several pathways. It plays a key role in environmental stress responses, global regulation of metabolism, energy conservation, antiviral defense, and development *(2)*. Evidence indicates SnRK1 uses the post-translational modification, protein phosphorylation, to induce catabolic reactions of key metabolic enzymes and to cause large scale transcription reprogramming by modulating transcription factors *(3, 4)*. Like AMPK and SNF1, SnRK1 is activated by an upstream kinase, which is GRIK in plants *(5, 6)*. How the GRIK-SNRK1 cascade modulates cell development and growth is not well understood.

To better understand how the GRIK-SnRK1 cascade modulates transcription, I showed that it phosphorylates more than half of the members of the Arabidopsis TCP transcription factor family. I characterized the phosphorylation site(s) of three TCPs and analyzed Arabidopsis cell proteins in a series of GRIK-SnRK1 kinase reactions to reveal a more specific motif for SnRK1 phosphorylation.

Exploring Functional Effects of TCP18 Phosphorylation by the GRIK-SnRK1 Cascade

TCP18 or BRC1 is required for axial bud dormancy. Comparing gene expression profiles of wild-type and *brc1* mutants identified several BRC1-dependent genes, including a set of up-regulated ABA-related genes (*7*). Although TCP18 function has been well studied, there is little information about its regulation in the literature, as is the case for most TCPs. I used LC/MS/MS to determine the TCP18 phosphorylation sites by the GRIK-SnRK1 cascade *in vitro* and verified the sites by site-directed mutagenesis (Chapter III). Ser-36 and Ser-38 have a clear impact on TCP18 phosphorylation, and Thr-233 has a mild but discernable impact as well. Plans are underway to collaborate with Dr. Pilar Cubas, an expert in TCP18 *in vivo* analysis, to determine the functional impact of TCP18 phosphorylation. These experiments will use phosphomutant and phosphomimic forms of TCP18 that I constructed.

Verification of TCP20 and TCP22 interaction with SnRK1 and GRIK *in vivo*

TCP20 binds the promoter regions of RPL24, RPS27 (*8*), PCNA2, RPS4, and CyCB1;1 (*9*). TCP20 is expressed proliferating tissues, including embryos, root buds and tips, cotyledons, and meristems (*9*). TCP20 regulates germination, shoot growth, and hypocotyl/cotyledon development (*9*). TCP20 also targets LIPOXYGENASE2 (LOX2) and TCP9 (*10*) and represses expression of subgroup Ib bHLH transcription factors (*11*).

TCP20 affects nitrate forging by binding the promoter region of NIA1.1 and NRT2.1, mediating root response to nitrate concentrations (*12*). TCP20 interacts with the Isochorismate Synthaase 1 (ICS1) gene, which codes for the key enzyme in salicylic acid biosynthesis, and may regulate it along with TCP8 (*13*). TCP22 localizes on the surface of newly formed leaves (*14*) and has been implicated in regulating leaf developmental traits, particularly the size of rosettes (*14*), plant growth, and reduced response to gibberellin (*15*).

We characterized phosphorylation sites of TCP20 and TCP22 and showed that phosphorylation status impacts their interactions with BRM, a subunit of the SWI/SNF chromatin remodeling complex (Chapter III). Although this functional implication for TCP20 and TCP22 were determined *in vivo*, direct interaction of SnRK1 with either TCP20 or TCP22 was not assessed. Future studies could address potential interactions in co-immunoprecipitation and LC/MS/MS analyses of transgenic Arabidopsis suspension cells expressing HA-tagged TCP20 or TCP22. This approach could identify binding partners of TCP20 and TCP22 including SnRK1 and their heterodimer partners (see Chapter I Fig.5)

SnRK1 Specificity and Phosphorylation of Other TCPs

SnRK1.1 is expressed throughout the seedling, but is more prevalent in leaf primordia, vascular tissue, and root tips (*16*). In contrast, SnRK1.2 is only present in hydathodes, leaf primordia, cotyledons, and vascular tissue of seedlings (*16*). SnRK1.1

over-expression lines are delayed for flowering and the onset of senescence under long-day conditions (*3*), SnRK1.2 over-expressing mutants have early flowering and larger rosettes (*16*).Therefore, it is likely that there are differences in the substrates targeted by the two SnRK1 isoforms. To date, the only report of post-transcriptional modification of a class I TCP is phosphorylation of TCP8 (*17*). Reports of regulation of class II members indicate that a subset of CIN-type mRNAs are targets of the microRNA, miR319 (*18*). Some class I TCPs and NAC homologues may also be regulated by miR319 (*19*). This microRNA, as well as others, is downregulated during energy deficient periods by SnRK1 (*20*). Additionally, TCP4 appears to regulate miR167, which is part of the miR159-miR167-miR319 circuit, indicating indirect TCP modulation of other TCP functions (*21*).

Regulation of TCP by protein interactions has recently been identified. TCPs can be negatively regulated by PNM1, a transcription factor that is found in both the nucleus and mitochondria and thought to act as a messenger from the mitochondria (*22*). TCP Interactor containing EAR motif protein (TIE1) modulates TCP activity, and when over-expressed, causes curly leaves similar to miR319 over-expressing mutants (*23*). TCP5, TCP13, and TCP 17 are also negatively regulated by RABBIT EARS (RBE) (*24*). It is hypnotized that introns might also have regulatory roles in these genes (*25*).

Phosphorylation events by the GRIK-SnRK1 cascade of several TCPs *in vitro* were observed, but only four were comprehensively analyzed via LC/MS/MS to determine phosphorylation sites (Chapter III). I propose that similar treatment of TCP1,

TCP3, TCP8, TCP10, TCP11, TCP12, TCP13, and TCP23 would likely yield identification of additional phosphorylation sites depending upon phosphorylation stoichiometry, stable protein expression, and the amount of material that could be obtained for analysis. Additionally, TCP9 and TCP19 appear to be substrates of GRIK, and they could also be analyzed in the same way. Unfortunately the GST fusion proteins that I constructed for TCP2, TCP4, TCP14, and TCP15 were poorly expressed and difficult to purify, but if an alternative tag were utilized, similar methods could be applied. With implications that SnRK1.1 and SnRK1.2 may have some differences in their substrates, using preactivated full-length SnRK1.1 and SnRK1.2 to analyze TCP phosphorylation should be performed.

Impact of Phosphorylation of Other TCPs on their Interactions with BRM

The SWI/SNF group of ATPases are a type of chromatin remodeling complex that is conserved in yeast, animals, and plants (*26*). In plants, there are three types of SWI/SNF subgroups: BRAHMA (BRM), SPLAYED (SYD), and MINUSCULE (MINU) (*26-28*). These subunits are part of a core complex that forms with proteins SWI3 and SNF5-domain proteins (*28, 29*). SWI/SNF complexes use ATP hydrolysis to alter histone–DNA interactions (*29, 30*) to increase or decrease accessibility of genomic DNA leading to activation or repression of transcription, respectively (*29, 30*). SYD and BRM physically interact with the transcription factors, which are necessary for the SWI/SNF complex interaction with DNA (*31*), and TCP4 has been verified to interact

with BRM (*32*). In Chapter III, TCP20 and TCP22 were shown to interact with BRM and SWI3C and that TCP phosphorylation by the GRIK-SnRK1 cascade disrupts these interactions. A yeast two-hybrid study (*32*) indicated that BRM also interacts with other TCPs, which I showed are also GRIK or SnRK1 substrates, suggesting that phosphorylation could impact these interactions as well.

In the yeast two-hybrid study, TCP1, TCP8, TCP13 and TCP19 were identified as partners of BRM and/or SWI3C (*32*). These interactions would need to be verified due to a high false positive rate associated with yeast-two hybrid assays. The GRIK-SnRK1 phosphorylation of TCP1, TCP4, TCP8, and TCP13 could be examined for impacts on their interactions with BRM and/or SWI3C. The effect of GRIK phosphorylation of TCP19 could be studied this way as well. The interactions of SWI/SNF components with TCP9, TCP10, TCP11, TCP12, TCP18, or TCP23 were not tested. However, because these TCPs also were positive for phosphorylation in GRIK-SnRK1 kinase assays, it would be worthwhile asking if they interact with BRM and/or SWI3C in yeast two-hybrid assays. These experiments would indicate if phosphorylation of selected TCPs by the GRIK-SnRK1 kinase cascade is a general mechanism for regulating TCP interaction with the SNF/SWI complex in plants.

Verifying SnRK1 Substrates Containing the RSxSF Motif

The site of protein phosphorylation is often influenced by the surrounding amino acid sequence known as the consensus sequence or motif (*33*). Even though

phosphorylation regulation is a complicated process in which target protein structures or other phosphorylation events can affect this post-translational modification, consensus sequences are a key part of kinase recognition and phosphorylation (*33*), enabling kinase specificity (*34*). Previously -LxRxxSxxxL- and -xxxxxxSxx(D/E)xx- were identified as SnRK1 consequence sequences for phosphorylation via a peptide assay and meta-analysis, respectively (*34, 35*). However when comparing SnRK1 phosphorylation sites of TGMV AL1 (*4*), CaLCuV AL2 (*36*), GRIK1 (*37*) and sites determined in Chapter III to these consensus motifs inconsistencies were found. Utilizing LC/MS/MS analysis of Arabidopsisculture cell lysates incubated with recombinant kinases, I was able to identify –xxxRSxSFxxxxx- as a motif of the GRIK-SnRK1 cascade (Chapter IV).

Another future experiment would be to confirm that the motif –xxxRSxSFxxxxx- is consensus site for the GRIK-SnRK1 cascade in the proteins associated with the phosphopeptides identified in Chapter IV. Potential target proteins include the ENTH/ANTH/VHS superfamily protein (AT4G32285.1), glycine-rich protein (AT4G22740.1), NagB/RpiA/CoA transferase-like superfamily protein (AT1G72340.1) and homeobox protein knotted-1-like 4 (AT5G11060). It is also important to determine if the –xxxRxxSPxxxxx- or –xxxxSxSPxxxxx- motif identified by the LC/MS/MS study from the proteins in the soluble protein of Arabidopsis cell lysates, whaich was not verified by the phosphopeptide assay, was background or if proteins with this sequence are phosphorylated due to other factors such as secondary/tertiary structural elements of the substrates. Potential protein substrates with these motifs are the arginine/serine-rich-

splicing factor RSP31 (AT3G61860), pollen Ole e 1 allergen and extensin family protein (AT2G34700), bromo-adjacent homology (BAH) domain-containing protein (AT4G11560.1), and AMP deaminase, putative / myoadenylate deaminase, putative (AT2G38280.1). In both cases, the putative GRIK-SnRK1 substrate proteins could be expressed in *E. coli* and analyzed in kinase assays *in vitro.*

Another consideration is the experimental model used to identify SnRK1 substrates. The proteomes of Arabidopsis cultured cells and seedlings are likely to different due to the differentiation of the cell types in seedlings. A comparative study could be performed to determine if additional substrates and additional GoTerms and motifs can be identified. Additionally, analysis of *grik1 and grik2* individual knock out mutants and the double knockout mutants could be compared with wild-type plants to determine if native GRIK1 and/or GRIK2 impact the observed phosphorylation events.

REFERENCES

1. Hawley, S. A., Pan, D. A., Mustard, K. J., Ross, L., Bain, J., Edelman, A. M., Frenguelli, B. G., and Hardie, D. G. (2005) Calmodulin-dependent protein kinase kinase-beta is an alternative upstream kinase for AMP-activated protein kinase, *Cell Metab 2*, 9-19.

2. Ghillebert, R., Swinnen, E., Wen, J., Vandesteene, L., Ramon, M., Norga, K., Rolland, F., and Winderickx, J. (2011) The AMPK/SNF1/SnRK1 fuel gauge and energy regulator: structure, function and regulation, *FEBS J 278*, 3978-3990.

3. Baena-Gonzalez, E., Rolland, F., Thevelein, J. M., and Sheen, J. (2007) A central integrator of transcription networks in plant stress and energy signalling, *Nature 448*, 938-942.

4. Shen, Q., Liu, Z., Song, F., Xie, Q., Hanley-Bowdoin, L., and Zhou, X. (2011) Tomato SlSnRK1 protein interacts with and phosphorylates betaC1, a pathogenesis protein encoded by a geminivirus beta-satellite, *Plant Physiol 157*, 1394-1406.

5. Halford, N. G., and Hey, S. J. (2009) Snf1-related protein kinases (SnRKs) act within an intricate network that links metabolic and stress signalling in plants, *Biochem J 419*, 247-259.

6. Crozet, P., Margalha, L., Confraria, A., Rodrigues, A., Martinho, C., Adamo, M., Elias, C. A., and Baena-Gonzalez, E. (2010) Mechanisms of regulation of SNF1/AMPK/SnRK1 protein kinases, *Front Plant Sci 5*, 190.

7. Gonzalez-Grandio, E., and Cubas, P. (2014) Identification of gene functions associated to active and dormant buds in Arabidopsis, *Plant Signal Behav 9*, e27994.

8. Li, C., Potuschak, T., Colon-Carmona, A., Gutierrez, R. A., and Doerner, P. (2005) Arabidopsis TCP20 links regulation of growth and cell division control pathways, *Proc Natl Acad Sci U S A 102*, 12978-12983.

9. Herve, C., Dabos, P., Bardet, C., Jauneau, A., Auriac, M. C., Ramboer, A., Lacout, F., and Tremousaygue, D. (2009) *In vivo* interference with AtTCP20 function induces severe plant growth alterations and deregulates the expression of many genes important for development, *Plant Physiol 149*, 1462-1477.

10. Danisman, S., van der Wal, F., Dhondt, S., Waites, R., de Folter, S., Bimbo, A., van Dijk, A. D., Muino, J. M., Cutri, L., Dornelas, M. C., Angenent, G. C., and Immink, R. G. (2012) Arabidopsis class I and class II TCP transcription factors regulate jasmonic acid metabolism and leaf development antagonistically, *Plant Physiol 159*, 1511-1523.

11. Andriankaja, M. E., Danisman, S., Mignolet-Spruyt, L. F., Claeys, H., Kochanke, I., Vermeersch, M., De Milde, L., De Bodt, S., Storme, V., Skirycz, A., Maurer, F., Bauer, P., Muhlenbock, P., Van Breusegem, F., Angenent, G. C., Immink, R. G., and Inze, D. (2014) Transcriptional coordination between leaf cell differentiation and chloroplast development established by TCP20 and the subgroup Ib bHLH transcription factors, *Plant Mol Biol 85*, 233-245.

12. Guan, P., Wang, R., Nacry, P., Breton, G., Kay, S. A., Pruneda-Paz, J. L., Davani, A., and Crawford, N. M. (2014) Nitrate foraging by Arabidopsis roots is mediated by the transcription factor TCP20 through the systemic signaling pathway, *Proc Natl Acad Sci U S A 111*, 15267-15272.

13. Wang, X., Gao, J., Zhu, Z., Dong, X., Wang, X., Ren, G., Zhou, X., and Kuai, B. (2015) TCP transcription factors are critical for the coordinated regulation of isochorismate synthase 1 expression in Arabidopsis thaliana, *Plant J 82*, 151-162.

14. Aguilar-Martinez, J. A., and Sinha, N. (2013) Analysis of the role of Arabidopsis class I TCP genes AtTCP7, AtTCP8, AtTCP22, and AtTCP23 in leaf development, *Front Plant Sci 4*, 406.

15. Daviere, J. M., Wild, M., Regnault, T., Baumberger, N., Eisler, H., Genschik, P., and Achard, P. (2014) Class I TCP-DELLA interactions in inflorescence shoot apex determine plant height, *Curr Biol 24*, 1923-1928.

16. Williams, S. P., Rangarajan, P., Donahue, J. L., Hess, J. E., and Gillaspy, G. E. (2014) Regulation of Sucrose non-Fermenting Related Kinase 1 genes in Arabidopsis thaliana, *Front Plant Sci 5*, 324.

17. Valsecchi, I., Guittard-Crilat, E., Maldiney, R., Habricot, Y., Lignon, S., Lebrun, R., Miginiac, E., Ruelland, E., Jeannette, E., and Lebreton, S. (2013) The intrinsically disordered C-terminal region of *Arabidopsis thaliana* TCP8 transcription factor acts both as a transactivation and self-assembly domain, *Mol Biosyst 9*, 2282-2295.

18. Nag, A., King, S., and Jack, T. (2009) miR319a targeting of TCP4 is critical for petal growth and development in Arabidopsis, *Proc Natl Acad Sci U S A 106*, 22534-22539.

19. Zhou, M., Li, D., Li, Z., Hu, Q., Yang, C., Zhu, L., and Luo, H. (2013) Constitutive expression of a miR319 gene alters plant development and enhances salt and drought tolerance in transgenic creeping bentgrass (Agrostis stolonifera L.), *Plant Physiol*.

20. Confraria, A., Martinho, C., Elias, A., Rubio-Somoza, I., and Baena-Gonzalez, E. (2013) miRNAs mediate SnRK1-dependent energy signaling in Arabidopsis, *Front Plant Sci 4*, 197.

21. Rubio-Somoza, I., and Weigel, D. (2013) Coordination of flower maturation by a regulatory circuit of three microRNAs, *PLoS genetics 9*, e1003374.

22. Hammani, K., Gobert, A., Small, I., and Giege, P. (2011) A PPR protein involved in regulating nuclear genes encoding mitochondrial proteins?, *Plant Signal Behav 6*, 748-750.

23. Tao, Q., Guo, D., Wei, B., Zhang, F., Pang, C., Jiang, H., Zhang, J., Wei, T., Gu, H., Qu, L. J., and Qin, G. (2013) The TIE1 transcriptional repressor links TCP transcription factors with TOPLESS/TOPLESS-RELATED corepressors and modulates leaf development in Arabidopsis, *Plant Cell 25*, 421-437.

24. Huang, T., and Irish, V. F. (2015) Temporal Control of Plant Organ Growth by TCP Transcription Factors, *Curr Biol 25*, 1765-1770.

25. Martin-Trillo, M., and Cubas, P. (2010) TCP genes: a family snapshot ten years later, *Trends Plant Sci 15*, 31-39.

26. Flaus, A., Martin, D. M., Barton, G. J., and Owen-Hughes, T. (2006) Identification of multiple distinct Snf2 subfamilies with conserved structural motifs, *Nucleic Acids Res 34*, 2887-2905.

27. Sang, Y., Silva-Ortega, C. O., Wu, S., Yamaguchi, N., Wu, M. F., Pfluger, J., Gillmor, C. S., Gallagher, K. L., and Wagner, D. (2012) Mutations in two non-canonical Arabidopsis SWI2/SNF2 chromatin remodeling ATPases cause embryogenesis and stem cell maintenance defects, *Plant J 72*, 1000-1014.

28. Kwon, C. S., and Wagner, D. (2007) Unwinding chromatin for development and growth: a few genes at a time, *Trends Genet 23*, 403-412.

29. Hargreaves, D. C., and Crabtree, G. R. (2011) ATP-dependent chromatin remodeling: genetics, genomics and mechanisms, *Cell Res 21*, 396-420.

30. Clapier, C. R., and Cairns, B. R. (2009) The biology of chromatin remodeling complexes, *Annu Rev Biochem 78*, 273-304.

31. Wu, M. F., Sang, Y., Bezhani, S., Yamaguchi, N., Han, S. K., Li, Z., Su, Y., Slewinski, T. L., and Wagner, D. (2012) SWI2/SNF2 chromatin remodeling ATPases overcome polycomb repression and control floral organ identity with the LEAFY and SEPALLATA3 transcription factors, *Proc Natl Acad Sci U S A 109*, 3576-3581.

32. Efroni, I., Han, S. K., Kim, H. J., Wu, M. F., Steiner, E., Birnbaum, K. D., Hong, J. C., Eshed, Y., and Wagner, D. (2013) Regulation of leaf maturation by chromatin-mediated modulation of cytokinin responses, *Developmental cell 24*, 438-445.

33. Nelson, D. L. (2005) *Lehninger Principles of Biochemistry*, 4th ed., W. H. Freeman and Company, New York, New York.

34. Vlad, F., Turk, B. E., Peynot, P., Leung, J., and Merlot, S. (2008) A versatile strategy to define the phosphorylation preferences of plant protein kinases and screen for putative substrates, *Plant J 55*, 104-117.

35. van Wijk, K. J., Friso, G., Walther, D., and Schulze, W. X. (2014) Meta-Analysis of *Arabidopsis thaliana* Phospho-Proteomics Data Reveals Compartmentalization of Phosphorylation Motifs, *Plant Cell 26*, 2367-2389.

36. Shen, W., Dallas, M. B., Goshe, M. B., and Hanley-Bowdoin, L. (2014) SnRK1 phosphorylation of AL2 delays Cabbage leaf curl virus infection in Arabidopsis, *J Virol 88*, 10598-10612.

37. Shen, W., Reyes, M. I., and Hanley-Bowdoin, L. (2009) Arabidopsis protein kinases GRIK1 and GRIK2 specifically activate SnRK1 by phosphorylating its activation loop, *Plant Physiol 150*, 996-1005.

APPENDICES

Appendix A

Table A. Plasmids for Expressing Recombinant Proteins Not Constructed in this Study

Fusion Protein	Method	Accession #	pNSB #	cDNA source	F Primer	R Primer	RE digestion	Vector	Resis-tence	Expression line
GST-TCP18(fl)S48A/T233A	Mutagenesis-Pfu	At3g18550	1957	pNSB1954	TCP18 S48A F	TCP18 S48A R	-	-	Amp	BL21 (DE3)
GST-TCP15(fl)S128A/S129A	Mutagenesis-Pfu	At1g69690	1958	pNSB1731	TCP15S128A S129A F	TCP15S128A S129A R	-	-	Amp	BL21 (DE3)
GST-TCP22(fl) S140E/S316A	Mutagenesis-Pfu	At1g72010	1968	pNSB1742	TCP22S316A F	TCP22S316A R	-	-	Amp	BL21 (DE3)
GST-TCP3(fl) S262E	Mutagenesis-Pfu	At1g53230	1969	pNSB1757	TCP3S262E F	TCP3S262E R	-	-	Amp	BL21 (DE3)
GST-TCP18(fl) S48A	Mutagenesis-Pfu	At3g18550	1933	pNSB1792	TCP18 S48A F	TCP18 S48A R	-	-	Amp	BL21 (DE3)
GST-TCP18C-term S234A/S235A	Mutagenesis-Pfu	At3g18550	1934	pNSB1890	TCP18C SS234+5AA F	TCP18C SS234+5AA R	-	-	Amp	BL21 (DE3)
GST-TCP18C-term T254A/T255A/T257A	Mutagenesis-Pfu	At3g18550	1935	pNSB1890	TCP18C TTET254-8AAEA F	TCP18C TTET254-8AAEA F	-	-	Amp	BL21 (DE3)
GST-TCP18C-term T279A	Mutagenesis-Pfu	At3g18550	1936	pNSB1890	TCP18C T279A F	TCP18C T279A R	-	-	Amp	BL21 (DE3)
GST-TCP18C-term S313A	Mutagenesis-Pfu	At3g18550	1937	pNSB1890	TCP18C S313A F	TCP18C S313A R	-	-	Amp	BL21 (DE3)
GST-TCP23(fl) S132A	Mutagenesis-Pfu	At1G35560	1944	pNSB1796	TCPS132A F2	TCP23S132A R2	-	-	Amp	BL21 (DE3)

Table A. Plasmids for Expressing Recombinant Proteins Not Constructed in this Study (Continued)

Fusion Protein	Method	Accession #	pNSB #	cDNA source	F Primer	R Primer	RE digestion	Vector	Resis-tence	Expression line
GST-TCP18(Cterm) T233AS336A	Mutagenesis -Q5	At3g18550	1987	pNSB1912	TCP18S336 A F	TCP18S336 A R	-	-	Amp	BL21 (DE3)
GST-TCP18(Cterm) T233AS336E	Mutagenesis -Pfu	At3g18550	1989	pNSB1912	TCP18S336 E F	TCP18S336 E R	-	-	Amp	BL21 (DE3)

Appendix B

ABBREVIATIONS

A

A	alanine
AA	amino acid
ABA	abscisic acid
Ace	acetyl
ADP	adensine diphosphate
AIS	auto-inhibitory sequence
AMP	adensine monophosphate
AMPK	AMP-activated protein kinase
AREB	ABA-Responsive Element Binding factor
ASC	association to the complex
ATP	adensine triphosphate

B

βIS	β-interacting sequence
bHLH	basic helix-loop-helix
BiFC	bimolecular fluorescence complementation
BRM	BRAHMA
BSH	BUSHY

C

C	cysteine
CaMK	calmodulin-dependent protein kinase
CaMKKα	calcium/calmodulin-dependentprotein kinase kinase α

Carb100	100 mg/ml carbenicillin
CBM	carbohydrate-binding module
CBS	cystathionine β–synthase
CCaMK	calcium and calmodulin-dependent protein kinase
CDPKs	calcium-dependent protein kinase
CID	collision-induced dissociation
Col-0	Columbia-0
CRK	CDPK-related kinase
CUC	CUP-SHAPED COTYLEDON
CyC	cycloidea

D

D	aspartic acid
DM	dodecyl maltoside
DNA	deoxyribonucleic acid
dsDNA	double-stranded DNA
DTT	dithiothreitol

E

E	glutamic acid
E. Coli	*Escherichia coli*
EDTA	ethylenediaminetetraacetic acid
ERLIC	electrostatic repulsion-hydrophilic interaction chromatography
ETD	electron transfer dissociation

F

F	phenylalanine
FA	formic acid

G

G	glycine
GFP	green fluorescent protein
GRIK	geminivirus Rep interacting kinase
GSP	gene specific primer
GST	glutathione S-transferase
GUS	beta-glucuronidase

H

H	histidine
HCD	higher-energy collisional dissociation

I

I	isoleucine
ICS1	isochorismate synthaase 1
IDD8	indeterminate domain 8
IMAC	immobilized metal affinity chromatography
IPTG	isopropyl β-D-1-thiogalactopyranoside

K

K	lysine
KA1	kinase-associated
Kan50	50 mg/ml kanamycin
KAT1	K+ channel in Arabidopsis thaliana 1
kD	kilo Dalton
KIS	kinase interacting sequence

L

L	leucine
LB	Luria broth
LC/MS/MS	liquid chromtography/ mass spectrometry/ mass spectrometry
LKB1	liver kinase B1
LOX2	LIPOXYGENASE2

M

M	methionine
MAP	microtubule-associated protein
MARK	microtubule affinity-regulating kinase
MINU	MINUSCULE
miR	microRNA

N

N	asparagine

P

P	proline
PAGE	polyacrylamide gel electrophoresis
PBS	phosphate-buffered saline
PBST	phosphate-buffered saline with Tween-20
PCF	PROLIFERATING CELL FACTORS
PCNA	proliferating cell nuclear antigen
PEPRK	PEP carboxylase kinase-related kinase
PPCK	phosphoenolpyruvate carboxylase kinase
PTL	Petal Loss
PTM	post-translational modification

Q

Q	glutamine

R

R	arginine
RBE	RABBIT EARS
RBOHF	Respiratory Burst Oxidase Homolog F
ROS	reactive oxygen species
rpm	revolutions per minute

S

S	serine
Ser	serine
SLAC1	Slow Anion Channel-Associated 1
SNF1	Sucrose Nonfermenting−1
SnRK	SNF1-related kinase
SWI/SNF	switch/sucrose non-fermentable
SYD	SPLAYED

T

T	threonine
TB1	teosinte branched 1
TCP	Teosinte branched 1 / Cycloidea / PROLIFERATING CELL FACTOR
TDP	T-DNA boarder sequence
Thr	threonine
TIE1	EAR motif protein
TiO_2	titanium oxide

U

UBA	ubiquitin-associated

V

V	valine

W

W	tryptophan

Y

Y	tyrosine
Y2H	yeast two-hybrid